Contribution of Dynamic Instability to Microtubule Organization

by

Simon Muriithi Karuku

A Thesis submitted to the Faculty of Graduate Studies of
The University of Manitoba
in partial fulfillment of the requirements for the degree of

MASTER OF SCIENCE

Department of Mathematics
University of Manitoba
Winnipeg, Manitoba

Abstract

Microtubules are hollow cylindrical protein structures found in all eukaryotic cells, and essential in several cellular processes, including cell motility, cell division, vesicle trafficking and maintenance of cell shape. The building block of microtubules, *tubulin*, is one of the proven targets for anticancer drugs. A microtubule exhibits a remarkable property, termed *dynamic instability*, in which it is able to switch stochastically between two distinct states. In one state, the microtubule grows while in the other, it shrinks. The balance between the growing and shrinking states is crucial for the normal functioning of the cell. One of the interesting questions that cell biologists have pondered over the years is: what is the biological function of dynamic instability? While some great strides have been made in answering this question, the details of the precise nature of the mechanism of dynamic instability in relation to their roles are not well understood. In this thesis some biologically plausible mathematical models for microtubule dynamics *in vitro* are developed. Two of the models are developed with the exclusion of dynamic instability while the others are with its inclusion. Also considered are two different modes of nucleation of microtubules: saturating and non-saturating mode. The models are analyzed and numerical simulations conducted, with an aim of mathematically assessing the role of dynamic instability in the integral microtubule dynamics *in vitro*. Results indicate that dynamic instability induces the formation of microtubules from the tubulin subunits, and that dynamic instability depends on the GTP-tubulin concentration.

Acknowledgements

I would first like to sincerely thank my advisor, Dr. Stéphanie Portet, for her expert advice, unwavering support and positive encouragement throughout the course of my Masters program. Her patience and kindness have immensely contributed to the timely completion of this thesis. Secondly, I thank my committee members, Dr. Julien Arino and Dr. Beni Sahai, for their constructive criticism and helpful suggestions. I gratefully acknowledge the financial support for my Masters studies through the Teaching Assistantship from the Department of Mathematics. I am greatly indebted to the administrative staff in the Department of Mathematics, Ms. Heather Aldwyn, Ms. Leanne Blondeau and Ms. Shirley Kangas, for their kindness. Finally, special thanks are due the members of the faculty, my friends and colleagues in the Department of Mathematics for their friendliness and support.

Dedication

To
my father, Gilbert Karuku Mũrĩithi,
and
my mother, Rose Mũthoni Werũ,
for all their sacrifices, love and prayers.

Table of Contents

List of Tables

List of Figures

Notations and abbreviations

Notation	meaning
$\mathbb{Z}^+$	the set $\{0, 1, 2, \cdots\}$ of nonnegative integers
$\mathbb{R}^+$	the set $(0, \infty)$ of positive real numbers
$\mathbb{R}_+$	the set $[0, \infty)$ of non-negative real numbers
$\mathbb{R}^n$	the n-dimensional Euclidean space
$\mathbb{R}^n_+$	the n-dimensional nonnegative orthant $\{(x_1, \cdots, x_n) \in \mathbb{R}^n : \ x_1 \geq 0, \cdots, x_n \geq 0\}$
$\mathrm{tr}(\cdot)$	the trace of a matrix
$\lvert \cdot \rvert$	the determinant of a matrix
$\lvert\lvert \cdot \rvert\rvert$	Euclidean norm
$\mathbf{I}$	The identity matrix
$\mathbf{A}^T$	the transpose of $\mathbf{A}$
$M_n(\mathbb{R})$	The set of real $n \times n$ matrices over $\mathbb{R}$
$M_{mn}(\mathbb{R})$	The set of real $m \times n$ matrices over $\mathbb{R}$

Abbreviation	meaning
GDP	guanosine diphosphate
GTP	guanosine triphosphate
E site	Exchangeable nucleotide binding site of tubulin
MT	microtubule
ODE	ordinary differential equation
RHS	right-hand side
LHS	left-hand side

Chapter 1

Biological background

> *The strange fact about* MTs[1] *is that they form when and where the cells need them − implying some complex regulation of spatial localization − and that in many instances they may construct, always at the same speed, extraordinarily complex assemblies...* ([22] pp. 430).

This chapter contains a basic introduction to cell biology. The content is focused on and constrained to motivating the object of this thesis, namely, an evaluation of the contribution of nucleation and dynamic instability to the overall microtubule dynamics.

1.1 The cell

The smallest structural unit of living things which, given the right conditions, can function independently is the *cell*. There are two major types of cells: *prokaryotes* and *eukaryotes*. Eukaryotic cells are structurally and biochemically more complex than prokaryotic cells. Prokaryotic cells contain non-membranous organelles and lack a cell nucleus. In contrast, eukaryotic cells have a nucleus as well as many membrane-bound organelles such as mitochondria, lysosomes, endoplasmic reticulum, Golgi apparatus and vacuoles (see Figure 1.1). Here, we focus on eukaryotes.
The nucleus contains deoxyribonucleic acid (DNA), the repository of genetic instructions for growth, development and replication. DNA is a polymer made up of four repeating subunits called nucleotides (A, C, G, and T)[2] with specific chemical and structural

[1] MT: Microtubule

[2] The letters A, C, G, and T represent the nucleic acid bases adenine, cytosine, guanine, and thymine, respectively.

properties, organized into linear structures called *chromosomes* within the cell nucleus. Eukaryotic cells reproduce by a complex process of cell division. In somatic (body) cells, chromosomes go through a process called *mitosis*, during which, a cell divides into two genetically identical daughter cells, each identical to the parent cell.

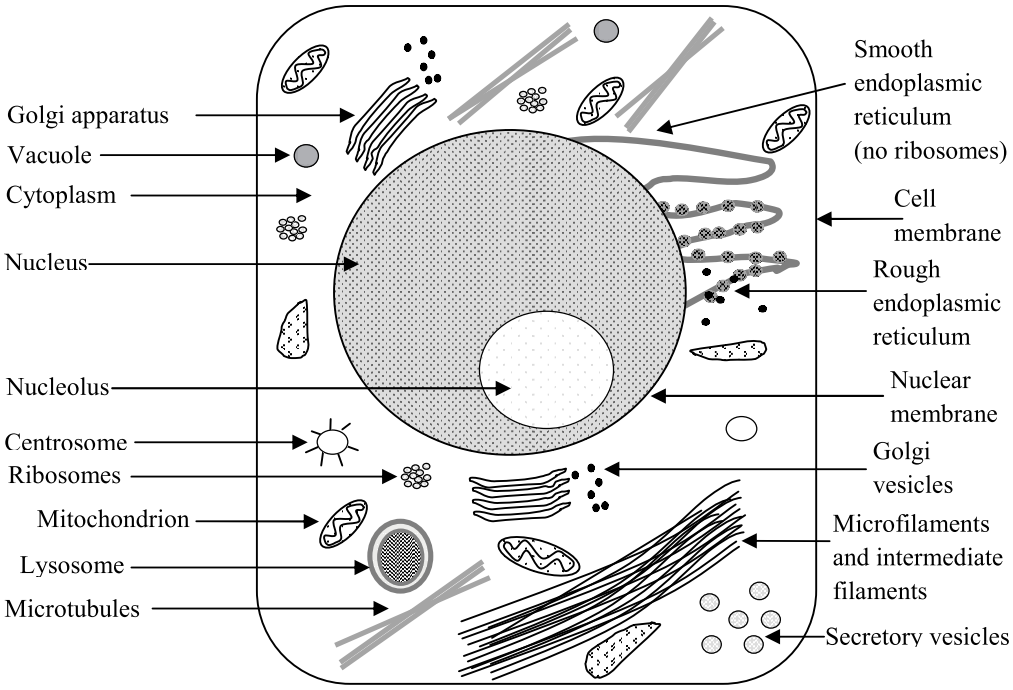

Figure 1.1: Illustration of a eukaryotic cell.

1.2 The cytoskeleton

In addition to the nucleus, nearly all eukaryotic cells have a *cytoskeleton*, a network of protein filaments and tubular structures that extends throughout the cytoplasm (the region of the cell that is between the nucleus and the cell membrane). The cytoskeleton is a highly dynamic structure that undergoes constant restructuring and modification in response to environmental stimulations, thus providing a structural framework for the cell. In addition to playing this structural role, the cytoskeleton plays many roles in nuclear and cell division, transport, signaling, determination of cell shape and polarity. It is comprised of three principal types of protein filaments: *microtubules*, *actin filaments*

(also called *microfilaments*), and *intermediate filaments*. Each type of filament is formed from a different protein subunit: *actin* for actin filaments, *tubulin* for microtubules, and a family of related fibrous proteins, such as vimentin or cytokeratin, for intermediate filaments [2]. In this work, we will focus on the microtubules, with a view to understand the significance of the key components in the *in vitro* assembly-disassembly dynamics of a microtubule. In particular, the significance of a unique microtubule behaviour, known as *dynamic instability*, in the overall microtubule dynamics will be examined.

1.3 The microtubules

Microtubules are hollow cylinders with an outer diameter of about 25 nm (nanometers[3]), inner diameter of about 15 nm, and a varying overall length, ranging from 200 nm to 25 μm [22, 72]. They are composed primarily of the protein *tubulin*. Each tubulin is found as a heterodimer, consisting of two similar, but not identical monomers, called α- and β-tubulin each of molecular weight of about 55 kilodaltons[4] (kDa) [22, 62, 72, 73]. Each $\alpha\beta$-tubulin heterodimer is about $4nm$ in diameter and $8nm$ long [2]. The α- and β-tubulin in a heterodimer are tightly bound together by noncovalent bonding, so that the heterodimer, under normal conditions, rarely dissociates into individual α- and β-tubulin monomers [51]. Each heterodimer contains two guanine nucleotide-binding sites: an *exchangeable* site (E-site) at the β-tubulin end, occupied by either energy-rich guanosine 5′-triphosphate (GTP) or guanine 5′-diphosphate (GDP), and a *nonexchangeable* site (N-site) between the α- and β- monomers, occupied by GTP [72]. The heterodimer with GTP bound to the β-tubulin subunit is referred to as a *GTP-tubulin* heterodimer. If GDP binds to the β-tubulin subunit, the resulting heterodimer is refered to as a *GDP-tubulin* heterodimer. From now on, we shall simply use the term "*dimer*" as a short for heterodimer. The GTP at the N-site is tightly bound, and cannot be removed without

[3] $25\,\text{nm} = 2.5 \times 10^{-5}\,\text{mm}$

[4] A "Dalton" (Da) is a measure of molecular weight or mass. 1 Dalton corresponds to one-twelfth the mass of a Carbon−12 atom; $1\text{Da} \approx 1.66 \times 10^{-24} g$

denaturing the dimer, while the GTP at the E-site is freely exchangeable with unbound GTP [43].

Microtubules are formed by the self assembly of the GTP-tubulin dimers [18, 21, 58, 72] in the presence of additional GTP and magnesium ions (Mg^{2+}) and at 37^oC [43]. The dimers bind in a head-to-tail fashion ($\alpha\beta\alpha\beta$) forming linear units known as *protofilaments* (Figure 1.2). In general, each microtubule is composed of thirteen protofilaments, which interact laterally (i.e., side-by-side) to form the hollow tubule − the microtubule [18, 21, 72, 73] (Figure 1.2).

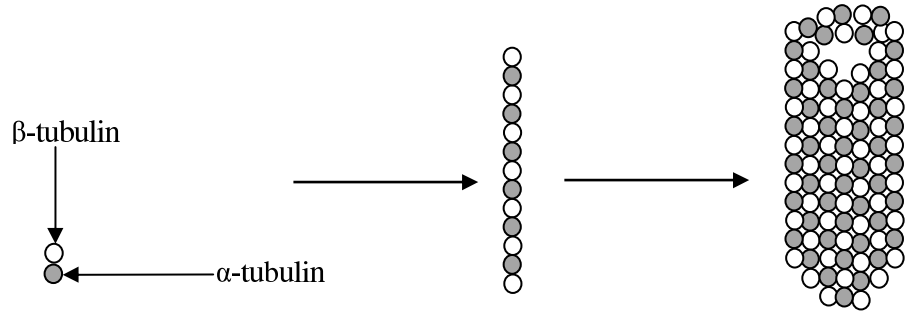

Figure 1.2: Microtubule structure. Each tubulin is found as a *heterodimer*, consisting of two similar, but not identical monomers, called α- and β-tubulin monomer. The heterodimers bind in a head-to-tail fashion forming the *protofilaments*. In general, each microtubule is composed of thirteen protofilaments, which interact laterally (i.e., side-by-side) to form the hollow tubule − the *microtubule*.

The head-to-tail orientation of dimers in the microtubule lattice results in an intrinsic structural polarity between the two ends of the microtubule: one end exposes only α-tubulin subunits, and the other only β-tubulin subunits. The end which starts with β-tubulin is called the *plus* end, while the end that starts with α-tubulin is called the *minus* end of the microtubule [18, 36, 47]. The rate at which polymerization takes place at the two ends is different, with the plus end growing much faster than the minus end [2, 18, 58, 81]. In most eukaryotic cells, the microtubule minus ends are embedded within the microtubule-organizing centre (MTOC) where initiation[5] of new filaments occurs, whilst

[5]Initiation of new filaments is usually referred to as *nucleation*.

the plus ends grow into the cytoplasm [2, 81]. During polymerization (assembly) of dimers to the ends of microtubules, the GTP at the E-site is hydrolyzed to GDP and the resulting GDP is unable to exchange. The result is that the body of the microtubule is made up of GDP-tubulin subunits that energetically favour depolymerization (disassembly) [61, 72]. When the microtubule disassembles (depolymerizes), the dimers are released and the GDP at the E-site is now able to exchange to GTP. In contrast, the GTP bound at the N-site is non-exchangeable and is not hydrolyzed to GDP during the addition of dimers to the ends of microtubules [18]. This unique GTP binding and hydrolysis properties at the E- and N-sites strongly influence the dynamic behaviour of microtubules. Microtubules undergo two interesting kinds of dynamics: *dynamic instability* [58] and *treadmilling* [53]. The former is a process in which individual microtubule ends switch abruptly and stochastically between periods of growth and shortening, while the latter is the net assembly at one microtubule end and the net disassembly at the opposite end with no net change in microtubule length. Treadmilling and dynamic instability are compatible behaviours, and a specific microtubule population can show primarily treadmilling behaviour, dynamic instability behaviour, or some mixture of both [44]. We now discuss each of these in greater detail in turn.

1.3.1 Dynamic instability

When observed *in vivo*, microtubules display a remarkable phenomenon. They rapidly grow toward the cell periphery at a constant rate for some period and then suddenly shrink rapidly back towards the centrosome [2, 22]. The microtubules may shrink partially and then recommence growing, or they may disappear completely, to be replaced by a different microtubule [2]. Thus in a population of microtubules, at any point in time, a subset of microtubules are rapidly growing while others are quickly shrinking [14]. Both states are known to coexist under identical conditions of tubulin availability. The random alternation between the two states is known as *dynamic instability* [58]. The transition from growth to shrinkage is termed a *'catastrophe'*, while the reverse reaction

− the transition from shrinking to growing − is referred to as a *'rescue'* [82]. Dynamic instability has also been observed *in vitro* [34, 58, 82]. To characterize dynamic instability, typically four parameters have been used in previous analyses: rate of polymerization, rate of depolymerization, frequency of catastrophe, and frequency of rescue [19, 26]. Dynamic instability is an energy-requiring phenomenon and is believed to be a function of GTP hydrolysis [58]. The most widely accepted model to explain dynamic instability is the "*GTP cap*" model [18, 48, 58]. During microtubule assembly, according to this model, the α-tubulin part of the dimer binds to the β-tubulin at the microtubule plus end. This binding triggers hydrolysis of β-tubulin-bound GTP (GTP-tubulin) to GDP (GDP-tubulin) [24]. A GDP-tubulin at the tip of a microtubule will fall off, while a GDP-tubulin in the middle of a microtubule will not. If non-hydrolyzable GTP is incorporated in the E-site of β-tubulin, the affected subunits will remain in the GTP-bound form after they polymerize into microtubules. The normal hydrolysis of GTP to GDP by the polymerized tubulin subunits renders the microtubule inherently unstable because the GDP-bound form makes the protofilaments curve slightly [61]. Since tubulin adds onto the end of the microtubule only in the GTP-bound state, there is generally a "cap" of GTP-tubulin at the tip of the microtubule, protecting it from disassembly. The stochastic shrinking and growing of microtubules is thus ascribable to random loss and regain of this cap. When hydrolysis takes place at the tip of the microtubule, the microtubule begins a rapid depolymerization and retraction. GTP-bound tubulin can begin adding to the tip of the microtubule again, providing a new cap and protecting the microtubule from shrinking. A catastrophe occurs when the GTP cap is lost allowing GDP-tubulin to dissociate. A rescue, on the other hand, is proposed to occur when a shrinking end is recapped with GTP-tubulin [18].

1.3.2 Treadmilling

This is the net gain of tubulin subunits at the plus end of a microtubule and an equivalent net loss from the minus end, producing a net flux of subunits through the microtubule.

Thus, the net polymerization at the plus end balances the net depolymerization at the minus end [53, 58]. Two models have been proposed in an attempt to understand the mechanism of treadmilling − the Wegner model and the differential dynamic instability model [28, 82]. The former model [84], initially proposed for actin filament assembly, assumes that there is no GTP cap at the microtubule ends, that only GDP-tubulin subunits would dissociate from the microtubule, and that there is only one single continuous phase of assembly of GTP-tubulin and disassembly of GDP-tubulin taking place at a given microtubule end. Upon polymerization of tubulin subunit at the microtubule end, GTP hydrolysis allows the critical tubulin concentrations for growth at opposite ends to be different. If the dimer pool concentration is at an intermediate value between the critical concentrations of the two ends, the end with the lower critical concentration will persistently grow while the end with the higher critical concentration will persistently shorten [53]. However, this theory has been contested from several points of view (see, for example, [82]). The differential dynamic instability model for treadmilling posits that for microtubule ends capable of dynamic instability, differences in the contributions of the assembly and disassembly phases between the two ends offer an alternative way to bias one end into net growth while the other end is biased into net shrinkage at steady-state assembly. Treadmilling will occur if the growth phase is dominant at one end while the shortening phase is dominant at the other end [28].

1.3.3 Mechanisms of microtubule assembly *in vitro*

In vitro, microtubule assembly proceeds in two phases, a *nucleation* phase followed by an *elongation* (growth) phase [18, 80]. During the nucleation phase, new microtubule ends are spontaneously generated from the dimers [41, 80]. Once the preformed microtubule nuclei (or seeds) are large enough to be stable, assembly of dimers onto the ends produces elongation [80]. The formation of the initial nuclei is energetically less favourable than the subsequent addition of dimers to the growing microtubule and, consequently, nucleation becomes negligible once elongation commences [52]. The elongation phase continues until

the dimer pool is reduced to the concentration in equilibrium with microtubules (critical concentration) [52, 80].

1.3.4 Functions of microtubules

While evidence concerning the cellular functions of microtubules is largely circumstantial [72], it is generally accepted that microtubules fulfill important functions in addition to the maintenance of the physical architecture of the cell [36, 44, 63, 73].

During cell division (mitosis), microtubules rearrange themselves into an array of fibres, called the *mitotic spindle* [22, 73]. It is this spindle that eventually pulls each set of chromosomes to opposite ends of the cell, ensuring accurate distribution of the genetic material to each daughter cell. Microtubules are also directly involved with the movement of chromosomes during cell division [22, 63].

Microtubules are the main components of the complex and highly organized axonemal structures found in cilia and flagella − hairlike structures projecting from the cell surface [22, 73, 77]. In vertebrates, the respiratory tract is lined with cilia that keep potentially harmful microorganisms from entering the lungs. The sperm tail (flagellum), on the other hand, propels the sperm cell in a vigorous forward motion through the seminal fluid, enabling the sperm penetrate the female egg in order to fertilize it [73].

Microtubules play an important role in intracellular trafficking of vesicles and organization of organelles by providing the tracks along which motor proteins, such as kinesin and dynein superfamily proteins, convey their cargoes [2, 36].

Microtubules are also involved in the transmission of nerve impulses (signal transduction) [5, 36, 63], and protein and hormone secretion [72, 73].

1.3.5 Diseases related to microtubule malfunction

Although each cell in the body maintains itself and carries out its specific function, it is part of a large colony of collaborating cells that constitute the whole organism. A cell

communicates with its surrounding cells by releasing chemical messages, through a process called *signal transduction*. The defining characteristics of malignant tumours (commonly referred to as "cancer") are abnormal, excessive and inappropriate cellular proliferation, invasiveness and ability to form secondary tumours. A hyperplastic (cancerous) cell will stimulate neighbouring cells to grow by secreting growth factors. As they proliferate, hyperplastic cells disrupt the normal function of surrounding tissues, leading to eventual organ failure and death. As noted in Section 1.3.4, the process of chromosome segregation during cell division is mediated by the mitotic spindle, which is composed primarily of microtubules. This role of microtubules has been exploited by cancer chemotherapists to develop drugs that are not only effective for cancer treatment, but have minimal effects on non-cancerous cells (a review can be found in, for example, [44]). The drugs are so designed as to disrupt microtubule assembly − prevent polymerization and/or promote depolymerization. For example, the drug *paclitaxel* (taxol), used in the treatment of cancer [44], blocks dynamic instability by stabilizing GDP-tubulin in the microtubule. Thus, even when hydrolysis of GTP reaches the tip of the microtubule, there is no depolymerization and the microtubule does not shrink back. Another drug *Colchicine* has the opposite effect: it blocks the polymerization of tubulin into microtubules.

Elsewhere, microtubules are actively involved in the growth and maintenance of the axon [5]. Here, microtubule assembly plays an important role: when growing axons are treated with microtubule depolymerizing drugs, the axons stop growing and retract (reviewed in [5]); while compounds that promote neurite growth also promote microtubule assembly. Therefore, understanding how microtubules assemble can lend valuable insight into important medical problems such as the treatment of cancer and neurodegenerative diseases.

1.4 Motivation

Since the discovery of microtubule dynamic instability in 1984 [58], cell biologists have been actively studying the role of this unique behaviour in biological functions of microtubules. Dynamic instability, for example, is known to provide the mechanism for the recycling of microtubules in the mitotic spindle [24]. While several hypotheses attempting to ascribe roles to dynamic instability have been advanced (for a review see, for example, [24]), details of the precise nature of the mechanism of dynamic instability in relation to these roles remain sketchy. A comprehensive model for the mechanism of dynamic instability would require a detailed study of all the key processes in microtubule assembly and disassembly dynamics. This work aims at providing some insight into the impact of dynamic instability on the assembly-disassembly dynamics of microtubules *in vitro*. We hope to mathematically evaluate the contribution of nucleation and dynamic instability in the assembly-disassembly dynamics of microtubules. We'll take a comparative approach and explore the dynamics of microtubules with the inclusion and exclusion of dynamic instability.

1.5 Thesis outline

The remainder of this thesis consists of five more chapters, organized as follows. Chapter two provides some mathematical background on dynamical systems analysis. A review of sensitivity analysis in modelling is also considered. Chapter three contains a review of some previous microtubule dynamics models. Chapter four and Chapter five describe the core of our own research work. In Chapter four, we describe the proposed microtubule dynamics models while in Chapter five, we analyze these models and give a discussion of this analysis. Finally, Chapter six provides conclusions and suggestions for future work.

Chapter 2

Mathematical preliminaries

This chapter reviews a few mathematical preliminaries usually required in the analysis of the behaviour of a generic dynamical system. Different notions of stability of equilibrium solutions of a dynamical system and related theorems are described.

2.1 Introduction to dynamical systems

Dynamical systems theory provides the mathematical tools for analyzing and describing systems that change over time. Informally, a dynamical system is a rule that determines how a system evolves over time. The rule determines what the state $\boldsymbol{x}_t$ is at a later time t given an initial condition or "state" $\boldsymbol{x}_0$.

Definition 2.1.1. [7] *A* ***dynamical system*** *is a triple* $\{\mathcal{T}, \mathcal{X}, \boldsymbol{\phi}_t\}$*, consisting of an ordered time set* $\mathcal{T}$*, a state (or phase) space* $\mathcal{X}$*, and an evolution operator* $\boldsymbol{\phi}_t : \mathcal{X} \longrightarrow \mathcal{X}$ *that transforms an initial state* $\boldsymbol{x}_0 \in \mathcal{X}$ *at time* $t_0 \in \mathcal{T}$ *to another state* $\boldsymbol{x}_t \in \mathcal{X}$ *at time* $t \in \mathcal{T}$*.*

The time set $\mathcal{T}$ may be continuous or discrete. The state space $\mathcal{X}$ may be continuous or discrete or a hybrid of the two, and it may be finite or infinite-dimensional depending on the number of variables required to fully describe the state of the system. $\boldsymbol{\phi}_t$ may be given explicitly or defined implicitly, it may be deterministic or stochastic, and it satisfies

the following properties[1] [65]:

(i) $\boldsymbol{\phi}_0$ is the identity operator; that is, $\boldsymbol{\phi}_0(\boldsymbol{x}) = \boldsymbol{x}, \quad \forall\, \boldsymbol{x} \in \mathcal{X}$;

(ii) $\boldsymbol{\phi}_{t+s}(\boldsymbol{x}) = \boldsymbol{\phi}_t\left(\boldsymbol{\phi}_s(\boldsymbol{x})\right), \quad \forall\, \boldsymbol{x} \in \mathcal{X}, \quad t, s \in \mathcal{T}$.

Remark. If $\boldsymbol{\phi}$ satisfies (i) and (ii), it is said to have the semigroup property.

In the discrete-time case, a dynamical system can be expressed as

$$\boldsymbol{x}(t+1) = \boldsymbol{f}(\boldsymbol{x}(t)),$$

where $\boldsymbol{x}(t)$ is the state of the system at time t, and $\boldsymbol{f}$ is called the *map* of the system. For a given initial condition, the iterates of the mapping $\boldsymbol{f}$ will yield a state-space *trajectory*. On the other hand, the evolution of a continuous dynamical system (also referred to as a *flow*) can mathematically be described by a number of different formalisms. One of the simplest of such formalisms is a set of first-order nonlinear ordinary differential equations (ODEs)

$$\frac{d\boldsymbol{x}(t)}{dt} = \boldsymbol{f}(\boldsymbol{x}(t), t).$$

The vector field $\boldsymbol{f}$ assigns an instantaneous direction and magnitude of change at each point in the state space. Starting from some initial state $\boldsymbol{x}_0$, the sequence of states generated by the action of the dynamics is called a *solution trajectory* or *orbit*. A solution trajectory has the property that its tangent at each point is given by the vector field at that point. The set of all possible solution trajectories graphically illustrates the action of the evolution operator $\boldsymbol{\phi}_t$ [7].

Often, the long-term behaviour of dynamical systems is of special interest. Over time, the state of many dynamical systems eventually ends up in a small subset of the state space called a *limit set* [7]. A limit set is *invariant* with respect to the dynamics of the system it represents, in the sense that if the system's state reaches a limit set, the dynamics will act to keep it there indefinitely [7]. Two simple types of limits sets are *equilibrium points* and *limit cycles*. An equilibrium point is a point in the system's phase space where the

[1] For simplicity, $\boldsymbol{\phi}(\cdot, t)$ is being denoted by $\boldsymbol{\phi}_t(\cdot)$

system's state does not change with time. On the other hand, a limit cycle is a closed trajectory such that once in cycle, the trajectory will repeat infinitely. An equilibrium point, and more generally, a limit set, can be *stable* or *unstable*. For a stable equilibrium point, the system trajectories can be kept arbitrarily close to the equilibrium point by starting sufficiently close to it. A limit set is said to be unstable if it is not stable. Formal definitions of these and other terms in dynamical systems will appear in the next section.

2.2 Some qualitative properties of dynamical systems

In the real world, most dynamical systems are nonlinear. Such a system can sometimes be represented by a set of first-order nonlinear ODEs in the form

$$\dot{\boldsymbol{y}}(t) = \mathbf{g}(\boldsymbol{y}(t), t), \quad \boldsymbol{y} \in \mathcal{S} \subset \mathbb{R}^n, \;\; t \in \mathbb{R}_+, \tag{2.1}$$

where $\mathbf{g} : \mathbb{R}_+ \times \mathcal{S} \longrightarrow \mathbb{R}^n$ is a vector field, and $\dot{\boldsymbol{y}}(t) = \frac{d\boldsymbol{y}(t)}{dt}$. These equations describe the time evolution of the variables and the system they represent.

Definition 2.2.1. *A function* $\mathbf{g} : \mathbb{R}^n \longrightarrow \mathbb{R}^m$ *is said to be* ***continuous at a point*** $\boldsymbol{y} \in \mathcal{S} \subset \mathbb{R}^n$ *if for every* $\epsilon > 0$*, there exists a* $\delta(\epsilon) > 0$ *such that*

$$||\boldsymbol{y} - \boldsymbol{z}|| < \delta \quad \Rightarrow \quad ||\mathbf{g}(\boldsymbol{y}) - \mathbf{g}(\boldsymbol{z})|| < \epsilon.$$

If $\mathbf{g}$ *is continuous at every point in its domain then* $\mathbf{g}$ *is said to be continuous.*

Remarks. A function $\mathbf{g}$ defined on a domain $\mathcal{S}$ is said to be C^k-continuous (or k times continuously differentiable, or of class C^k), $k \in \mathbb{Z}^+$, (and we write $\mathbf{g} \in C^k(\mathcal{S})$) iff all the partial derivatives of $\mathbf{g}$ of order less than or equal to k exist and are continuous functions on $\mathcal{S}$. In particular, $\mathbf{g} \in C^1(\mathcal{S})$ in $\boldsymbol{y}$ iff $\mathbf{g}$ is continuous and all the first partial derivatives

$$\frac{\partial g_i(\boldsymbol{y}, t)}{\partial y_j}, \;\; i, j = 1, \cdots, n$$

exist and are continuous on $\mathcal{S}$. In this case (that is $\mathbf{g} \in C^1(\mathcal{S})$), we say that $\mathbf{g}$ is continuously differentiable in $\boldsymbol{y}$ on $\mathcal{S}$. Conventionally, we say that $\mathbf{g}$ is C^0 if $\mathbf{g}$ is continuous.

Definition 2.2.2. *A function $\boldsymbol{g} : \mathbb{R}^n \longrightarrow \mathbb{R}^m$ is said to be **piecewise continuous** on a finite interval $\mathcal{S} \subset \mathbb{R}^n$ if*

(a) *$\boldsymbol{g}$ is continuous on $\mathcal{S}$ except for a finite number of points of discontinuity, and*

(b) *$\boldsymbol{g}$ has finite right-hand and left-hand limits at each point of discontinuity.*

A function is piecewise continuous on an infinite interval if it is piecewise continuous on every finite subinterval.

Definition 2.2.3. [31] *Let $\mathcal{E} \subseteq \mathbb{R}^n \times \mathbb{R}$ be an open set and consider the dynamical system* (2.1)*. Denote the time interval for which* (2.1) *is defined as $\mathbb{I} \subseteq \mathbb{R}$. A function $\boldsymbol{y} : \mathbb{I} \longrightarrow \mathbb{R}^n$ is said to be a **solution** of* (2.1) *on $\mathbb{I}$ if $\boldsymbol{y}$ is a continuously differentiable function defined on $\mathbb{I}$, $(\boldsymbol{y}(t), t) \in \mathcal{E}$, $t \in \mathbb{I}$ and $\boldsymbol{y}(t)$ satisfies* (2.1) *$\forall\, t \in \mathbb{I}$. We refer to $\mathbf{g}$ as a **vector field** on $\mathcal{E}$. Suppose $(\boldsymbol{y}_0, t_0) \in \mathcal{E}$ is given. An **initial value problem*** (IVP) *for Eq.* (2.1) *consists of finding an interval $\mathbb{I}$ containing t_0 and a solution $\boldsymbol{y}$ of* (2.1) *satisfying $\boldsymbol{y}(t_0) = \boldsymbol{y}_0$. We write this problem symbolically as*

$$\dot{\boldsymbol{y}}(t) = \mathbf{g}(\boldsymbol{y}(t), t), \quad \boldsymbol{y}(t_0) = \boldsymbol{y}_0, \quad t \in \mathbb{I}. \tag{2.2}$$

If there exists an interval $\mathbb{I}$ containing t_0 and a $\boldsymbol{y}$ satisfying (2.2), we refer to this as a solution of (2.1) passing through $(\boldsymbol{y}_0, t_0)$ [31]. In other words, an IVP consists in finding the trajectory $\boldsymbol{\varphi}_t$ passing through a given initial state $(\boldsymbol{y}_0, t_0)$. The graph of $\boldsymbol{\varphi}_t$ is the curve $\boldsymbol{\Gamma}$ lying in the region $\mathcal{E} \subset \mathbb{R}^{n+1}$, where each point of the curve has the coordinate $(\boldsymbol{\varphi}_t, t)$ and where the tangent to $\boldsymbol{\Gamma}$ at each point is represented by $\mathbf{g}(\boldsymbol{\varphi}_t, t)$.
When considering the IVP (2.2), two questions are of fundamental interest:

(i) Does a solution to the problem always exist?

(ii) If a solution exists, is it unique?

The first question is addressed in Cauchy-Peano's existence theorem, stated next.

Theorem 2.2.4 (Cauchy-Peano existence theorem [31]). *Let $\mathcal{E} \subseteq \mathbb{R}^n \times \mathbb{R}$ be an open set and consider the dynamical system* (2.1). *If the function $\mathbf{g} : \mathcal{E} \longrightarrow \mathbb{R}^n$ is continuous in $\mathcal{E}$, then for any $(\boldsymbol{y}_0, t_0) \in \mathcal{E}$, system* (2.1) *has a solution $\boldsymbol{\varphi}$ in $\mathbb{R}^n$ satisfying $\boldsymbol{\varphi}(t_0) = \boldsymbol{y}_0$.*

Corollary 2.2.5. [31] *If $\mathcal{U}$ is a compact set of $\mathcal{E}$, $\mathcal{U} \subset \mathcal{V}$, an open set in $\mathcal{E}$ with the closure $\bar{\mathcal{V}}$ of $\mathcal{V}$ in $\mathcal{E}$, then there is an $\alpha > 0$ such that, for any initial value $(\boldsymbol{y}_0, t_0) \in \mathcal{U}$, there is a solution to the IVP* (2.2), *which exists at least on the interval $[t_0 - \alpha,\ \ t_0 + \alpha]$.*

For the second question, on the uniqueness of solutions of (2.2), an additional hypothesis must be imposed on Theorem 2.2.4; namely, local Lipschitz hypothesis. The following definition characterizes the notion of Lipschitzness of a function.

Definition 2.2.6. *Let $\mathcal{E} \subseteq \mathbb{R}^n \times \mathbb{R}$ be an open set. A function $\mathbf{g} : \mathcal{E} \longrightarrow \mathbb{R}^n$ is said to be **locally Lipschitz** in $\boldsymbol{y}(t)$ (or with respect to $\boldsymbol{y}(t)$) if for every compact set $\boldsymbol{\Omega} \subseteq \mathcal{E}$, there exists a positive constant $L = L_{\boldsymbol{\Omega}}$ such that for all $t \in \mathbb{R}$, and any $\boldsymbol{y}_1(t), \boldsymbol{y}_2(t) \in \mathbb{R}^n$ satisfying $(\boldsymbol{y}_1(t), t), (\boldsymbol{y}_2(t), t) \in \boldsymbol{\Omega}$, we have*

$$||\mathbf{g}(\boldsymbol{y}_1(t), t) - \mathbf{g}(\boldsymbol{y}_2(t), t)|| \leq L_{\boldsymbol{\Omega}} ||\boldsymbol{y}_1(t) - \boldsymbol{y}_2(t)||. \tag{2.3}$$

If the Lipschitz condition (2.3) *holds for all $\boldsymbol{y}_1(t),\ \boldsymbol{y}_2(t) \in \mathbb{R}^n,\ t \in \mathbb{R}_+$, then $\mathbf{g}$ is said to be **globally Lipschitz** (with respect to $\boldsymbol{y}(t)$).*

Remark. The constant $L_{\boldsymbol{\Omega}}$ in (2.3) is called a **Lipschitz constant** for $\mathbf{g}$.

The following Lemma implies that a continuously differentiable function is locally Lipschitz.

Lemma 2.2.7. [33] *Let $\mathcal{E} \subseteq \mathbb{R}^{n+1}$ be open. If the function $\mathbf{g} : \mathcal{E} \longrightarrow \mathbb{R}^n$ is C^1 in $\boldsymbol{y}$, then $\mathbf{g}$ is locally Lipschitz in $\boldsymbol{y}$.*

Theorem 2.2.8 (Picard-Lindelöf theorem [31, 33]). *Let $\mathcal{E} \subseteq \mathbb{R}^{n+1}$ be an open set and consider the dynamical system* (2.1). *If the function $\mathbf{g} : \mathcal{E} \longrightarrow \mathbb{R}^n$ is continuous in $\mathcal{E}$ and locally Lipschitz with respect to $\boldsymbol{y}(t)$ in $\mathbb{R}^n$, then for any $(\boldsymbol{y}_0, t_0) \in \mathcal{E}$, system* (2.1) *has a unique solution $\boldsymbol{\varphi}$ in $\mathbb{R}^n$ satisfying $\boldsymbol{\varphi}(t_0) = \boldsymbol{y}_0$.*

Dynamical systems are classified as autonomous and non-autonomous, based on the independence or dependence of the system on the time variable.

Definition 2.2.9 (Autonomous system). *The nonlinear system* (2.1) *is said to be* ***autonomous*** *if* $\mathbf{g}$ *does not depend explicitly on time t; i.e., if the system's state equations can be written as*

$$\dot{\boldsymbol{y}} = \mathbf{g}(\boldsymbol{y}).$$

Otherwise, the system is called ***non-autonomous****.*

Remark. When (2.1) is autonomous, the domain of $\mathbf{g}$ in (2.1) is of dimension n, otherwise it is of dimension $(n + 1)$.

Definition 2.2.10 (Equilibrium point). *Consider the dynamical system* (2.1). *A point $\boldsymbol{y}^* \in \mathcal{S}$ is said to be an* ***equilibrium point*** *of* (2.1) *if*

$$\mathbf{g}(\boldsymbol{y}^*, t) = \mathbf{0}, \qquad \forall\, t \geq 0.$$

An equilibrium point $\boldsymbol{y}^*$ has the property that for any $t \geq t_0 > 0$, if the state of the system starts at $\boldsymbol{y}^*$, it will remain at $\boldsymbol{y}^*$ for all future time.

We now present the basic notions of stability of equilibria of dynamical systems. Roughly speaking, an equilibrium point $\boldsymbol{y}^*$ is Lyapunov stable if any trajectory that starts sufficiently close to $\boldsymbol{y}^*$ stays arbitrarily close to $\boldsymbol{y}^*$ for all future time. Lyapunov stability does not, however, imply asymptotic stability. An equilibrium point $\boldsymbol{y}^*$ is asymptotically stable if it is Lyapunov stable and, in addition, any trajectory starting close to $\boldsymbol{y}^*$ ultimately converges to $\boldsymbol{y}^*$ as time progresses. Both Lyapunov stability and asymptotic stability of an equilibrium point are local, in the sense that they are expressed in terms

of a neighbourhood of a given initial condition. A stronger notion of stability - global asymptotic stability- exists. An equilibrium point $\boldsymbol{y}^*$ is globally asymptotically stable if all trajectories regardless of starting point (initial condition) will converge to $\boldsymbol{y}^*$ as time approaches infinity. Formal definitions of these notions of stability are now given.

Definition 2.2.11 (Stability of non-autonomous systems [30, 46])**.** *Consider the nonlinear dynamical system* (2.1) *where* $\boldsymbol{g} : \mathcal{S} \times \mathbb{R}_+ \longrightarrow \mathbb{R}^n$ *is locally Lipschitz in* $\boldsymbol{y}$ *and piecewise continuous in* t*. Let* $\boldsymbol{\varphi}_t$ *be the solution of* (2.1) *at time* t *corresponding to the initial condition* $\boldsymbol{\varphi}_{t_0} = \boldsymbol{y}_0$*. Let* $\boldsymbol{y}^* \in \mathcal{S}$ *be an equilibrium point of* (2.1)*; i.e.,* $\boldsymbol{g}(\boldsymbol{y}^*, t) = \boldsymbol{0}, \ \forall\, t \geq t_0 \geq 0$*. Then,* $\boldsymbol{y}^*$ *is said to be*

- ***stable*** *in the sense of Lyapunov* (*or* ***Lyapunov stable***, *or* ***locally stable***) *if for any given* $t_0 \geq 0$ *and* $\varepsilon > 0$*, there exists a* $\delta > 0$ (*depending on* ε *and* t_0) *such that*

$$||\boldsymbol{\varphi}_{t_0} - \boldsymbol{y}^*(t_0)|| < \delta \quad \Rightarrow \quad ||\boldsymbol{\varphi}_t - \boldsymbol{y}^*(t)|| < \varepsilon, \quad \forall\, t \geq t_0 \geq 0.$$

- ***unstable*** *if it is not Lyapunov stable.*

- ***asymptotically stable*** *if it is stable in the sense of Lyapunov, and for each* $t_0 \geq 0$ *there exists a positive constant* $\delta_1 = \delta_1(t_0)$ *such that*

$$||\boldsymbol{\varphi}_{t_0} - \boldsymbol{y}^*(t_0)|| < \delta_1 \quad \Rightarrow \quad \lim_{t \to \infty} ||\boldsymbol{\varphi}_t - \boldsymbol{y}^*(t)|| = 0.$$

- ***globally asymptotically stable*** *if it is stable in the sense of Lyapunov, and*

$$\lim_{t \to \infty} ||\boldsymbol{\varphi}_t - \boldsymbol{y}^*(t)|| = 0, \quad \forall\, \boldsymbol{\varphi}_{t_0} \in \mathcal{S}, \ \ t_0 \geq 0.$$

Now let $\boldsymbol{y}^*(t)$ be the equilibrium solution of (2.1) with $\boldsymbol{y}^*(0) = \boldsymbol{y}_0$ and consider a perturbation of the initial condition of (2.1) so that $\boldsymbol{y}(0) = \boldsymbol{y}_0 + \delta \boldsymbol{y}_0$. If we now replace $\boldsymbol{y}(t)$ by a new variable $\boldsymbol{x}(t) = \boldsymbol{y}(t) - \boldsymbol{y}^*(t)$, and noting that both $\boldsymbol{y}^*(t)$ and $\boldsymbol{y}(t)$ are solutions

of (2.1), then $\boldsymbol{x}(t)$ satisfies the following non-autonomous differential equation:

$$\dot{\boldsymbol{x}} = \boldsymbol{g}(\boldsymbol{y}^*(t) + \boldsymbol{x}, t) - \boldsymbol{g}(\boldsymbol{y}^*(t), t) \equiv \boldsymbol{f}(\boldsymbol{x}, t)$$

with initial condition $\boldsymbol{x}(0) = \delta\boldsymbol{y}(0) \equiv \boldsymbol{x}_0$. Since $\boldsymbol{f}(\boldsymbol{0}, t) = \boldsymbol{0}$ for every $t \in \mathbb{R}$, the new dynamical system,

$$\dot{\boldsymbol{x}} = \boldsymbol{f}(\boldsymbol{x}, t) \tag{2.4}$$

has an equilibrium point at the origin of the state space. Therefore, instead of studying the deviation of $\boldsymbol{y}(t)$ from $\boldsymbol{y}^*(t)$ for system (2.1), we may simply study the pertubation dynamics of (2.4) with respect to the equilibrium point $\boldsymbol{0}$.
Consequently, we summarize the above definitions of stability using the origin as the equilibrium point for a time-invariant dynamical system.

Definition 2.2.12 (Stability of autonomous systems [30, 46])**.** *Consider the autonomous dynamical system*

$$\dot{\boldsymbol{x}}(t) = \boldsymbol{f}(\boldsymbol{x}), \quad \boldsymbol{x} \in \mathcal{D} \subseteq \mathbb{R}^n, \ \ t \in \mathbb{R}_+ \tag{2.5}$$

where $\boldsymbol{f} : \mathcal{D} \longrightarrow \mathbb{R}^n$ is locally Lipschitz in $\boldsymbol{x}$ and piecewise continuous in t. Let $\boldsymbol{\phi}(t)$ be the solution of system (2.5) at time t corresponding to the initial condition $\boldsymbol{\phi}(0) = \boldsymbol{x}_0$. Assume that $\boldsymbol{x}^* = \boldsymbol{0}$ is an equilibrium point of (2.5); i.e., $\boldsymbol{f}(\boldsymbol{0}) = \boldsymbol{0}$. Then, $\boldsymbol{x}^* = \boldsymbol{0}$ is

- ***Lyapunov stable*** *if, for each $\epsilon > 0$, there exists a $\delta = \delta(\epsilon) > 0$ such that*

$$||\boldsymbol{\phi}(0)|| < \delta \quad \Rightarrow \quad ||\boldsymbol{\phi}(t)|| < \epsilon, \quad \forall\, t \geq 0.$$

- ***unstable*** *if it is not Lyapunov stable.*

- ***asymptotically stable*** *if it is Lyapunov stable, and there exists a $\delta_1 > 0$ such that*

$$||\boldsymbol{\phi}(0)|| < \delta_1 \quad \Rightarrow \quad \lim_{t\to\infty} ||\boldsymbol{\phi}(t)|| = 0.$$

- ***globally asymptotically stable*** *if it is Lyapunov stable and*

$$\lim_{t\to\infty} ||\boldsymbol{\phi}(t)|| = 0, \quad \forall\, \boldsymbol{\phi}(0) \in \mathcal{D}.$$

Definition 2.2.13. *Let $\boldsymbol{\phi}_t$ be the solution of system (2.5) at time t corresponding to the initial condition $\boldsymbol{\phi}_{t_0} = \boldsymbol{x}_0$. Then*

- *the **forward** (or **positive**) **orbit** of (through) $\boldsymbol{x}$ is the set*

$$O^+(\boldsymbol{x}) = \{\boldsymbol{\phi}_t(\boldsymbol{x}) : t \geq 0\};$$

- *the **backward** (or **negative**) **orbit** of (through) $\boldsymbol{x}$ is the set*

$$O^+(\boldsymbol{x}) = \{\boldsymbol{\phi}_t(\boldsymbol{x}) : t \leq 0\};$$

- *the **orbit** of (through) $\boldsymbol{x}$ is the union of forward and backward orbits:*

$$O(\boldsymbol{x}) = O^+(\boldsymbol{x}) \cup O^-(\boldsymbol{x}).$$

Remark. In defining a backward orbit in Definition 2.2.13, we are assuming that system (2.5) is defined for $t \in \mathbb{R}$ so that trajectories can evolve backwards in time.

Definition 2.2.14. [65] *A point $\boldsymbol{p} \in \mathcal{D} \subseteq \mathbb{R}^n$ is called an ω-**limit point** of the solution $\boldsymbol{\phi}_t$ of the dynamical system (2.5) iff there is a sequence $\{t_n\}_{n=0}^{\infty}$, with $t_n \to \infty$ as $n \to \infty$, such that $\boldsymbol{\phi}_{t_n} \to \boldsymbol{p}$ as $n \to \infty$. Similarly, if there is a sequence $\{t_n\}_{n=0}^{\infty}$, with $t_n \to -\infty$ as $n \to \infty$, such that $\lim_{n\to\infty} \boldsymbol{\phi}_{t_n} = \boldsymbol{q}$, and a point $\boldsymbol{q} \in \mathcal{D} \subseteq \mathbb{R}^n$, then $\boldsymbol{q}$ is called an α-**limit point** of the solution $\boldsymbol{\phi}_t$ of (2.5). The set of all ω-limit points of a trajectory $\boldsymbol{\phi}_t$ is called the ω-**limit set** of $\boldsymbol{\phi}_t$. The set of all α-limit points of a trajectory $\boldsymbol{\phi}_t$ is called the α-**limit set** of $\boldsymbol{\phi}_t$. The set of all limit points of $\boldsymbol{\phi}_t$ is called the **limit set** of $\boldsymbol{\phi}_t$.*

Theorem 2.2.15. [65] *The α- and ω-limit sets of a trajectory $\boldsymbol{\phi}_t$ of (2.5) are closed subsets of $\mathcal{D}$ and if $\boldsymbol{\phi}_t$ is contained in a compact subset of $\mathbb{R}^n$, then the α- and ω-limit sets of $\boldsymbol{\phi}_t$ are non-empty, compact, connected subsets of $\mathcal{D}$.*

Definition 2.2.16. *A set $\mathcal{S} \subseteq \mathcal{D} \subseteq \mathbb{R}^n$ is said to be*

- ***forward invariant** with respect to the dynamical system (2.5) if for any $\boldsymbol{x}_0 \in \mathcal{S}$, there is a t_0 such that $\boldsymbol{\phi}_t(\boldsymbol{x}_0) \equiv \boldsymbol{\phi}(t; t_0, \boldsymbol{x}_0) \in \mathcal{S}, \quad \forall\, t \geq t_0$,*

- ***backward invariant*** *with respect to the dynamical system* (2.5) *if for any* $\boldsymbol{x}_0 \in \mathcal{S}$, *there is a* t_0 *such that* $\boldsymbol{\phi}_t(\boldsymbol{x}_0) \in \mathcal{S}, \quad \forall\, t \leq t_0$,

- ***invariant*** *if it is both forward and backward invariant.*

Remark. Simply put, a set $\mathcal{S}$ is an invariant set for system (2.5) if every trajectory $\boldsymbol{\phi}_t$ starting from a point in $\mathcal{S}$ will remain in $\mathcal{S}$ for all times (that is, $\boldsymbol{x}_0 \in \mathcal{S} \;\Rightarrow\; \boldsymbol{\phi}_t(\boldsymbol{x}_0) \in \mathcal{S}, \quad \forall\, t \in \mathbb{R}$).

2.3 Stability analysis

Stability analysis of equilibrium solutions is a fundamental and important problem in establishing the qualitative behaviour of dynamical systems. In this section, a review of commonly used techniques in stability analysis is considered.

2.3.1 Lyapunov's first (indirect) method

In the Lyapunov's first method, the strategy is to make a Taylor series expansion of (2.5) in the neighbourhood of an equilibrium solution $\boldsymbol{x}^*$ of (2.5), and approximate the vector field by the linear part of this expansion. Consider the nonlinear dynamical system (2.5) where $\boldsymbol{x} \in \mathcal{D} \subseteq \mathbb{R}^n$, and $\boldsymbol{f}(\boldsymbol{x})$ is continuously differentiable. Let $\boldsymbol{x}^*$ be an equilibrium solution of (2.5); that is, $\boldsymbol{f}(\boldsymbol{x}^*) = \mathbf{0}$. The Jacobian matrix of system (2.5) is given by

$\mathbf{J}(\boldsymbol{x}) = \frac{\partial \boldsymbol{f}}{\partial \boldsymbol{x}}(\boldsymbol{x})$, with the (i,j)th entry

$$J_{ij}(\boldsymbol{x}) = \frac{\partial \dot{x}_i(\boldsymbol{x})}{\partial x_j} \equiv \frac{\partial f_i(\boldsymbol{x})}{\partial x_j}, \quad i,j = 1,\ldots,n.$$

Consider a small perturbation, $\boldsymbol{z} = \boldsymbol{x} - \boldsymbol{x}^*$, around $\boldsymbol{x}^*$. Then,

$$\frac{d\boldsymbol{z}}{dt} = \frac{d}{dt}(\boldsymbol{x} - \boldsymbol{x}^*) = \frac{d\boldsymbol{x}}{dt} = \boldsymbol{f}(\boldsymbol{x}).$$

The Taylor series expansion of $\boldsymbol{f}(\boldsymbol{x})$ around $\boldsymbol{x}^*$ is given by

$$\boldsymbol{f}(\boldsymbol{x}) = \boldsymbol{f}(\boldsymbol{x}^*) + \boldsymbol{f}'(\boldsymbol{x}^*)(\boldsymbol{x} - \boldsymbol{x}^*) + \mathcal{O}\left(|\boldsymbol{x} - \boldsymbol{x}^*|^2\right)$$

$$= \boldsymbol{f}'(\boldsymbol{x}^*)(\boldsymbol{x} - \boldsymbol{x}^*) + \mathcal{O}\left(|\boldsymbol{x} - \boldsymbol{x}^*|^2\right) \qquad (\text{since } \boldsymbol{f}(\boldsymbol{x}^*) = \mathbf{0})$$

$$\approx \mathbf{J}^*\boldsymbol{z}, \qquad \text{where } \mathbf{J}^* = \left.\frac{\partial \boldsymbol{f}}{\partial \boldsymbol{x}}(\boldsymbol{x})\right|_{\boldsymbol{x}=\mathbf{x}^*}$$

That is, for a small perturbation $\boldsymbol{z}$, only the first term in the above expansion is significant, since the higher order terms involve powers of the small perturbation from the equilibrium solution $\boldsymbol{x}^*$. The time evolution of our new variable, $\boldsymbol{z}$ will then be governed by the linearized system

$$\dot{\boldsymbol{z}} = \mathbf{J}^*\boldsymbol{z} \tag{2.6}$$

The new system (2.6) is referred to as the *linearization* (or *linear approximation*) of the nonlinear dynamical system (2.5) at the equilibrium point $\boldsymbol{x}^*$. Note that since $\mathbf{J}^*$ is a constant matrix, (2.6) is an autonomous linear differential equation[2] whose solution is given by

$$\boldsymbol{z}(t) = \exp(\mathbf{J}^* t)\boldsymbol{z}_0, \quad t \geq 0,$$

where $\boldsymbol{z}_0$ is the initial condition of (2.6) at $t = 0$. The stable and centre manifold theorems establish the relationship between the nonlinear system (2.5) and its linearization (2.6).

Theorem 2.3.1 (Stable Manifold Theorem [65]). *Let $\boldsymbol{f} \in C^1(\mathcal{D})$ where $\mathcal{D}$ is an open subset of $\mathbb{R}^n$ containing the origin, and let $\boldsymbol{\phi}_t$ be the flow of the nonlinear system* (2.5)*. Suppose that $\boldsymbol{x}^* = \mathbf{0}$ is an equilibrium solution for* (2.5)*, and that $\mathbf{A} = \left.\frac{\partial \boldsymbol{f}}{\partial \boldsymbol{x}}(\boldsymbol{x})\right|_{\boldsymbol{x}^*=\mathbf{0}}$ has k*

[2]The solution, $\boldsymbol{x}(t)$, of a continuous-time autonomous linear dynamical system

$$\dot{\boldsymbol{x}} = \mathbf{A}\boldsymbol{x}, \quad \boldsymbol{x}(0) = \boldsymbol{x}_0, \qquad \boldsymbol{x} \in \mathbb{R}^n, \ \mathbf{A} \in M_n(\mathbb{R}), \ t \in \mathbb{R}_+$$

is given by

$$\boldsymbol{x}(t) = e^{\mathbf{A}t}\boldsymbol{x}_0, \qquad t \geq 0,$$

where $e^{\mathbf{A}t} = \mathbf{I} + \sum_{k=1}^{\infty} \frac{t^k}{k!}\mathbf{A}^k$.

eigenvalues with negative real part and $n-k$ eigenvalues with positive real part. Then

- *there exists a k-dimensional differentiable manifold S tangent to the stable subspace E^s of the linear system*

$$\dot{\boldsymbol{x}} = \mathbf{A}\boldsymbol{x} \tag{2.7}$$

  at $\mathbf{0}$ such that for all $t \geq 0$, $\boldsymbol{\phi}_t(S) \subset S$ and for all $\boldsymbol{x}_0 \in S$, $\lim_{t\to\infty} \boldsymbol{\phi}_t(\boldsymbol{x}_0) = \mathbf{0}$; and

- *there exists an $n-k$ dimensional differentiable manifold U tangent to the unstable subspace E^u of (2.7) at $\mathbf{0}$ such that for all $t \leq 0$, $\boldsymbol{\phi}_t(U) \subset U$ and for all $\boldsymbol{x}_0 \in U$, $\lim_{t\to-\infty} \boldsymbol{\phi}_t(\boldsymbol{x}_0) = \mathbf{0}$.*

Remark. By the stable (resp. unstable) subspace, we mean the span of the generalized eigenvectors corresponding to the eigenvalues with negative (resp. positive) real parts.

Theorem 2.3.2 (Centre Manifold Theorem [65])**.** *Let $\boldsymbol{f} \in C^r(\mathcal{D})$ where $\mathcal{D}$ is an open subset of $\mathbb{R}^n$ containing the origin and $r \geq 1$. Suppose that $\boldsymbol{x}^* = \mathbf{0}$ is an equilibrium solution of (2.5), and that $\mathbf{A} = \frac{\partial \boldsymbol{f}}{\partial \boldsymbol{x}}(\boldsymbol{x})\Big|_{\boldsymbol{x}^*=\mathbf{0}}$ has k eigenvalues with negative real part, j eigenvalues with positive real part, and $m = n-k-j$ eigenvalues with zero real part. Then there exists an m-dimensional centre manifold $W^c(\mathbf{0})$ of class C^r tangent to the centre subspace[3] E^c of (2.7) at $\mathbf{0}$, which is invariant under the flow $\boldsymbol{\phi}_t$ of (2.5).*

Remark. By Theorem 2.3.2, we know that the linearized system (2.6) is tangent to the nonlinear system (2.5) and, hence, the local behaviour of (2.5) will be approximated by the behaviour of its linearization; that is, by system (2.6), at $\boldsymbol{x}^* = \mathbf{0}$ [65].
The classical Hartman-Grobman's theorem asserts that on a topological level, the linear approximation (2.6) captures all the local dynamics of (2.5), providing that the equilibrium solution $\boldsymbol{x}^*$ of (2.5) is *hyperbolic* (see Definition 2.3.3). In other words, near a hyperbolic equilibrium solution, the nonlinear system (2.5) has the same qualitative

[3]By the centre subspace, we mean the span of the generalized eigenvectors corresponding to the eigenvalues with zero real parts.

structure as the linear system (2.6). Before stating the theorem, some definitions are in order.

Definition 2.3.3. *Let $\boldsymbol{x}^* \in \mathcal{D} \subseteq \mathbb{R}^n$ be an equilibrium point of the nonlinear dynamical system (2.5); $\boldsymbol{x}^*$ is said to be **hyperbolic** if all the eigenvalues of the Jacobian matrix $\frac{\partial \boldsymbol{f}}{\partial \boldsymbol{x}}(\boldsymbol{x})\Big|_{\boldsymbol{x}=\boldsymbol{x}^*}$ has nonzero real parts.*

Definition 2.3.4. *A function $h : \mathcal{U} \longrightarrow \mathcal{V}$ is a **homeomorphism** if h is a bijection (that is, one-to-one and onto), and both h and h^{-1} are continuous.*

Definition 2.3.5. [65] *Let*

$$\dot{\boldsymbol{x}}(t) = \boldsymbol{f}_1(\boldsymbol{x}), \quad \boldsymbol{f}_1 \in C^1(\mathcal{D}_1), \quad \mathcal{D}_1 \subset \mathbb{R}^n \tag{2.8}$$

and

$$\dot{\boldsymbol{x}}(t) = \boldsymbol{f}_2(\boldsymbol{x}), \quad \boldsymbol{f}_2 \in C^1(\mathcal{D}_2), \quad \mathcal{D}_2 \subset \mathbb{R}^n \tag{2.9}$$

*be two autonomous dynamical systems, where $\mathcal{D}_1$ and $\mathcal{D}_2$ are open neighbourhoods of the origin. The two systems are said to be **topologically equivalent** or to have the same qualitative structure in a neighbourhood of the origin, if there is a homeomorphism $h : \mathcal{D}_1 \longrightarrow \mathcal{D}_2$ which maps trajectories $\boldsymbol{\phi}_t$ of (2.8) onto trajectories $\boldsymbol{\psi}_t$ of (2.9) and preserves the orientation. If the homeomorphism h preserves the parameterization by time (that is, $h \circ \boldsymbol{\phi}_t(\boldsymbol{x}) = \boldsymbol{\psi}_t(h(\boldsymbol{x})), \ \forall\, \boldsymbol{x}, t$), then the systems (2.8) and (2.9) are said to be **topologically conjugate** in a neighbourhood of the origin.*

Theorem 2.3.6 (Hartman-Grobman Theorem [65])**.** *Let $\boldsymbol{f} \in C^1(\mathcal{D})$ where $\mathcal{D}$ is an open subset of $\mathbb{R}^n$ containing the origin, and let $\boldsymbol{\phi}_t$ be the flow of the nonlinear system (2.5). Suppose that $\boldsymbol{x}^* = \mathbf{0}$ is a hyperbolic equilibrium solution of (2.5).Then there exist neighbourhoods $\mathcal{U}$, $\mathcal{V}$ of the origin and a homeomorphism $h : \mathcal{U} \longrightarrow \mathcal{V}$, such that for each $\tilde{\boldsymbol{x}} \in \mathcal{U}$, there is an open interval $\tilde{\mathbb{I}} \subset \mathbb{R}$ containing the origin such that for all $\tilde{\boldsymbol{x}} \in \mathcal{U}$ and $t \in \tilde{\mathbb{I}}$*

$$h \circ \boldsymbol{\phi}_t(\tilde{\boldsymbol{x}}) = \exp(\mathbf{A}t) h(\tilde{\boldsymbol{x}});$$

that is, h maps trajectories of (2.5) near the origin onto trajectories of (2.6) near the origin and preserves the parameterization.

Remarks.

(i) Theorem 2.3.6 says nothing about the non-hyperbolic case.

(ii) From Definition 2.3.5, the Hartman-Grobman theorem can be stated thus: "If the origin is a hyperbolic equilibrium solution of (2.5), then the flow of (2.5) is topologically conjugate to the flow of (2.6) near the origin."

The following theorem gives the conditions under which we can draw conclusions about the stability of the origin as an equilibrium point for the nonlinear system (2.5) by investigating its stability as an equilibrium solution for the linearized system (2.6).

Theorem 2.3.7. [46] *Let* $\boldsymbol{x}^* = \mathbf{0}$ *be a hyperbolic equilibrium solution for the nonlinear dynamical system* (2.5) *where* $\boldsymbol{f} : \mathcal{D} \subset \mathbb{R}^n \longrightarrow \mathbb{R}^n$ *is continuously differentiable and* $\mathcal{D}$ *is a neighbourhood of the origin. Let* $\mathbf{A} = \frac{\partial \boldsymbol{f}}{\partial \boldsymbol{x}}(\boldsymbol{x})\Big|_{\boldsymbol{x}^*=\mathbf{0}}$ *be the Jacobian matrix of* $\boldsymbol{f}$ *evaluated at the origin.*

(i) *If all the eigenvalues of* $\mathbf{A}$ *have negative real parts, then* $\boldsymbol{x}^* = \mathbf{0}$ *is asymptotically stable.*

(ii) *If* $\mathbf{A}$ *has at least one eigenvalue with a positive real part, then* $\boldsymbol{x}^* = \mathbf{0}$ *is unstable.*

Remarks.

· Since the solution of the linearized system (2.6) is of the form $\boldsymbol{z}(t) = e^{\mathbf{A}t}\mathbf{z}_0$, it follows that if all the eigenvalues of $\mathbf{A}$ have negative real parts, then all the trajectories will decay exponentially to the equilibrium solution, otherwise if there is an eigenvalue with a positive real part, then the trajectories will grow exponentially in time; hence Theorem 2.3.7.

· If the Jacobian matrix $\mathbf{A}$ in Theorem 2.3.7 has some eigenvalues with a zero real part with the rest of the eigenvalues having negative real parts, then linearization fails to determine stability of the origin.

2.3.2 Routh-Hurwitz criterion

Consider the nonlinear dynamical system (2.5) where $\boldsymbol{x} \in \mathcal{D} \subseteq \mathbb{R}^n$ and $\boldsymbol{f} : \mathcal{D} \longrightarrow \mathbb{R}^n$ is continuously differentiable. Let $\boldsymbol{x}^* = \mathbf{0}$ be an equilibrium solution of (2.5); that is, $\boldsymbol{f}(\mathbf{0}) = \mathbf{0}$.

Let $\mathbf{A}$ be the Jacobian matrix of $\boldsymbol{f}$ evaluated at the equilibrium solution; that is, $\mathbf{A} = \frac{\partial \boldsymbol{f}}{\partial \boldsymbol{x}}(\boldsymbol{x})\Big|_{\boldsymbol{x}^*=\mathbf{0}}$. The eigenvalues of $\mathbf{A}$ are the solutions of the characteristic equation $|\mathbf{A} - \lambda\mathbf{I}| = 0$, which expands to

$$c_0\lambda^n + c_1\lambda^{n-1} + \cdots + c_{n-1}\lambda + c_n = 0. \tag{2.10}$$

By Theorem 2.3.7, the equilibrium solution is asymptotically stable if all eigenvalues of $\mathbf{A}$ have negative real parts. The Routh-Hurwitz criterion gives necessary and sufficient conditions for all the roots of (2.10) to have a negative real part, and thus for the equilibrium solution to be asymptotically stable [23].

Theorem 2.3.8 (Routh-Hurwitz criterion)**.** *Consider the characteristic equation* (2.10) *where* $c_i \in \mathbb{R},\ i = 0, 1, 2, \ldots, n;\ c_0 > 0$. *A necessary and sufficient condition for all the roots of* (2.10) *to have negative real parts is that the inequalities*

$$H_1 = |c_1| = c_1 > 0, \qquad H_2 = \begin{vmatrix} c_1 & c_3 \\ c_0 & c_2 \end{vmatrix} > 0, \qquad H_3 = \begin{vmatrix} c_1 & c_3 & c_5 \\ c_0 & c_2 & c_4 \\ 0 & c_1 & c_3 \end{vmatrix} > 0,$$

$$H_4 = \begin{vmatrix} c_1 & c_3 & c_5 & c_7 \\ c_0 & c_2 & c_4 & c_6 \\ 0 & c_1 & c_3 & c_5 \\ 0 & c_0 & c_2 & c_4 \end{vmatrix} > 0, \quad \ldots, \quad H_n = \begin{vmatrix} c_1 & c_3 & c_5 & \ldots & 0 \\ c_0 & c_2 & c_4 & \ldots & 0 \\ 0 & c_1 & c_3 & \ldots & 0 \\ 0 & c_0 & c_2 & \ldots & 0 \\ \ldots & \ldots & \ldots & \ldots & \ldots \\ \ldots & \ldots & \ldots & \ldots & c_n \end{vmatrix} > 0$$

hold.

Remark. From Theorem 2.3.8, it can be shown that:

(a) for a two-dimensional system, a necessary and sufficient condition for the real parts of the two eigenvalues to be negative is that

  (i) $|\mathbf{A}| > 0$, and

  (ii) $\text{tr}(\mathbf{A}) < 0$

(b) for a three-dimensional system, a necessary and sufficient condition for the real parts of all the three eigenvalues to be negative is that

  (i) $|\mathbf{A}| < 0$,

  (ii) $\text{tr}(\mathbf{A}) < 0$, and

  (iii) $|\mathbf{A}| - \text{tr}(\mathbf{A}) \cdot M > 0$, where M is the sum of all 2×2 principal minors of $\mathbf{A}$.[4]

2.3.3 Lyapunov's second (direct) method

Linear stability analysis examines the behaviour of a dynamical system in the vicinity of an equilibrium solution. The analysis, however, does not give an insight into the stability of the system away from the equilibrium solution. Lyapunov's second method can used to establish the global stability of a dynamical system. This method entails systematic exploitation of special auxiliary functions, termed *Lyapunov functions*, for the investigation of stability.

Definition 2.3.9. *Let $\boldsymbol{x}^* = \mathbf{0}$ be an equilibrium solution for system (2.5), and let $\mathcal{D} \subseteq \mathbb{R}^n$ be an open neighbourhood of $\mathbf{0}$. Let $V : \mathcal{D} \longrightarrow \mathbb{R}$ be a continuously differentiable function. The (total) derivative, $\dot{V}(\boldsymbol{x}(t))$, of $V(\boldsymbol{x}(t))$ along an arbitrary solution $\boldsymbol{x}(t)$ of (2.5) is given by*

$$\dot{V}(\boldsymbol{x}(t)) = \frac{dV(\boldsymbol{x}(t))}{dt} = \frac{\partial V(\boldsymbol{x}(t))}{\partial \boldsymbol{x}} \cdot \frac{d\boldsymbol{x}(t)}{dt} = \nabla V(\boldsymbol{x}(t)) \cdot \boldsymbol{f}(\boldsymbol{x})$$

[4] If $A = \begin{bmatrix} a_{11} & a_{12} & a_{13} \\ a_{21} & a_{22} & a_{23} \\ a_{31} & a_{32} & a_{33} \end{bmatrix}$, then the 2×2 principal minors of A are $\begin{vmatrix} a_{11} & a_{12} \\ a_{21} & a_{22} \end{vmatrix}$, $\begin{vmatrix} a_{11} & a_{13} \\ a_{31} & a_{33} \end{vmatrix}$, and $\begin{vmatrix} a_{22} & a_{23} \\ a_{32} & a_{33} \end{vmatrix}$.

Then V is a ***weak Lyapunov function*** *for system (2.5) on the set $\mathcal{D}$ iff*

(i) *V is continuously differentiable on $\mathcal{D}$;*

(ii) $V(\mathbf{0}) = 0$ *and* $V(\boldsymbol{x}) > 0, \quad \forall\, \boldsymbol{x} \in \mathcal{D} \setminus \{\mathbf{x}^*\}$,[5]

(iii) $\dot{V}(\boldsymbol{x}) \leq 0, \quad \forall\, \boldsymbol{x} \in \mathcal{D}$.[6]

Remarks.

· If we have a strict inequality in part (*iii*) of Definition 2.3.9, then V is known as a **strong** (or strict) Lyapunov function.

· Notice that at each point on the $(\boldsymbol{x}, t)$ space, $V(\boldsymbol{x})$ is a function of position. Thus, the sign of $\dot{V}(\boldsymbol{x})$ determines whether $V(\boldsymbol{x})$ is increasing or decreasing along the solutions of (2.5). Hence the following theorem.

Theorem 2.3.10 (Lyapunov's stability theorem [33, 65])**.** *Consider the dynamical system (2.5), where $\mathcal{D} \subseteq \mathbb{R}^n$ is a nonempty open set, and let $\boldsymbol{x}^* \in \mathcal{D}$ be an equilibrium solution of (2.5). Suppose that for some neighbourhood $\mathcal{U}$ of $\boldsymbol{x}^*$, there exists a continuous function $V : \mathcal{U} \longrightarrow \mathbb{R}$, which is continuously differentiable on $\mathcal{U} \setminus \{\boldsymbol{x}^*\}$ and satisfies the conditions $V(\boldsymbol{x}^*) = 0$ and $V(\boldsymbol{x}) > 0, \quad \forall\, \boldsymbol{x} \in \mathcal{U} \setminus \{\boldsymbol{x}^*\}$.*

(i) *If $\dot{V}(\boldsymbol{x}) \leq 0$, for all $\boldsymbol{x} \in \mathcal{D}$, then $\boldsymbol{x}^*$ is stable;*

(ii) *If $\dot{V}(\boldsymbol{x}^*) = 0$ and $\dot{V}(\boldsymbol{x}) < 0$, for all $\boldsymbol{x} \in \mathcal{U} \setminus \{\boldsymbol{x}^*\}$, then $\boldsymbol{x}^*$ is asymptotically stable.*

(iii) *If $\dot{V}(\boldsymbol{x}) > 0$, for all $\boldsymbol{x} \in \mathcal{U} \setminus \{\boldsymbol{x}^*\}$, then $\boldsymbol{x}^*$ is unstable.*

The power of Lyapunov's direct method lies in its independence on information about solutions of a dynamical system. In other words, to establish the stability of a dynamical system, we do not require any information regarding the solutions of the system. The

[5] i.e., $V(\boldsymbol{x})$ is positive definite in $\mathcal{D}$

[6] i.e., $\dot{V}(\boldsymbol{x})$ is negative semi-definite in $\mathcal{D}$

drawback for this method, however, is that finding a Lyapunov function for a given system is, to a great extent, a hard and challenging task, in fact, often impossible.

The following theorem can be regarded as an extension of Theorem 2.3.10, and can be used to prove asymptotic stability of system (2.5) if a Lyapunov function satisfying condition (i) in Theorem 2.3.10 exists.

Theorem 2.3.11 (LaSalle's theorem [46])**.** *Consider the nonlinear autonomous dynamical system* (2.5) *and let*

(i) $\boldsymbol{\Omega} \subset \mathcal{D} \subset \mathbb{R}^n$ *be a compact positively invariant set with respect to* (2.5)*,*

(ii) $V : \mathcal{D} \longrightarrow \mathbb{R}$ *be a continuously differentiable function such that* $\dot{V}(\boldsymbol{x}) \leq 0 \ \ \forall\, \boldsymbol{x} \in \boldsymbol{\Omega}$*,*

(iii) $E \subset \boldsymbol{\Omega}$ *be the set of all points in* $\boldsymbol{\Omega}$ *where* $\dot{V}(\boldsymbol{x}) = 0$*,*

(iv) $\mathcal{M} \subset E$ *be the largest invariant set in* E*.*

Then every solution starting in $\boldsymbol{\Omega}$ *approaches* $\mathcal{M}$ *as* $t \to \infty$*.*

Corollary 2.3.12 (Barbashin-Krasovskii's theorem [46])**.** *Let* $\boldsymbol{x}^* = \mathbf{0}$ *be an equilibrium solution for* (2.5)*. Let* $V : \mathcal{D} \longrightarrow \mathbb{R}$ *be a continuously differentiable function on a domain* $\mathcal{D}$ *containing the origin* $\boldsymbol{x}^* = \mathbf{0}$*, such that*

(i) $V(\mathbf{0}) = 0$ *and* $V(\boldsymbol{x}) > 0, \quad \forall\, \boldsymbol{x} \neq \mathbf{0}$*,*

(ii) $\dot{V}(\boldsymbol{x}) \leq 0, \quad \forall\, \boldsymbol{x} \in \mathcal{D}$*.*

Let $\mathcal{S} = \left\{ \boldsymbol{x} \in \mathcal{D} : \ \dot{V}(\boldsymbol{x}) = 0 \right\}$ *and suppose that no solution can stay identically in* $\mathcal{S}$*, other than the trivial solution,* $\boldsymbol{x}(t) \equiv \mathbf{0}$*. Then, the origin is locally asymptotically stable.*

In order to state the next result on the global stability of an equilibrium solution using Lyapunov's direct method, we need the following definition.

Definition 2.3.13. [46] *A real function* $V : \mathbb{R}^n \longrightarrow \mathbb{R}$ *is said to be* ***radially unbounded*** *if* $\lim\limits_{||\boldsymbol{x}|| \to \infty} V(\boldsymbol{x}) = \infty$*.*

Remark. If, in addition to the hypothesis of Corollary 2.3.12, $V(\boldsymbol{x})$ is radially unbounded, then the origin is globally asymptotically stable.

Theorem 2.3.14 (Barbashin-Krasovskii's theorem [46]). *Let $\boldsymbol{x}^* = \mathbf{0}$ be an equilibrium solution for* (2.5). *Let $V : \mathbb{R}^n \longrightarrow \mathbb{R}$ be a continuously differentiable, radially unbounded function such that*

(i) $V(\mathbf{0}) = 0 \quad$ *and* $V(\boldsymbol{x}) > 0, \quad \forall\, \boldsymbol{x} \neq \mathbf{0}$,

(ii) $\dot{V}(\boldsymbol{x}) < 0, \quad \forall\, \boldsymbol{x} \neq \mathbf{0}$.[7]

Then, $\boldsymbol{x}^* = \mathbf{0}$ is globally asymptotically stable.

2.3.4 Comparison principle

The comparison theorem is a powerful tool for analyzing the stability of solutions of dynamical systems. As the name suggests, comparison theorem compares the unknown solutions of one differential equation (or differential inequality) with known behaviour of another differential equation [10]. A scalar version of the comparison theorem is presented.

Theorem 2.3.15 (Comparison theorem [10, 70]). *Let $f : \mathbb{R} \times \mathbb{R} \longrightarrow \mathbb{R}$ satisfy a Lipschitz condition* (2.3) *for $t \geq t_0$. If the continuous function $x(t)$ satisfies the differential inequality*

$$\dot{x}(t) \leq f(x(t), t),$$

for $t \geq t_0$, and if $v(t)$ is a solution of the differential equation

$$\dot{v}(t) = f(v(t), t)$$

satisfying the initial condition

$$v(t_0) = x(t_0),$$

then

$$x(t) \leq v(t)$$

for $t \geq t_0$.

[7] i.e., $\dot{V}(\boldsymbol{x})$ is negative definite in $\mathbb{R}^n$

The generalization of Theorem 2.3.15 requires a few more details, which can be found in, for example, [50, 57, 70]. The comparison theorem allows one to replace the difficult problem of analyzing a given dynamical system $\dot{\boldsymbol{x}}_1 = \boldsymbol{f}_1(\boldsymbol{x}_1, t)$, say, by the comparatively simple problem of analyzing another dynamical system $\dot{\boldsymbol{x}}_2 = \boldsymbol{f}_2(\boldsymbol{x}_2, t)$, provided it is known that

- $\boldsymbol{f}_1(\boldsymbol{y}, t) \leq \boldsymbol{f}_2(\boldsymbol{y}, t)$ (componentwise),
- $\boldsymbol{x}_1(0) \leq \boldsymbol{x}_2(0)$, and
- $\boldsymbol{f}_2$ is quasi-monotone nondecreasing (or more generally, quasi-monotone).

When these conditions are satisfied, the conclusion is that the solutions $\boldsymbol{x}_1(t)$ of $\boldsymbol{f}_1$ are bounded by the solutions $\boldsymbol{x}_2(t)$ of $\boldsymbol{f}_2$ for all $t \geq 0$ for which both solutions are defined, thus the qualitative behaviour of the former system is inferred from the latter (see [57] pp. 140).

2.4 Special case: planar dynamical systems

In this section, we present a few results that are special to the two-dimensional system. Consider the nonlinear autonomous planar dynamical system

$$\begin{aligned} \dot{x} &= f_1(x, y) \\ \dot{y} &= f_2(x, y) \\ x(0) &= x_0, \qquad y(0) = y_0 \end{aligned} \tag{2.11}$$

where $(x, y) \in \mathcal{A} \subset \mathbb{R}^2$, f_1 and f_2 are real-valued, continuously differentiable functions on $\mathcal{A}$, and $\boldsymbol{F} = (f_1, f_2) : \mathcal{A} \longrightarrow \mathbb{R}^2$ is a continuous vector field. Assume that at each point $(x, y) \in \mathcal{A}$, sufficient conditions for existence and uniqueness of the solutions of (2.11) are fulfilled[8].

[8] see Theorems 2.2.4 and 2.2.8

Definition 2.4.1. *A solution* $(x(t), y(t)) \in \mathcal{A} \subset \mathbb{R}^2$ *of system* (2.11) *is called a* ***closed orbit*** *or a* ***periodic solution****, if for a fixed* $\tau > 0$*,*

$$(x(t), y(t)) = (x(t+\tau), y(t+\tau)), \quad \forall\, t. \tag{2.12}$$

The smallest such number τ *satisfying* (2.12) *is called the* **period**.

The trajectory of a periodic solution is either a simple closed curve or, in the case of constant (trivial) solutions, a single point − the equilibrium point.
A limit cycle of (2.11) is a periodic solution of (2.11) with the additional property that it is isolated, in the sense that any neighbouring trajectory of the limit cycle is not closed, they spiral either towards or away from the limit cycle.

Definition 2.4.2. [33] *A* ***limit cycle*** *is a closed orbit* $\boldsymbol{\Gamma}$ *for which there exists at least one* $\boldsymbol{z} \notin \boldsymbol{\Gamma}$ *such that either* $\boldsymbol{\Gamma}$ *is the* ω*-limit set of* $\boldsymbol{z}$*, or* $\boldsymbol{\Gamma}$ *is the* α*-limit set of* $\boldsymbol{z}$*. In the first case,* $\boldsymbol{\Gamma}$ *is called an* ω*-limit cycle; in the second case, an* α*-limit cycle.*

We now present the celebrated Poincaré-Bendixson's theorem for planar systems, which says that every bounded solution must either be an equilibrium solution, a closed orbit, or the solution must approach one of these in forwards and backwards time.

Theorem 2.4.3 (Poincaré-Bendixson's theorem [33])**.** *A non-empty compact limit set of a continuously differentiable planar dynamical system, which contains no equilibrium point, is a closed orbit.*

According to Theorem 2.4.3, if a trajectory enters and does not leave a compact region of phase space, and this region contains no equilibria, then the trajectory must approach a periodic orbit as $t \to \infty$. An alternative form of Theorem 2.4.3 is stated:

Corollary 2.4.4 (Poincaré-Bendixson's theorem [17])**.** *Let* $\mathcal{A}$ *be a positively invariant region for the vector field* $\boldsymbol{F}$ *of* (2.11)*, where* $\boldsymbol{F} \in C^1$*. If* $\mathcal{A}$ *is compact, then* $\mathcal{A}$ *contains either a closed orbit or an equilibrium point.*

Recall that a curve $\mathcal{C} \in \mathbb{R}^2$ is called *simple* if it does not intersect itself.

Definition 2.4.5. *A region $\mathcal{A}$ is said to be **simply connected** if for any simple closed curve $\mathcal{C}$ lying entirely within $\mathcal{A}$, all points inside $\mathcal{C}$ are points of $\mathcal{A}$.*

The following theorem provides us a technique for excluding periodic orbits in planar dynamical systems.

Theorem 2.4.6 (Dulac's criterion [65])**.** *Let $\boldsymbol{F} \in C^1(\mathcal{A})$ where $\mathcal{A}$ is a simply connected region in $\mathbb{R}^2$. If there exists a function $B(x, y) \in C^1(\mathcal{A})$ such that the divergence of $B\boldsymbol{F}$; namely $\nabla \cdot (B\boldsymbol{F}) = \frac{\partial (Bf_1)}{\partial x} + \frac{\partial (Bf_2)}{\partial y}$, is not identically zero and does not change sign in $\mathcal{A}$, then there are no closed orbits of* (2.11) *contained entirely in $\mathcal{A}$.*

Remarks.

1. In Theorem 2.4.6, by "does not change sign," we mean that the quantity is entirely negative or entirely positive on $\mathcal{A}$.

2. The function $B(x, y)$ in Theorem 2.4.6 is called a *Dulac function* for $\boldsymbol{F}$ in the region $\mathcal{A}$. When $B(x, y) \equiv 1$, Theorem 2.4.6 is called Bendixson's criterion (Theorem 2.4.7), which rules out the possibility of closed orbits.

Theorem 2.4.7 (Bendixson's criterion [65])**.** *Let $\boldsymbol{F} \in C^1(\mathcal{A})$ where $\mathcal{A}$ is a simply connected region in $\mathbb{R}^2$. If the divergence of the vector field $\boldsymbol{F}$, $\nabla \cdot \boldsymbol{F} = \frac{\partial f_1}{\partial x} + \frac{\partial f_2}{\partial y}$, is not identically zero and does not change sign in $\mathcal{A}$, then* (2.11) *has no nontrivial closed orbit lying entirely in $\mathcal{A}$.*

Recall that from Theorem 2.3.8 we remarked that for a planar dynamical system, a hyperbolic equilibrium point is asymptotically stable, iff the trace and the determinant of the Jacobian evaluated at the equilibrium solution are negative and positive, respectively. Notice that the expression $\nabla \cdot \boldsymbol{F}$ in Theorem 2.4.7 is nothing new but the trace of the Jacobian matrix of (2.11). Thus, if $\nabla \cdot \boldsymbol{F}$ does not change sign on $\mathcal{A}$, then this suggests that if (x^*, y^*) is the only equilibrium solution of (2.11), then (x^*, y^*) is everywhere

asymptotically stable or everywhere unstable on $\mathcal{A}$, in this case ruling out the possibility of closed orbit in $\mathcal{A}$. Hence the Bendixson's criterion.

2.5 Qualitative stability analysis

In this section, we present a method of examining the stability of an equilibrium solution of a dynamical system when the entries of the linearization (Jacobian) matrix are specified in terms of sign values; that is, the entries of the Jacobian matrix are elements of the set $\{+, -, 0\}$. The idea of qualitative stability has some rather interesting applications in such areas as ecology [56] and economics [66].

Definition 2.5.1. *A matrix $\mathbf{A} \in M_n(\mathbb{R})$ is said to be* **stable** *if and only if each eigenvalue of $\mathbf{A}$ has a negative real part.*

Definition 2.5.2. *A* ***sign pattern matrix*** *is a matrix $\mathbf{B} = (b_{ij})$ whose entries b_{ij} are elements of the set $\{+, -, 0\}$.*

Given a matrix $\mathbf{A} \in M_{mn}(\mathbb{R})$, the sign pattern matrix of $\mathbf{A}$ is the matrix $\operatorname{sgn}(\mathbf{A}) = (\operatorname{sgn}(a_{ij}))$, where

$$\operatorname{sgn}(a_{ij}) = \begin{cases} -, & \text{if } a_{ij} < 0 \\ 0, & \text{if } a_{ij} = 0 \\ +, & \text{if } a_{ij} > 0 \end{cases}$$

Example.

$$\text{If} \quad \mathbf{A} = \begin{bmatrix} 1 & -1 & 0 \\ 0 & 1 & -2 \\ -2 & 0 & -4 \end{bmatrix}, \quad \text{then} \qquad \operatorname{sgn}(\mathbf{A}) = \begin{bmatrix} + & - & 0 \\ 0 & + & - \\ - & 0 & - \end{bmatrix}$$

Definition 2.5.3. *Let $\mathbf{A} = (a_{ij})$ be an $n \times n$ sign pattern matrix. The set of all matrices $\mathbf{B} \in M_n(\mathbb{R})$ with the same sign pattern as $\mathbf{A}$ is called the* **sign pattern class** (*or* **qualitative class**) *of $\mathbf{A}$, and is denoted by $Q(\mathbf{A})$; that is,*

$$Q(\mathbf{A}) = \{\mathbf{B} = (b_{ij}) \in M_n(\mathbb{R}) : \operatorname{sgn}(b_{ij}) = a_{ij}, \quad \forall\, i, j = 1, \cdots, n\}$$

Qualitative (or sign) stability of matrices is motivated by the following question: Are all the matrices formed by randomly changing the magnitude (but not the sign) of the nonzero entries a_{ij} of a stable matrix $\mathbf{A} \in M_n(\mathbb{R})$ stable in the sense of definition 2.5.1?

Definition 2.5.4. *A matrix* $\mathbf{A} \in M_n(\mathbb{R})$ *is said to be* **sign stable** (*or* **qualitatively stable**) *if* $\mathbf{B}$ *is stable for every* $\mathbf{B} \in Q(\mathbf{A})$.

The following theorem, due to Quirk & Ruppert [66], gives the necessary conditions for qualitative stability of a real square matrix.

Theorem 2.5.5 (Necessary conditions for qualitative stability [66])**.** *Let* $\mathbf{A} = (a_{ij}) \in M_n(\mathbb{R})$. *Then the following conditions are necessary for qualitative stability of* $\mathbf{A}$.

M1 $a_{ii} \leq 0$ *for all* i.

M2 $a_{ii} < 0$ *for at least one* i.

M3 $a_{ij}a_{ji} \leq 0$ *for all* $i \neq j$.

M4 $a_{ij}a_{jk} \cdots a_{qr}a_{ri} = 0$ *for any sequence of* 3 *or more distinct indices* $i, j, \cdots, q, r$.

M5 $\mathbf{A}$ *is nonsingular.*

We remark that Theorem 2.5.5 gives necessary but not sufficient conditions for qualitative stability. By introducing the so-called 'colour test', Jeffries [40] formulated the necessary and sufficient conditions for qualitative stability of a real square matrix.

Definition 2.5.6. *A directed graph* (*or a* ***digraph***) *is a pair* $\mathcal{D} = \mathcal{D}(\mathcal{N}, \mathcal{A})$, *where* $\mathcal{N}$ *is a finite set of* ***nodes*** (*or vertices*) *and* $\mathcal{A} \subseteq \mathcal{N} \times \mathcal{N}$ *is a finite set of* ***directed edges*** (*or arcs*) *between the nodes.*

An arc $a \in \mathcal{A}$ from node n_i to node n_j, $n_i, n_j \in \mathcal{N}$, is represented by a tuple (n_i, n_j). We then call n_i the **initial node** (or head) of a and n_j the **terminal node** (or tail) of a. A **signed digraph** is a digraph in which each directed arc has a plus (+) or minus (−) sign associated with it.

Definition 2.5.7. *A digraph $\mathcal{D}' = (\mathcal{N}', \mathcal{A}')$ is a **subgraph** of a digraph $\mathcal{D} = (\mathcal{N}, \mathcal{A})$ if $\mathcal{N}' \subseteq \mathcal{N}$ and $\mathcal{A}' \subseteq \mathcal{A}$.*

Definition 2.5.8. [40] *A **predation link** in a signed digraph is a pair of nodes connected by one arc with a $+$ sign and another arc with a $-$ sign.*

Definition 2.5.9. [40] *A* **predation community** *is a subgraph consisting of all interconnected predation links.*

Colour test [40]

A predation community passes the colour test provided each node in the associated digraph may be coloured black or white with the result that

C1 Each self-regulating node is black;

C2 There is at least one white node;

C3 Each white node is connected by a predation link to at least one other white node;

C4 Each black node connected by a predation link to one white node, is connected by a predation link to at least one other white node.

A predation community fails the colour test if at least one of the conditions **C1** - **C4** fails.

Theorem 2.5.10 (Necessary and sufficient conditions for qualitative stability [40, 66])**.** *A matrix $\mathbf{A} = (a_{ij}) \in M_n(\mathbb{R})$ is qualitatively stable if and only if it satisfies the following conditions:*

M1 $a_{ii} \leq 0$ *for all* i.

M2′ *Each predation community in the digraph associated with* $\mathbf{A}$ *fails the colour test.*

M3 $a_{ij}a_{ji} \leq 0$ *for all* $i \neq j$.

M4 $a_{ij}a_{jk} \cdots a_{qr}a_{ri} = 0$ *for any sequence of* 3 *or more distinct indices* $i, j, \cdots, q, r$.

M5 **A** *is nonsingular.*

Matrices that are qualitatively stable are necessarily stable in the ordinary sense. In other words, if in system (2.6), $\mathbf{J}^*$ is qualitatively stable, then each eigenvalue of $\mathbf{J}^*$ has a negative real part and, by Theorem 2.3.8, the equilibrium solution $\boldsymbol{x}^*$ of system (2.5), is locally asymptotically stable. However, if $\mathbf{J}^*$ is not qualitatively stable, it does not necessarily mean that $\mathbf{J}^*$ is unstable. Rather, a detailed knowledge of the actual magnitudes of the elements of $\mathbf{J}^*$ (instead of merely their signs) is needed [56].

2.6 Sensitivity analysis

Virtually all physical/biological processes, are governed by a set of rules, such as chemical reactions, conservation of mass, and mass action law. A mathematical model of such a process necessarily contain physical parameters that make the model specific to the process system of interest. When analyzing a mathematical model, therefore, computation of model solutions offers limited insight into the ensemble dynamics of the system. It is hence important to determine systematically the influence of parameter variations on the model solutions. Sensitivity analysis involves the use of analytical and/or computational tools to evaluate the changes in the output of a dynamical system in response to specified changes in the system's input parameters.

Sensitivity analysis can be divided into two categories; *local* and *global* sensitivity analysis. Local sensitivity analysis focuses on the estimates of the model sensitivity to parameter variation in the neighbourhood of a certain parameter value. Global sensitivity analysis, on the other hand, is concerned with the whole set of parameters and aims to describe how the output varies in response to parameter variations within the whole parameter space.

There are several local sensitivity analysis techniques in the literature that have been developed to assess parameter importance. We discuss two of the most commonly used approaches: "*brute-force*" method and *differential sensitivity analysis*.

2.6.1 "Brute-force" approach (Indirect method)

In this method, input parameters are perturbed, one-at-a-time, and the model equations are solved anew for each new set of values of the parameters. The sensitivity coefficients (partial derivatives of the output functions with respect to the parameters) are then calculated from appropriate finite difference approximations.

Let the process of interest be described by a system of nonlinear first-order ordinary differential equations of the generic form

$$\dot{\boldsymbol{x}}(\boldsymbol{p}, t) = \boldsymbol{f}(\boldsymbol{x}(\boldsymbol{p}, t), \boldsymbol{p}, t), \tag{2.13a}$$

$$\boldsymbol{x}(\boldsymbol{p}, t_0) = \boldsymbol{x}_0(\boldsymbol{p}) \tag{2.13b}$$

where $\boldsymbol{x} \in \mathbb{R}^n$ is the vector of variables, $\boldsymbol{p} \in \mathbb{R}^m$ is the vector of parameters, $\boldsymbol{f} \in \mathbb{R}^n$ is the right-hand-side of the differential equations, and $\boldsymbol{x}_0 \in \mathbb{R}^n$ is the vector of initial values of the variables. The vectors $\boldsymbol{x}$ and $\boldsymbol{f}$ depend on the parameters $\boldsymbol{p}$.

The first-order sensitivity coefficient of the ith variable, x_i, with respect to the jth parameter, p_j, is given by

$$s_{ij} = \frac{\partial x_i(p_j, t)}{\partial p_j} \approx \lim_{\Delta p_j \to 0} \frac{x_i(p_j + \Delta p_j, t) - x_i(p_j, t)}{\Delta p_j},$$

using forward difference scheme, or

$$s_{ij} = \frac{\partial x_i(p_j, t)}{\partial p_j} \approx \lim_{\Delta p_j \to 0} \frac{x_i(p_j + \Delta p_j, t) - x_i(p_j - \Delta p_j, t)}{2\Delta p_j},$$

using centred difference scheme [75] - here, Δp_j is the perturbation value. The local sensitivity coefficients, $s_{ij}(t)$, show the effect of a small perturbation of parameter j on variable i. The brute-force method is widely used since it does not require any extra modification to be made above that needed to solve Eq. (2.13) [67, 75].

2.6.2 Differential sensitivity analysis (Direct method)

An alternative to the brute force method is to treat sensitivity coefficients themselves as dynamic variables and to develop differential equations describing their evolution.
Taking the derivatives on both sides of Eq. (2.13) with respect to $\boldsymbol{p}$, and interchanging the order of differentiation, we obtain a system of ordinary differential equations, written in compact matrix notation as

$$\dot{\mathbf{S}} = \mathbf{JS} + \mathbf{P}, \qquad \mathbf{S}(\boldsymbol{p}, t_0) = \mathbf{S}_0(\boldsymbol{p}).$$

That is,

$$\frac{d}{dt}\left[\frac{\partial \boldsymbol{x}}{\partial \boldsymbol{p}}\right] = \frac{\partial \boldsymbol{f}}{\partial \boldsymbol{x}}\frac{\partial \boldsymbol{x}}{\partial \boldsymbol{p}} + \frac{\partial \boldsymbol{f}}{\partial \boldsymbol{p}}, \qquad \frac{\partial \boldsymbol{x}(\boldsymbol{p}, t_0)}{\partial \boldsymbol{p}} = \frac{\partial \boldsymbol{x}_0(\boldsymbol{p})}{\partial \boldsymbol{p}}. \tag{2.14}$$

Here,

- $\mathbf{S}(t) = \left(s_{ij}(t)\right) = \left(\frac{\partial x_i}{\partial p_j}\right)$ is the $n \times m$ sensitivity matrix,
- $\mathbf{J} = \left(\frac{\partial f_i}{\partial x_j}\right)$ is the $n \times n$ Jacobian matrix, and
- $\mathbf{P} = \left(\frac{\partial f_i}{\partial p_j}\right)$ is the $n \times m$ matrix composed of derivatives of each of n-functions on the right-hand side in Eq. (2.13a) with respect to each of the parameters.

The initial condition for $\frac{\partial \boldsymbol{x}}{\partial \boldsymbol{p}_j}$ is the zero vector if p_j is not an initial condition, otherwise if p_j is an initial condition for the ith variable, then

$$\frac{\partial \boldsymbol{x}}{\partial \boldsymbol{p}_j} = [0 \cdots 0\ 1\ 0 \cdots 0]^T$$

where 1 is in the ith position [67].
Equations (2.13) and (2.14) are coupled through matrices $\frac{\partial \boldsymbol{f}}{\partial \boldsymbol{x}}$ and $\frac{\partial \boldsymbol{f}}{\partial \boldsymbol{p}}$; that is, Eq. (2.14) can only be solved if the variable values, to be calculated by Eq. (2.13a), are available at times where the above matrices are calculated during the numerical solution of the sensitivity Eq. (2.14) [75]. Thus, complete sensitivity analysis of system (2.13) requires solving Eqs. (2.13) and (2.14) simultaneously. This system of ordinary differential

equations has $n(m+1)$ equations. The explicit calculation and implementation of the expression appearing on the right-hand side of (2.14) can be a tedious task.
The existence of derivatives of the solution to (2.13) is given by Gronwall's theorem [29].

Theorem 2.6.1 (Gronwall's Theorem [29])**.** *If the partial derivatives* $\frac{\partial \boldsymbol{f}}{\partial \boldsymbol{x}}$ *and* $\frac{\partial \boldsymbol{f}}{\partial \boldsymbol{p}}$ *exist and are continuous in the neighbourhood of the solution* $\boldsymbol{x}(\boldsymbol{p}, \boldsymbol{x}_0(\boldsymbol{p}), t)$*, then the derivatives of the solution with respect to* $\boldsymbol{p}$ *exist, are continuous, and satisfy the linear inhomogeneous matrix differential equation* (2.14)*.*

2.6.3 Normalization of sensitivity

The sensitivity coefficient $s_{ij} = \frac{\partial x_i}{\partial p_j}$ is of limited applicability in its original form due to its dependence on the physical units of variables and parameters in the model. The parameters and the variables of model (2.13) may have different physical units. To separate the sensitivity results from the units of the model, the usual solution is to introduce normalized sensitivity coefficients. These coefficients form the normalized sensitivity matrix $\bar{\mathbf{S}}$, whose ijth element is given by

$$\bar{s}_{ij} = \frac{p_j}{x_i}\frac{\partial x_i}{\partial p_j} = \frac{\partial \ln x_i}{\partial \ln p_j}$$

The normalized sensitivity coefficients $\bar{s}_{ij}$ are now dimensionless real numbers that represent the fractional change in variable x_i caused by a fractional change of parameter p_j. $\bar{s}_{ij}$ could be either positive or negative.
The sensitivity coefficients can be interpreted as the ratio between the change in the process behaviour and the perturbation in the parameter that causes this change. A low sensitivity magnitude with respect to a parameter indicates a robust behaviour in which variations in this parameter have little effect on the output. On the other hand, a large sensitivity magnitude means that variations in the parameter are increased, causing large output changes.

Chapter 3

A review of previous works on microtubule dynamics modelling

Several mathematical models addressing different aspects of the microtubule behaviour have been developed over the years. In this chapter, we review some of the models that have been proposed in an attempt to capture the dynamic nature of microtubules.

3.1 Introduction

Numerous mathematical models have been developed over the last two decades to describe the process of microtubule dynamics. We review five categories of models:

(i) those that use the classical chemical kinetics approach,

(ii) those that use the chemical master equation approach,

(iii) those that use the mechanical approach,

(iv) those that use the cellular automata modelling approach, and

(v) those that use the agent-based modelling approach.

In our modelling later on, we will be adopting the chemical kinetics approach. The master equation approach is closely related to the chemical kinetics approach, save for the fact

that the former is stochastic while the latter is deterministic. In our review, therefore, we will detail these two approaches, with a view to providing the necessary background for our work.

3.2 Chemical kinetics approach

In the chemical kinetics approach, the variables of interest are the concentrations of individual proteins within an ensemble of microtubules. The reaction rates in the model are governed by the *mass action law*, which states that for a reaction in a homogeneous system, the reaction rate is proportional to the concentrations of the individual reactants involved. Thus, for example, if A and B react irreversibly at a rate constant k_1 to produce C, then the rate of change of the concentration of C would be

$$\frac{d[C]}{dt} = k_1[A][B]$$

where $[x]$ denotes the concentration of x. Thus, in the chemical kinetics approach, the models consist of a system of coupled first-order ordinary differential equations. This approach is deterministic, in the sense that given a set of initial conditions, the model can estimate what happens to the system in the future. Sept *et al.* [69], for example, developed a chemical kinetics model for microtubule dynamics with a focus on microtubule oscillations. The model is based on the following reactions:

(i) **Nucleation** – n_c GTP-tubulin dimers, T aggregate at a rate constant k_n to form a nucleus (seed) of length n_c.

$$n_c T \xrightarrow{k_n} M_{n_c}$$

(ii) **Growth** – a GTP-tubulin dimer adds to a microtubule of length n at a rate constant k_g to produce a microtubule of length $n+1$.

$$M_n + T \xrightarrow{k_g} M_{n+1}$$

(iii) **Decay** – a microtubule of length n decays at a rate constant k_d, forming n GDP-tubulin dimers.

$$M \xrightarrow{k_d} nD$$

(iv) **Conversion** – GDP-tubulin dimers are converted to GTP-tubulin dimers at a rate constant k_c.

$$D \xrightarrow{k_c} T$$

These reactions give rise to the following system of ordinary differential equations.

$$\dot{C}_t = -k_n C_t - k_g M C_t + k_c C_d \tag{3.1a}$$

$$\dot{C}_d = k_d C_a - k_c C_d \tag{3.1b}$$

$$\dot{C}_a = k_n C_t + k_g M C_t - k_d C_a \tag{3.1c}$$

$$\dot{M} = k_n C_t - k_d M \tag{3.1d}$$

System (3.1) gives the time evolution of GTP-tubulin dimers, C_t, GDP-tubulin dimers C_d, assembled tubulin, C_a, and microtubules, M. In this model, it is assumed that all the variables depend only on time. It is further assumed that $n_c = 1$, and that a microtubule completely decays. The latter assumption is rather too strong though.

The authors demonstrate that for system (3.1) to exhibit an oscillatory behaviour, an extra reaction in addition to the above four reactions must be added. This observation had earlier been made by Marx & Mandelkow [54]. Sept *et al.* [69] chose microtubule decay induced by excess GDP-tubulin dimers to produce oscillations:

$$M_n + D \xrightarrow{k_d^*} (n+1)D$$

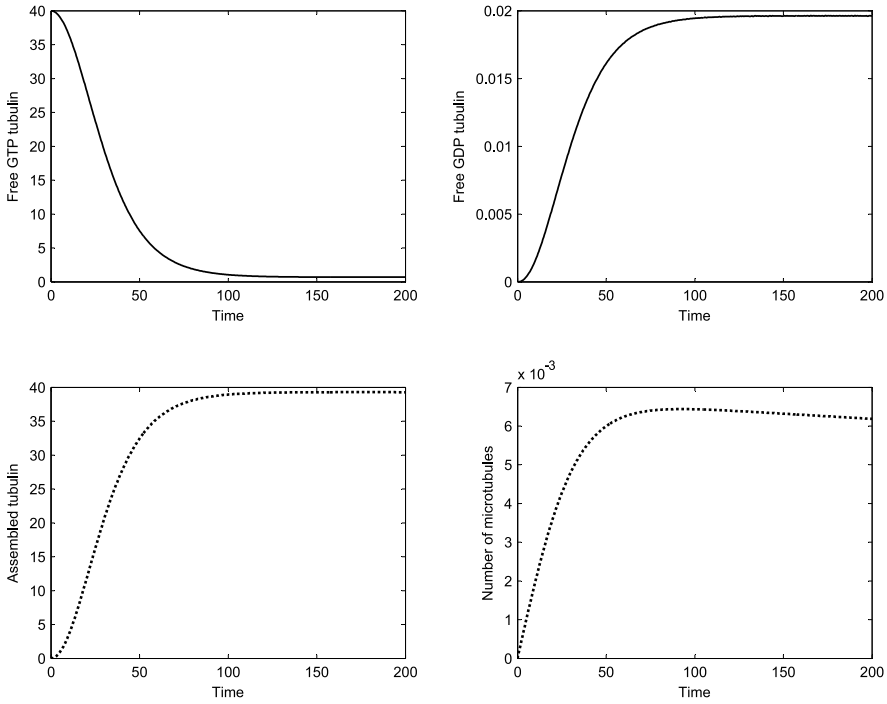

Figure 3.1: Solutions for C_t, C_d, C_a and M for model (3.1). Simulations were performed for initial tubulin concentration of $c = 40\mu M$ and at temperature 37^oC [69].

After adding this reaction, system (3.1) becomes

$$\dot{C}_t = -k_g M C_t - k_n C_t + k_c C_d \tag{3.2a}$$

$$\dot{C}_d = k_d C_a - k_c C_d + k_d^* C_a C_d \tag{3.2b}$$

$$\dot{C}_a = k_g M C_t - k_d C_a + k_n C_t - k_d^* C_a C_d \tag{3.2c}$$

$$\dot{M} = -k_d M + k_n C_t - k_d^* M C_d \tag{3.2d}$$

Sept [68] extended system (3.2) by incorporating spatial dependence.

$$\dot{C}_t = -k_g M C_t - n_c k_n C_t^{n_c} + k_c C_d + D_0 \nabla^2 C_t, \tag{3.3a}$$

$$\dot{C}_d = k_d C_a - k_c C_d + k_d^* C_a C_d + D_0 \nabla^2 C_d, \tag{3.3b}$$

$$\dot{C}_a = k_g M C_t - k_d C_a + k_n C_t^{n_c} - k_d^* C_a C_d, \tag{3.3c}$$

$$\dot{M} = -k_d M + k_n C_t - k_d^* M C_d, \tag{3.3d}$$

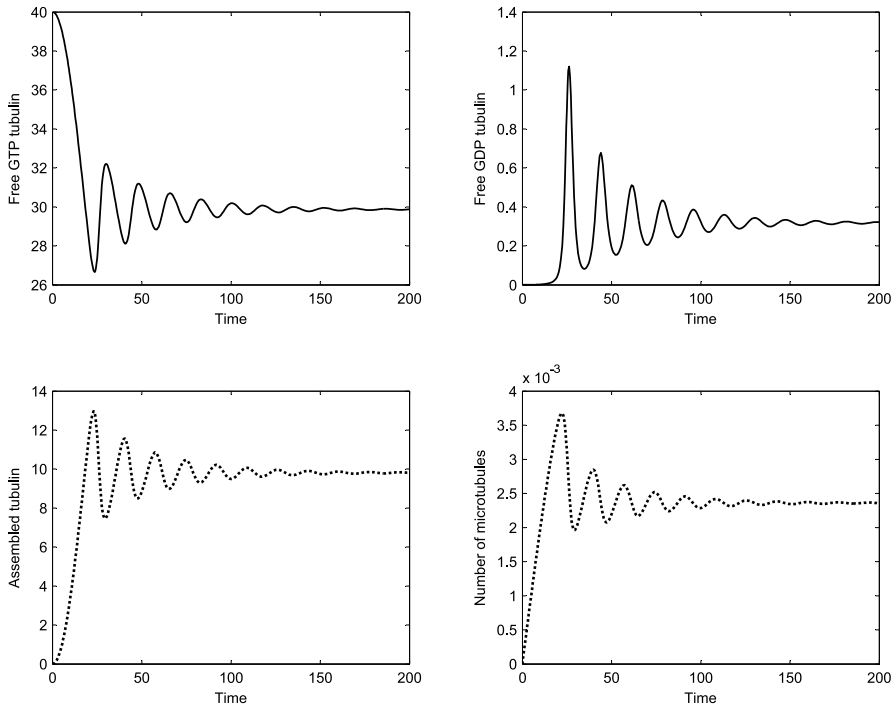

Figure 3.2: Solutions for C_t, C_d, C_a and M for model (3.2). Simulations were performed for initial tubulin concentration of $c = 40\mu M$ and at temperature 37^oC [69].

where D_0 is the diffusion coefficient, assumed same for all the tubulin dimers. Simulation results of the reaction-diffusion model (3.3) show that microtubule oscillations can be produced in both space and time. Qualitatively similar results to those in [69] are produced. Another model using the chemical kinetics approach is [54].

3.3 Master equation approach

In the master equation formalism, the chemical reactions in the microtubule dynamics are treated as random processes, based on the premise that it is impossible to say with complete certainty the state of an ensemble of microtubules at a future time. Stochastic dynamic models are thus developed to describe the evolution of the probability distribution $P(i,t)$, characterizing the system in the ith state at time t. The probability distribution is essentially the difference between the transition probabilities for the processes entering a given state and the processes leaving the state:

$$\frac{dP(i,t)}{dt} = \begin{bmatrix}\text{transition probabilities for the}\\ \text{processes leading into state } i\end{bmatrix} - \begin{bmatrix}\text{transition probabilities for the}\\ \text{processes leading out of state } i\end{bmatrix}$$

For example, Dogterom & Leibler [19] used the master equation approach to develop a two-state model for individual microtubules. Denoting the probability density for finding at time t a microtubule end in the growing (shrinking) state with a length between l and $l + dl$ by $P_g(l,t)$ ($P_s(l,t)$), they proposed the following model for the time evolution of the probability distributions of the microtubule ends:

$$\frac{\partial P_g(l,t)}{\partial t} = k_{\text{res}} P_s(l,t) - k_{\text{cat}} P_g(l,t) - k_g \frac{\partial P_g(l,t)}{\partial l}, \tag{3.4a}$$

$$\frac{\partial P_s(l,t)}{\partial t} = k_{\text{cat}} P_g(l,t) - k_{\text{res}} P_s(l,t) + k_s \frac{\partial P_s(l,t)}{\partial l}, \tag{3.4b}$$

where

- k_{cat} is the catastrophe frequency; that is, the rate at which a microtubule end switches from a growing to a shrinking state,
- k_{res} is the rescue frequency; that is, the rate at which a microtubule end switches from a shrinking to a growing state,
- k_g is the assembly rate, and
- k_s is the disassembly rate.

Dogterom and co-workers [20] extended Eqns. (3.4) further by considering the dynamics of the population of GDP- and GTP-tubulin dimers:

$$\begin{aligned}
\frac{\partial P_g(l,t)}{\partial t} &= k_{\text{res}} P_s(l,t) - k_{\text{cat}} P_g(l,t) - k_g \frac{\partial P_g(l,t)}{\partial l}, \\
\frac{\partial P_s(l,t)}{\partial t} &= k_{\text{cat}} P_g(l,t) - k_{\text{res}} P_s(l,t) + k_s \frac{\partial P_s(l,t)}{\partial l}, \\
\frac{\partial C_t(l,t)}{\partial t} &= k_c C_d(l,t) - k_g s_0 \left(\frac{L^2}{l^2}\right) P_g(l,t) + D\nabla^2 C_t(l,t), \\
\frac{\partial C_d(l,t)}{\partial t} &= -k_c C_d(l,t) + k_s s_0 \left(\frac{L^2}{l^2}\right) P_s(l,t) + D\nabla^2 C_d(l,t),
\end{aligned}$$

where $C_d(l,t)$ and $C_t(l,t)$ are the concentrations of GDP- and GTP-tubulin dimers, respectively, D is the diffusion coefficient, k_c is a rate at which GTP-tubulin dimers are regenerated from the GDP-tubulin dimers, L is the radius of the centrosome[1], and s_0, $0 \leq s_0 \leq 1$, is the total surface density of nucleation sites (that is, the fraction of the centrosome area capable of microtubule nucleation).

[1]The centrosome is the main microtubule organizing centre in the cell.

Antal *et al.* [3] also use the master equation approach to describe microtubule dynamics. Their model includes the following equations:

$$\frac{dP(n,t)}{dt} = -(n+k_g)P(n,t) + k_g P(n-1,t) + (n+1)P(n+1,t), \tag{3.5}$$

$$\frac{dP(l,t)}{dt} = k_g\big[P(l-1,t) - P(l,t)\big], \tag{3.6}$$

$$\frac{dP(l,n,t)}{dt} = k_g P(l-1,n-1,t) - (n+k_g)P(l,n,t) + (n+1)P(l,n+1,t), \tag{3.7}$$

$$\frac{dP(r,t)}{dt} = k_g\big[P(r-1,t) - P(r,t)\big] - rP(r,t) + \sum_{s\geq r+1} P(s,t). \tag{3.8}$$

Equation (3.5) gives the probability distribution $P(n,t)$ for a microtubule with n GTP-tubulin dimers at time t, taking into account two processes; namely, microtubule elongation at a rate constant k_g, and conversion of GTP-tubulin dimers to GDP-tubulin dimers at a rate 1. Equation (3.6), on the other hand gives the length distribution $P(l,t)$ for the microtubule. The joint probability distribution, $P(l,n,t)$, for a microtubule of length l containing n GTP-tubulin dimers at time t is given by Eq. (3.7). Finally, Eq. (3.8) gives the probability distribution, $P(r,t)$, for a microtubule GTP-tubulin cap of length r at time t.

In Eq. (3.5), the conversion events from GTP-tubulin dimers to GDP-tubulin dimers occur with total rate n. Using the generating function method (see [4] for details), the solution to Eq. (3.5) can be shown to be the Poisson distribution

$$P(n,t) = \frac{[k_g(1-e^{-t})]^n}{n!} e^{-k_g(1-e^{-t})},$$

giving the mean number of GTP-tubulin dimers and its variance as

$$\langle n\rangle = k_g(1-e^{-t}), \quad \langle n^2\rangle - \langle n\rangle^2 = k_g(1-e^{-t}).$$

For the initial condition $P(l,0) = \delta_{l,0}$, the solution to (3.6) is again the Poisson distribution

$$P(l,t) = \frac{(k_g t)^l}{l!} e^{-k_g t},$$

whose mean and variance are given as

$$\langle\, l\,\rangle = k_g t, \quad \langle\, l^2\,\rangle - \langle\, l\,\rangle^2 = k_g t.$$

Thus the growth rate of the microtubule and the diffusion coefficient of the microtubule end are, respectively, k_g and $\frac{k_g}{2}$ [3, 4].

From Eq. (3.8), the GTP-tubulin cap length distribution is shown [4] to be

$$P(r,t) = \frac{\Gamma(1+k_g)}{\Gamma(2+k_g+r)}(r+1)(k_g)^r, \tag{3.9}$$

where $\Gamma(k) = (k-1)!, \quad k \in \mathbb{Z}^+$. From Eq. (3.9), the average GTP-tubulin cap length approaches $\sqrt{\frac{\pi k_g}{2}}$ as $k_g \to \infty$ [4], implying that even though the average number of GTP-tubulin dimers equals k_g, only $\sqrt{k_g}$ of them organize themselves into the microtubule GTP cap [3]. Other microtubule dynamics models adopting the master equation approach include [11, 12, 45]. In [45], microtubule dynamics is considered in a detailed one-dimensional approximation in a region of section S and length L. The model considers three populations; namely, GTP-tubulin, GDP-tubulin and the plus end of a microtubule.

3.4 Mechanical approach

To fulfill their role in various cellular functions, microtubules possess certain mechanical properties. In a bid to understand these properties, a number of mechanical models have been developed. These models make use of the existing experimental data and the increasing knowledge on the interactions between the tubulin molecules and the elastic properties of microtubule protofilaments. For example, Jánosi and co-workers [38] developed an 'elastic sheet model' of microtubule wall material. This model reproduced various microtubule morphologies, yielding estimates on longitudinal and lateral bond strengths and intrinsic curvatures. The model also addressed the elastic properties of microtubule ends, and provided insight into the intrinsic metastability of growing microtubules.

VanBuren *et al.* [78] developed a mechanical model of microtubule assembly dynamics to estimate tubulin-tubulin bond energies, mechanical energy stored in the lattice, and the size of the GTP-tubulin cap at the microtubule tips. Using the model, the authors

were able to estimate important mechanical parameters such as the flexural rigidity[2] of tubulin subunits and important thermodynamic parameters such as the free energy of the interactions of tubulin dimers. The authors also confirmed that the longitudinal bonds between tubulin dimers along protofilaments are much stronger than the lateral bonds between adjacent protofilaments. Computer simulations of the model provided a framework for assessing the influence of mechanical properties of microtubules and tubulin dimers on dynamic instability. The microtubule dynamic instability generated by the model has rates and transition frequencies (catastrophe and rescue) that are similar to those measured experimentally.

The mechanochemical model by VanBuren *et al.* [79] incorporated the three-dimensional nature of tubulin building blocks. The model incorporated mechanical stress and strain within the microtubule lattice, relating conformational changes in tubulin dimers to the standard Gibbs free energy of the noncovalent interactions of tubulin molecules. Computer simulations of the model reproduced the growing and shrinking phases of microtubules. The model also recapitulated the three-dimensional microtubule-end structures and rates of assembly and disassembly for microtubules grown under standard conditions. The authors established that sheet-like microtubule ends are more likely to undergo catastrophe than blunt ends.

Designed to understand the process of dynamic instability, the model by Molodtsov *et al.* uses the structural and biochemical properties of tubulin to predict the shape and stability of microtubules [59]. This model provides a link between the biophysical characteristics of tubulin and the physiological behaviour of microtubules. Using the model, the authors confirmed the hypothesis of the 'GTP-cap model' of dynamic instability [18, 48, 58]; namely, a microtubule with a GTP-tubulin cap is stable.

Other examples of mechanical-based modelling of microtubule dynamics include [37, 60, 76, 83].

[2]Flexural rigidity is the resistance of a structure to bending forces.

3.5 Cellular automata (CA) modelling approach

A cellular automaton is a discrete dynamical system - the space, time and states of the system are discrete. Thus, in cellular automata (CA) modelling approach, the physical system is idealized as a regular (discrete) lattice [1, 74], whose points (called *cells*) can take a finite set of values. The configuration of the system at a given time step is governed by a set of rules. A formal definition of a cellular automaton is given in [64] as follows:

Definition 3.5.1. *A cellular automaton is a 4-tuple* $\left(L, \Sigma, N, f\right)$ *consisting of an n-dimensional lattice of cells indexed by integers,* $L = \mathbb{Z}^n$*, a finite set* Σ *of cell states, a finite neighbourhood scheme* $N \subseteq \mathbb{Z}^n$*, and a local transition function* $f : \Sigma^N \longrightarrow \Sigma$*.*

Ermentrout & Edelstein-Keshet [25] divide the CA models into three classes;

(i) deterministic (or Eulerian) automata,

(ii) lattice-gas models, and

(iii) solidification models.

In a deterministic automaton, the spatial domain of the model is divided into a fixed lattice and each cell has a state associated with it. The state at the next time step is determined solely from earlier states of the cell and those of the cells in its neighbourhood [1, 25].

In lattice gas models, again the system consists of a discrete spatial grid on which particles move about and interact in some prescribed manner. Unlike the deterministic automata, however, the rules governing the evolution of the particles in lattice-gas models are probabilistic.

In solidification models, the rules for the evolution of the particles in the lattice resemble those of the lattice-gas models, except that particles may be irreversibly bound at grid points, or cells may undergo irreversible configuration changes [25].

A model that subtly uses this approach is Bassetti *et al.* [6]. By discretizing space, time

and the orientation of microtubules, the authors defined a two-dimensional square lattice to represent the motor[3]-microtubule interactions. Each cell in the lattice is either empty or occupied by the centre of mass of a microtubule. Using the model, the authors successfully produced inhomogeneous stripe patterns, demonstrating that spatial patterns are obtained as non-equilibrium solutions of the system dynamics. Their model neglects dynamic instability in microtubules.

Casati *et al.* [15] used the CA modelling approach to investigate the influence of an electromagnetic field on microtubule assembly dynamics. The authors used a two-dimensional hexagonal uniform lattice to represent a portion of the cytoplasm through which the electromagnetic field propagates. Their modelling approach accounts for the changes that biological material induces on the electromagnetic field. They demonstrated that an electromagnetic field is capable of generating filamentary structures through the action of the ponderomotive force[4], despite the mixing effect of cytoplasmic hydrodynamic flows.

Another model that uses the CA approach is Kunwar *et al.* [49]. The authors used the model to describe the intra-cellular traffic of a family of microtubule motor proteins called *dynein* from the cell periphery towards the nucleus of the cell.

3.6 Agent-based modelling (ABM) approach

Agent-based modelling (ABM) is a technique that treats the components of a given system as agents, each of which has a set of behavioural rules that determine how the agents' states evolve in response to their current state and the state of their local environment. Thus, the agents in an ABM framework are assumed to have the ability to perceive and interact with each other and their environment. A typical ABM consists of

- a system of agents,

[3]Motor proteins are responsible for a wide range of intracellular activities, including transportation of vesicles and organelles along microtubules. There are two types of microtubule motors; *kinesin* and *dynein* (see, for example, [2] for details).

[4]A ponderomotive force is the force acting on a charged particle as the particle moves in an electromagnetic field.

- a set of agent relationships, and
- an environment or framework for simulating agent behaviours and interactions.

ABM can be considered a generalization of CA, where the model system is not required to be on a lattice and the rules can take any form including adaptive elements and goals-directed behaviour [74].

To our knowledge, very few models of microtubule dynamics adopt the ABM approach. The only model that we are aware of is that developed by Bouchard and co-workers [13]. Using stochastic AB simulations, the authors illustrated how the dynamic instability of microtubules can be harnessed to aid in building nanostructures.

Chapter 4

Modelling microtubule dynamics

In this chapter, we develop biologically plausible mathematical models of microtubule dynamics. These models attempt to describe microtubule assembly and disassembly kinetics *in vitro*. In the first two models in section 4.1, we model microtubule dynamics in the absence of dynamic instability. The other two models in section 4.2, introduce dynamic instability in the system.

4.1 Microtubule dynamics in the absence of dynamical instability

In this section, we model the temporal evolution of concentration *in vitro*, tracking the rates of change of the concentrations stemming from the chemical kinetics of microtubule assembly and disassembly in the absence of dynamic instability. We consider the following chemical reactions.

(i) **Nucleation** – n GTP-tubulin dimers, T aggregate at a rate constant k_n to form a nucleus (seed), M^1. The nucleus provides the site to which more dimers can add by the elongation process.

$$nT \xrightarrow{k_n} M \tag{4.1}$$

(ii) **Elongation** – a GTP-tubulin dimer adds to the newly formed nucleus or to a microtubule[1](of any length) at a rate constant k_g.

$$M + T \xrightarrow{k_g} M \tag{4.2}$$

(iii) **Shrinkage** – a microtubule shrinks at a rate constant k_s, losing GDP-tubulin dimer, D.

$$M \xrightarrow{k_s} M + D \tag{4.3}$$

(iv) **Reactivation** – the GDP-tubulin dimers liberated during the shrinkage process are converted to GTP-tubulin dimers at a rate constant k_c. These GTP-tubulin dimers are then available to be incorporated into the microtubule during the elongation process, or to form new seeds during the nucleation process.

$$D \xrightarrow{k_c} T \tag{4.4}$$

Reaction (4.4) is oversimplified, in the sense that it does not include the reactant (GTP) and byproduct (GDP). We are making an assumption that there is excess GTP in the solution. In their model, Katrukha and Guriya [45] have actually taken into account the concentrations of GTP and GDP in the microtubule dynamics. The concentrations are, however, treated as parameters and not as variables. A flow diagram for reactions (4.1-4.4) is shown in Figure 4.1.

We consider three state variables, namely,

(i) $C_m(t)$, the concentration of microtubules,

(ii) $C_t(t)$, the concentration of GTP-tubulin, and

(iii) $C_d(t)$, the concentration of GDP-tubulin.

[1]Since we are tracking the rates of change of concentration, no distinction is made between the seed in reaction (4.1) and the microtubules in reactions (4.2) and (4.3).

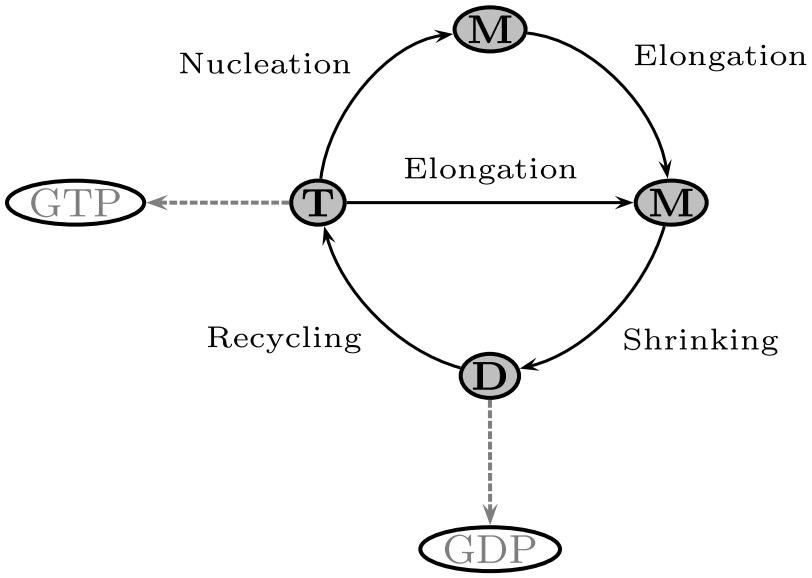

Figure 4.1: A flow diagram for the assembly and disassembly of microtubules in the absence of dynamic instability. Here, M denotes a microtubule, while D and T denote the GDP- and the GTP-tubulin dimer, respectively. GTP-tubulin dimers aggregate to form a microtubule nucleus from which a microtubule elongate by addition of more GTP-tubulin dimers. A microtubule can also undergo shrinkage, losing GDP-tubulin dimers in the process. GTP-tubulin dimers are regenerated when the excess GDP-tubulin dimers interact with GTP molecules.

Two approaches for the microtubule nucleation kinetics are explored; namely, saturating and nonsaturating nucleation kinetics.

Model I: Microtubule dynamics with non-saturating nucleation

Assuming the law of mass action, the kinetic equations describing reactions (4.1 - 4.4) are:

$$\frac{dC_t}{dt} = k_c C_d - k_n C_t^n - k_g C_m C_t \tag{4.5a}$$

$$\frac{dC_d}{dt} = k_s C_m - k_c C_d \tag{4.5b}$$

$$\frac{dC_m}{dt} = k_n C_t^n + k_g C_m C_t - k_s C_m \tag{4.5c}$$

In system (4.5), the rate of microtubule nucleation is assumed to exponentially depend on the concentration of GTP-tubulin dimers; that is, we have a nonsaturating nucleation kinetics (illustrated in Figure 4.2). This has indeed been established experimentally [42],

with the nucleation exponents ranging from 6 to 12 [16] (see also [41] for details).

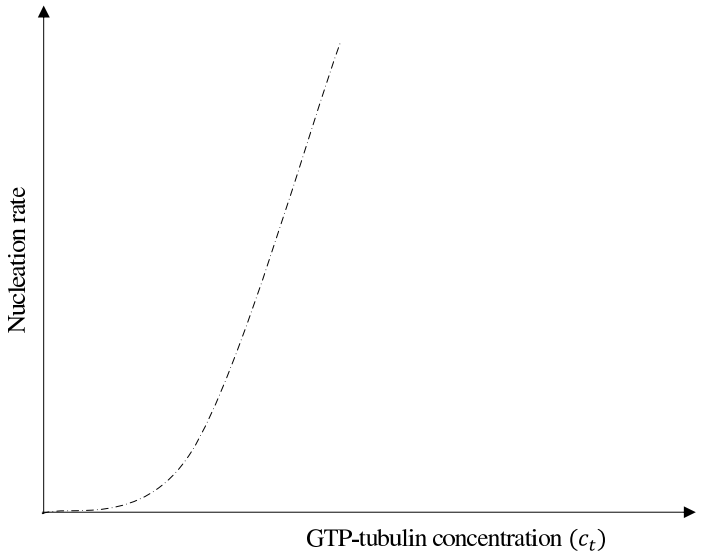

Figure 4.2: An illustration of non-saturating nucleation kinetics. As the GTP-tubulin concentration (C_t) increases, the nucleation rate increases unboundedly.

System (4.5) is considered with nonnegative initial conditions

$$C_m(0) \geq 0, \quad C_t(0) \geq 0, \quad C_d(0) \geq 0.$$

The parameters used in system (4.5), and their meaning, are summarized in Table 4.1.

Model II: Microtubule dynamics assuming saturating nucleation

In model I, we have assumed that the nucleation rate depends exponentially on the GTP-tubulin concentration. We now consider an alternative mechanism. Using a form similar to the Hill's function, we assume a rate-limiting nucleation mechanism for reaction (4.1). Figure 4.3 illustrates this mechanism.

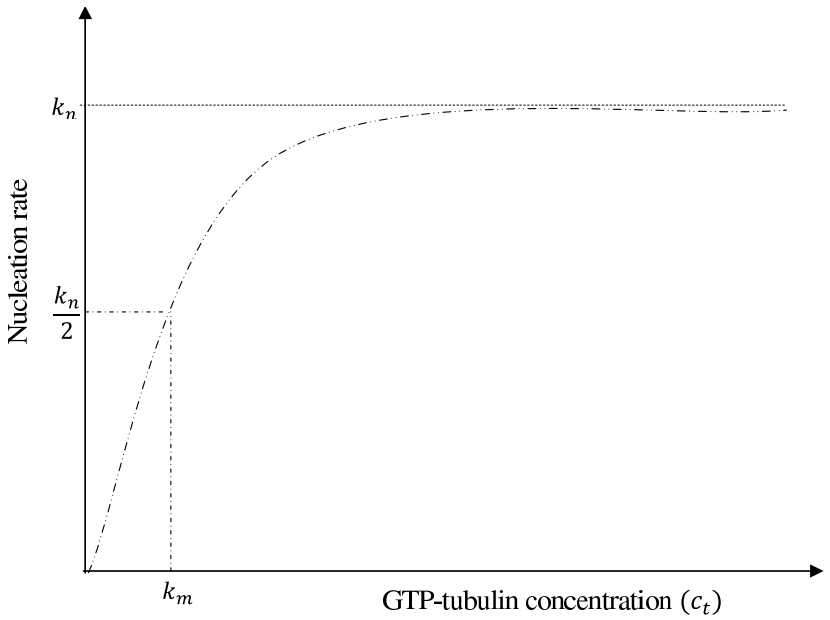

Figure 4.3: An illustration of saturating nucleation kinetics. As the GTP-tubulin concentration (C_t) increases, the rate of nucleation initially increases, but eventually reaches a maximum (k_n). When the rate of nucleation is $\frac{k_n}{2}$, GTP-tubulin concentration equals k_m.

And assuming the law of mass action for reactions (4.2), (4.3), and (4.4), the kinetic equations describing reactions (4.1 - 4.4) are:

$$\frac{dC_t}{dt} = k_c C_d - \frac{k_n C_t^n}{k_m + C_t^n} - k_g C_m C_t \tag{4.6a}$$

$$\frac{dC_m}{dt} = \frac{k_n C_t^n}{k_m + C_t^n} + k_g C_m C_t - k_s C_m \tag{4.6b}$$

$$\frac{dC_d}{dt} = k_s C_m - k_c C_d, \tag{4.6c}$$

The parameters used in system (4.6), and their meaning, are summarized in Table 4.1.

System (4.6) is considered with nonnegative initial conditions

$$C_m(0) \geq 0; \quad C_t(0) \geq 0; \quad C_d(0) \geq 0.$$

4.2 Microtubule dynamics in the presence of dynamical instability

In Section 4.1, we have modeled microtubule dynamics in the absence of dynamical instability. In this section, we now incorporate this process in our models and, thus, consider microtubules as occurring in two distinct states; namely, growing state, and shrinking state. The following chemical reactions are considered

(i) **Nucleation** – n GTP-tubulin dimers, T aggregate at a rate constant k_n to form a nucleus (seed), G - we are taking nucleus to be in the growing state.

$$nT \xrightarrow{k_n} G \tag{4.7}$$

(ii) **Elongation** – a GTP-tubulin dimer adds to the newly formed nucleus or to a growing microtubule (of any length) at a rate constant k_g.

$$G + T \xrightarrow{k_g} G \tag{4.8}$$

(iii) **Shrinkage** – a microtubule in the shrinking state shrinks at a rate constant k_s, losing GDP-tubulin dimer, D.

$$S \xrightarrow{k_s} S + D \tag{4.9}$$

(iv) **Reactivation** – the GDP-tubulin dimers liberated during the shrinkage process are converted to GTP-tubulin dimers at a rate constant k_c. These GTP-tubulin dimers are then available to be incorporated into the microtubule during the elongation process, or to form new seeds during the nucleation process.

$$D \xrightarrow{k_c} T \tag{4.10}$$

(v) **Rescue** – a microtubule in the shrinking state switches to the growing state at a rate constant k_{res}[2]

$$S \xrightarrow{k_{\text{res}}} G \tag{4.11}$$

(vi) **Catastrophe** – a microtubule in the growing state switches to the shrinking state at a rate constant k_{cat}[2]

$$G \xrightarrow{k_{\text{cat}}} S \tag{4.12}$$

These chemical reactions are represented in Figure 4.4.

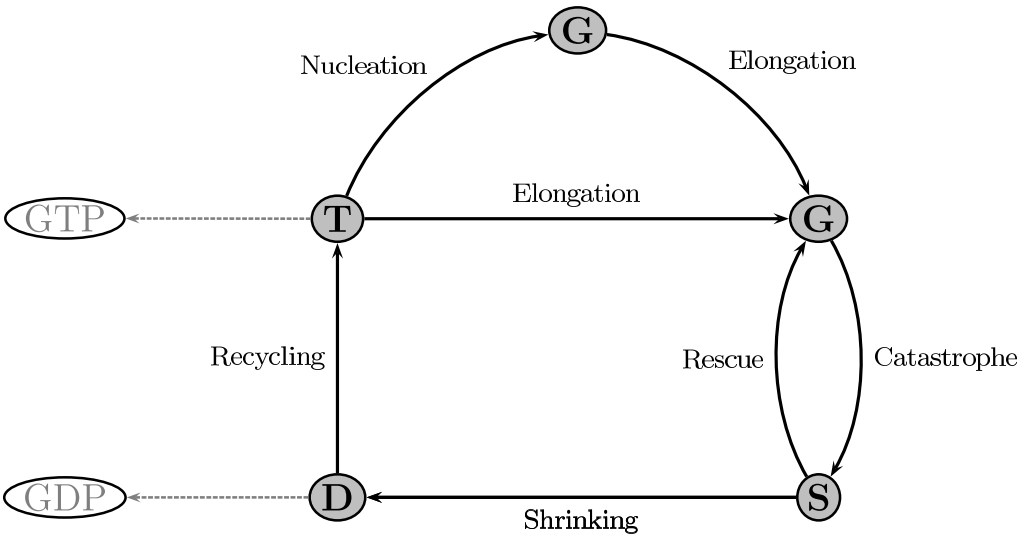

Figure 4.4: A flow diagram for the assembly and disassembly of microtubules in the presence of dynamic instability. Here, G and S denote, respectively, the growing and shrinking microtubule, while D and T denote the GDP- and GTP-tubulin dimer, respectively. GTP-tubulin dimers aggregate to form microtubule nuclei from which growing microtubules elongate by addition of more GTP-tubulin dimers. A growing microtubule may switch to a shrinking one through the catastrophe process. A shrinking microtubule can also switch to a growing microtubule via the rescue process. A shrinking microtubule can also undergo shrinkage, losing GDP-tubulin dimers in process. GTP-tubulin dimers are regenerated when the excess GDP-tubulin dimers interact with GTP molecules.

[2] k_{res} is the rescue frequency; it is the average number of rescues per unit of time of microtubule shrinkage. On the other hand, k_{cat} is the catastrophe frequency; namely, the average number of catastrophes per unit of time of microtubule growth [39].

We consider four state variables, namely,

(i) $C_t(t)$, the concentration of GTP-tubulin,

(ii) $C_d(t)$, the concentration of GDP-tubulin,

(iii) $C_s(t)$, the concentration of shrinking microtubules, and

(iv) $C_g(t)$, the concentration of growing microtubules.

Model III: Microtubule dynamics with non-saturating nucleation in the presence of dynamical instability

We assume that the law of mass action governs reactions (4.8 - 4.12) and that we have a non-saturating nucleation mode (Figure 4.2). With these assumptions, the kinetic equations describing reactions (4.8 - 4.12) are:

$$\frac{dC_t}{dt} = k_c C_d - k_n C_t^n - k_g C_g C_t \tag{4.13a}$$

$$\frac{dC_d}{dt} = k_s C_s - k_c C_d \tag{4.13b}$$

$$\frac{dC_s}{dt} = k_{\text{cat}} C_g - (k_{\text{res}} + k_s) C_s \tag{4.13c}$$

$$\frac{dC_g}{dt} = k_n C_t^n + k_g C_g C_t + k_{\text{res}} C_s - k_{\text{cat}} C_g \tag{4.13d}$$

This model has nonnegative initial conditions

$$C_t(0) \geq 0, \quad C_d(0) \geq 0, \quad C_s(0) \geq 0, \quad C_g(0) \geq 0.$$

The parameters used in system (4.13), and their meaning, are summarized in Table 4.1.

Model IV: Microtubule dynamics with saturating nucleation in the presence of dynamic instability

This model differs from model III above in the nucleation reaction mechanism. As in Model II, we assume that the system has a rate-limiting nucleation rate (Figure 4.3). The model thus becomes

$$\frac{dC_t}{dt} = k_c C_d - \frac{k_n C_t^n}{k_m + C_t^n} - k_g C_g C_t \tag{4.14a}$$

$$\frac{dC_d}{dt} = k_s C_s - k_c C_d \tag{4.14b}$$

$$\frac{dC_s}{dt} = k_{\text{cat}} C_g - (k_s + k_{\text{res}})\, C_s \tag{4.14c}$$

$$\frac{dC_g}{dt} = \frac{k_n C_t^n}{k_m + C_t^n} + (k_g C_t - k_{\text{cat}}) C_g + k_{\text{res}} C_s, \tag{4.14d}$$

with the initial conditions

$$C_t(0) \geq 0, \quad C_d(0) \geq 0, \quad C_s(0) \geq 0, \quad C_g(0) \geq 0.$$

A summary of the parameters used in model (4.14) and their meaning is given in Table 4.1.

Model V: Microtubule dynamics with non-saturating nucleation in the presence of dynamic instability − dependence of k_{cat} and k_{res} on GTP-tubulin concentration

Following Walker *et al.* [82], we assume dependence of k_{cat} and k_{res} on the concentration of GTP-tubulin using linear functions [39]:

$$k_{\text{cat}} = b_{\text{cat}} - a_{\text{cat}} C_t,$$

$$k_{\text{res}} = b_{\text{res}} + a_{\text{res}} C_t,$$

where a_{cat}, b_{cat}, a_{res}, and b_{res} are positive constants. Thus k_{cat} decreases with increasing C_t, whereas k_{res} increases with increasing C_t (Figure 4.5).

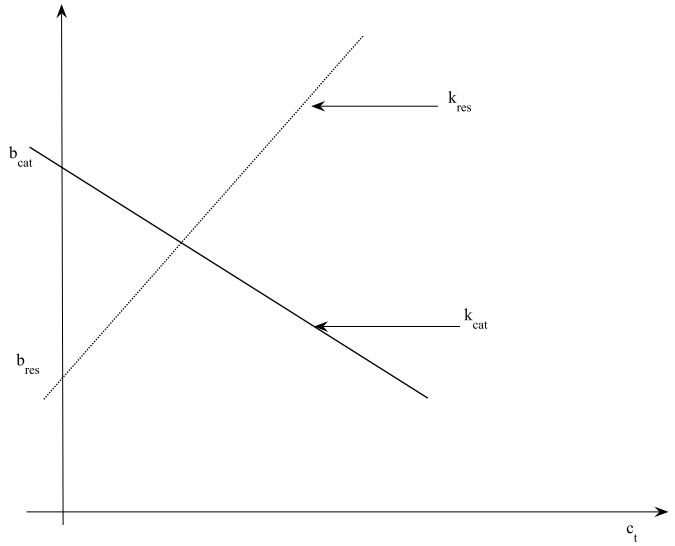

Figure 4.5: An illustration of the dependence of catastrophe and rescue rates on GTP-tubulin concentration.

Substituting these values in system (4.13), we have

$$\frac{dC_t}{dt} = k_c C_d - k_n C_t^n - k_g C_g C_t \tag{4.15a}$$
$$\frac{dC_d}{dt} = k_s C_s - k_c C_d \tag{4.15b}$$
$$\frac{dC_s}{dt} = (b_{\text{cat}} - a_{\text{cat}} C_t) C_g - (a_{\text{res}} C_t + b_{\text{res}} + k_s) C_s \tag{4.15c}$$
$$\frac{dC_g}{dt} = k_n C_t^n + k_g C_g C_t + (a_{\text{res}} C_t + b_{\text{res}}) C_s - (b_{\text{cat}} - a_{\text{cat}} C_t) C_g \tag{4.15d}$$

System (4.15) is considered with nonnegative initial conditions

$$C_t(0) \geq 0, \quad C_d(0) \geq 0, \quad C_s(0) \geq 0, \quad C_g(0) \geq 0.$$

A summary of the parameters used in model (4.15) and their meaning is given in Table 4.1.

Symbol	Meaning
All models	
k_n	Rate at which GTP-tubulin aggregates to form a nucleus
k_g	Rate at which a microtubule grows (elongates)
k_s	Rate at which a microtubule shrinks (disassembles)
k_c	Rate at which GDP-tubulin is converted to GTP-tubulin
Model II and IV only	
k_{m}	Maximal rate of nucleation
Model III and IV only	
k_{cat}	Catastrophe frequency
k_{res}	Rescue frequency
Model V only	
a_{cat}	Velocity of the catastrophe rate
a_{res}	Velocity of the rescue rate
b_{cat}	Maximal magnitude of the catastrophe rate
b_{res}	Minimal magnitude of the rescue rate

Table 4.1: Parameters used in the models and their meaning

Chapter 5

Mathematical analysis and simulation results

In this chapter, we analyze the models developed in Chapter 4. We also give the numerical simulations and sensitivity analysis results of the models. We conclude the chapter with a discussion, based on these results, of the emerging scenario from these models.

5.1 Mathematical analysis

Mathematical analysis of model I

$$\frac{dC_t}{dt} = k_c C_d - k_n C_t^n - k_g C_m C_t, \tag{5.1a}$$

$$\frac{dC_d}{dt} = k_s C_m - k_c C_d, \tag{5.1b}$$

$$\frac{dC_m}{dt} = k_n C_t^n + k_g C_m C_t - k_s C_m, \tag{5.1c}$$

$$C_m(0) \geq 0, \quad C_t(0) \geq 0, \quad C_d(0) \geq 0.$$

Summing the three equations in system (5.1), the conservation equation

$$\frac{d}{dt}[C_t(t) + C_d(t) + C_m(t)] = 0$$

is obtained. This implies that the total concentration of all the variables in system (5.1) is a positive constant; that is,

$$C_t(t) + C_d(t) + C_m(t) = C_0, \qquad \forall\, t \geq 0. \tag{5.2}$$

It is first noted that the origin $(0,\ 0,\ 0)$ is an equilibrium solution of (5.1). This is the trivial equilibrium point, corresponding to the absence of the quantities represented by the variables of system (5.1). The Jacobian matrix of system (5.1), evaluated at the origin, is given by

$$\mathbf{J}_{(0,0,0)} = \begin{bmatrix} 0 & k_c & 0 \\ 0 & -k_c & k_s \\ 0 & 0 & -k_s \end{bmatrix}$$

This matrix has two negative eigenvalues, $-k_c$ and $-k_s$, and one zero eigenvalue. Thus $(0,\ 0,\ 0)$ is a non-hyperbolic equilibrium solution. The stable manifold theorem (Theorem 2.3.1) implies that there exists a local two-dimensional stable manifold through the origin. That is, all trajectories asymptotically approaching the origin as $t \to \infty$ lie on a two-dimensional invariant manifold. Further, by the centre manifold theorem (Theorem 2.3.2), the topology of the flow near the origin is characterized by a one-dimensional local centre manifold intersecting the origin. Since the presence of a zero eigenvalue is a direct consequence of the conservation of mass, we conclude that the origin is locally asymptotically stable.

Remark 5.1.1. Note that the trivial equilibrium corresponds to the case when $C_0 = 0$; that is, when there is no tubulin in the experiment.

We now look for the non-trivial equilibrium solution(s) of (5.1); that is, the case when $C_0 > 0$.

The set

$$\widehat{\boldsymbol{\Omega}} = \{(C_t, C_d, C_m) \in \mathbb{R}^3_+ : C_t \geq 0;\ C_d \geq 0;\ C_m \geq 0;\ C_t + C_d + C_m = C_0\},$$

where $\mathbb{R}^3_+$ denotes the nonnegative orthant of $\mathbb{R}^3$, is positively invariant under the flow induced by (5.1). It therefore follows that system (5.1) is well posed with bounded solutions. Using (5.2), we can replace C_m with $C_0 - C_t - C_d$ in (5.1) to obtain a two-dimensional system

$$\begin{aligned}\frac{dC_t}{dt} &= k_c C_d - k_n C_t^n - k_g C_t(C_0 - C_t - C_d)\\ \frac{dC_d}{dt} &= k_s(C_0 - C_t - C_d) - k_c C_d\end{aligned}$$

That is

$$\frac{dC_t}{dt} = k_c C_d - k_n C_t^n + k_g C_t^2 - (C_0 - C_d)k_g C_t \tag{5.3a}$$

$$\frac{dC_d}{dt} = (C_0 - C_t)k_s - (k_s + k_c)C_d \tag{5.3b}$$

It is convenient to describe system (5.1) in terms of relative proportions; that is,

$$\bar{C}_t = \frac{C_t}{C_0},\ \ \bar{C}_d = \frac{C_d}{C_0},\ \ \bar{C}_m = \frac{C_m}{C_0}.$$

This gives the evident conditions

$$\bar{C}_t \leq 1,\ \ \bar{C}_d \leq 1,\ \ \bar{C}_m \leq 1,\ \ \bar{C}_t + \bar{C}_d + \bar{C}_m = 1,$$

and system (5.3) can be expressed as

$$\begin{aligned}\frac{d\bar{C}_t}{dt} &= k_c \bar{C}_d - k_n C_0^{n-1} \bar{C}_t^n + k_g C_0 \bar{C}_t^2 - (1 - \bar{C}_d)k_g C_0 \bar{C}_t\\ \frac{d\bar{C}_d}{dt} &= (1 - \bar{C}_t)k_s - (k_s + k_c)\bar{C}_d\end{aligned}$$

Dropping the bars, for notational simplicity, we have

$$\frac{dC_t}{dt} = k_c C_d - k_n C_0^{n-1} C_t^n + k_g C_0 C_t^2 - (1 - C_d)k_g C_0 C_t \tag{5.4a}$$

$$\frac{dC_d}{dt} = (1 - C_t)k_s - (k_s + k_c)C_d \tag{5.4b}$$

The set

$$\boldsymbol{\Omega} = \{(C_t, C_d) \in \mathbb{R}^2_+ : C_t \geq 0;\ C_d \geq 0;\ C_t + C_d \leq 1\}$$

is positively invariant under the flow of system (5.4); that is, solutions starting in $\boldsymbol{\Omega}$ remain there forever. Therefore, (5.4) is well posed, with bounded solutions.

Remark 5.1.2. From (5.4), the dynamics of C_m (in proportions) is deduced from

$$C_m(t) = 1 - C_t(t) - C_d(t).$$

The equivalence of system (5.1) and system (5.4) is thus established by noting that the solutions of (5.1) can be obtained from the solutions of (5.4) together with (5.2). That is, by multiplying the solutions of (5.4) by C_0 and using (5.2), we have the solutions of (5.1).

Let us now analyze system (5.4).

Equilibrium of system (5.4)

Theorem 5.1.3. *If $C_0 > 0$, then on the set $\boldsymbol{\Omega}$, system* (5.4) *admits a unique positive equilibrium*

$$E_1^* = \left(C_t^*, \frac{k_s(1 - C_t^*)}{k_s + k_c}\right),$$

where C_t^* is the unique positive root in the interval $(0, 1)$ to the equation

$$(k_s + k_c)k_n C_0^{n-1} C_t^n - k_c k_g C_0 C_t^2 + (k_g C_0 + k_s)k_c C_t - k_s k_c = 0$$

In particular,

$$C_t^* \in \left(0,\ \min\big(1, \frac{k_s}{k_g C_0}\big)\right).$$

Proof. Suppose that $C_0 > 0$. Setting the time derivatives in Eqs. (5.4a) and (5.4b) equal to zero, we obtain

$$k_c C_d - k_n C_0^{n-1} C_t^n + k_g C_0 C_t^2 - (1 - C_d)k_g C_0 C_t = 0 \tag{5.5a}$$

$$(1 - C_t)k_s - (k_s + k_c)C_d = 0 \tag{5.5b}$$

From Eq. (5.5b), we have

$$C_d = \frac{k_s}{k_s + k_c}(1 - C_t)$$

Substituting this value of C_d in Eq. (5.5a) and simplifying, we obtain an n-th degree polynomial in C_t:

$$(k_s + k_c)k_n C_0^{n-1} C_t^n - k_c k_g C_0 C_t^2 + (k_g C_0 + k_s)k_c C_t - k_s k_c = 0 \tag{5.6}$$

Thus, the positive roots, C_t^*, of Eq. (5.6) are the C_t-components of the equilibrium solutions of (5.5).
Let us write the left hand side of Eq. (5.6) as a difference of two polynomials $P_1(C_t) - P_2(C_t)$, where

$$P_1(C_t) = (k_s + k_c)k_n C_0^{n-1} C_t^n$$

and

$$P_2(C_t) = k_c \left[k_g C_0 C_t^2 - (k_g C_0 + k_s)C_t + k_s\right]$$

The polynomial P_1 is an increasing function on $\mathbb{R}_+$ such that $P_1(0) = 0$.
On the other hand, P_2 is a quadratic polynomial such that

- $P_2(0) = k_s k_c > 0$,
- its roots are 1 and $\frac{k_s}{k_g C_0}$, both positive,
- it is upwardly concave with a critical value at $C_t = \frac{k_g C_0 + k_s}{2k_g C_0}$,
- it is decreasing on $\left(0, \frac{k_g C_0 + k_s}{2k_g C_0}\right)$ and increasing on $\left(\frac{k_g C_0 + k_s}{2k_g C_0}, \infty\right)$, and
- it is positive on $\left(0, \min\left(1, \frac{k_s}{k_g C_0}\right)\right)$ and $\left(\max\left(1, \frac{k_s}{k_g C_0}\right), \infty\right)$.

It follows that P_1 and P_2 have a unique intersection for $0 < C_t < \min\left(1, \frac{k_s}{k_g C_0}\right)$. The second positive intersection, if it exists, has $C_t > \max\left(1, \frac{k_s}{k_g C_0}\right) \geq 1$. Since the state variables in (5.4) are in proportions, a biologically meaningful equilibrium must satisfy the condition $C_t \leq 1$. Consequently, C_t^* is unique and satisfies

$$0 < C_t^* < \min\left(1, \frac{k_s}{k_g C_0}\right), \tag{5.7}$$

This completes the proof of Theorem 5.1.3. □

Biological Remark. The ratio $\frac{k_s}{k_g}$ is termed the *critical concentration* of GTP-tubulin

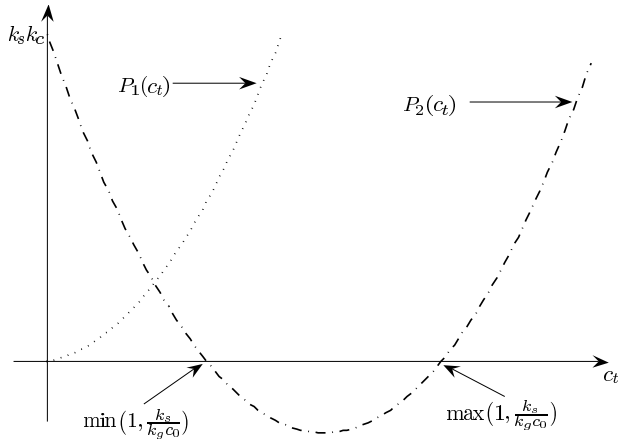

Figure 5.1: Illustrations of the functions $P_1(C_t)$ and $P_2(C_t)$ of Eq. (5.6)

dimers [80, 82] and is usually denoted by C_c. At GTP-tubulin concentrations above C_c, the GTP-tubulin dimers assemble into microtubules, while below the C_c, microtubules disassemble. At concentrations near C_c, some microtubules assemble, while others disassemble. Since we are working in proportions, the term $\frac{k_s}{k_g C_0}$ on the right hand side of (5.7) agrees perfectly with theoretical and experimental results in literature. For example, Bicout & Rubin [9] point out that below the critical concentration and in the presence of nucleation sites (nucleus), a stable population of microtubules will be maintained as long as the GTP-tubulin concentration is maintained.

Stability analysis of E_1^*

Theorem 5.1.4. *The equilibrium solution E_1^* of system* (5.4) *is globally asymptotically stable with respect to the set $\boldsymbol{\Omega}$.*

Proof. The Jacobian of system (5.4) is

$$\mathbf{J} = \begin{bmatrix} -nk_n(C_0C_t)^{n-1} + (2C_t + C_d - 1)k_gC_0 & k_gC_0C_t + k_c \\ \\ -k_s & -(k_s + k_c) \end{bmatrix}$$

Evaluated at the equilibrium E_1^*, the Jacobian becomes

$$\mathbf{J}_{E_1^*} = \begin{bmatrix} -nk_n(C_0C_t^*)^{n-1} + \left[2C_t^* - \frac{(k_sC_t^*+k_c)}{k_s+k_c}\right] k_gC_0 & k_gC_0C_t^* + k_c \\ \\ -k_s & -(k_s+k_c) \end{bmatrix}$$

The trace of $\mathbf{J}_{E_1^*}$,

$$\begin{aligned} \mathrm{tr}(\mathbf{J}_{E_1^*}) &= -nk_n(C_0C_t^*)^{n-1} + \left[2C_t^* - \frac{(k_sC_t^*+k_c)}{k_s+k_c}\right] k_gC_0 - k_s - k_c \\ &= -nk_n(C_0C_t^*)^{n-1} + \frac{(k_s+2k_c)k_gC_0}{k_s+k_c}C_t^* - \left[\frac{k_ck_gC_0}{k_s+k_c} + k_s + k_c\right], \end{aligned}$$

can be written as a difference of two polynomials $P_3(C_t^*) - P_4(C_t^*)$, where

$$P_3(C_t^*) = \frac{(k_s+2k_c)k_gC_0}{k_s+k_c}C_t^* - \left(\frac{k_ck_gC_0}{k_s+k_c} + k_s + k_c\right),$$

and

$$P_4(C_t^*) = nk_n(C_0C_t^*)^{n-1}$$

Then the sign of $\mathrm{tr}(\mathbf{J}_{E_1^*})$ depends on the relative positions of the graphs of P_3 and P_4.

Now P_3 is a straight line with a positive slope and negative intercept. It is negative for

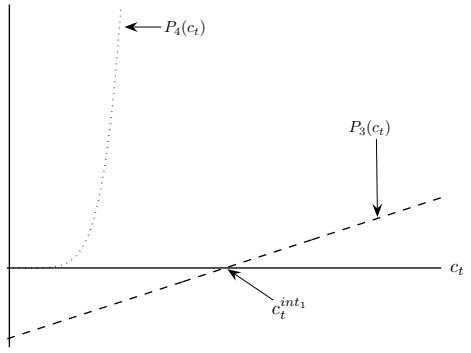

Figure 5.2: Illustrations of the functions $P_3(C_t)$ and $P_4(C_t)$ of the trace of $\mathbf{J}_{E_1^*}$

all $C_t^* < C_t^{\text{int}_1}$, where

$$C_t^{\text{int}_1} = \frac{(k_s + k_c)^2 + k_c k_g C_0}{(k_s + 2k_c)k_g C_0}$$

P_4, on the other hand, is an increasing function with $P_4(0) = 0$. Thus, $P_4 > 0, \ \forall\, C_t^* > 0$ and, therefore,

$$\forall\, C_t^* \in \left[0, C_t^{\text{int}_1}\right], \ \ P_3(C_t^*) < P_4(C_t^*),$$

which implies that

$$\forall\, C_t^* \in \left[0, C_t^{\text{int}_1}\right], \ \ \text{tr}(\mathbf{J}_{E_1^*}) < 0$$

Recall, from (5.7), that $C_t^* < 1$. Hence if $C_t^{\text{int}_1} \geq 1$, we have that $\text{tr}(\mathbf{J}_{E_1^*}) < 0$. Now suppose that $C_t^{\text{int}_1} < 1$; then,

$$k_s + k_c < k_g C_0 \tag{5.8}$$

And using (5.7), we deduce that, in this case, $\min\left(1, \frac{k_s}{k_g C_0}\right) = \frac{k_s}{k_g C_0}$; that is, $C_t^* \in \left(0, \frac{k_s}{k_g C_0}\right)$. There are two possibilities for the relative positions of $\frac{k_s}{k_g C_0}$ and $C_t^{\text{int}_1}$ along the C_t-axis.

(a) $\frac{k_s}{k_g C_0} < C_t^{\text{int}_1}$ – in this case, it follows that $\left(0, \frac{k_s}{k_g C_0}\right) \subset \left[0, C_t^{\text{int}_1}\right]$. Thus for any C_t^*, $P_3(C_t^*) - P_4(C_t^*) < 0$.

(b) $\frac{k_s}{k_g C_0} > C_t^{\text{int}_1}$ – in this case, $k_g C_0 < -k_c$, contradicting inequality (5.8). We therefore rule out this possibility.

It follows that $\text{tr}(\mathbf{J}_{E_1^*}) < 0$. From Bendixson's criterion (Theorem 2.4.7), it follows that there are no non-constant periodic solutions in the positive quadrant. We have shown that the solutions to system (5.4) are bounded. Furthermore, we have established, from Theorem 5.1.3, that E_1^* is unique. By Poincaré-Bendixson theorem (Theorem 2.4.3), it follows that all trajectories limit to the equilibrium E_1^*; that is, that E_1^* is globally asymptotically stable. This completes the proof of Theorem 5.1.4. □

Remark 5.1.5. From Remark 5.1.2, the following theorem on the uniqueness and stability of the equilibrium solution of system (5.1) is trivially true.

Theorem 5.1.6. *If $C_0 > 0$, then on the set $\widehat{\boldsymbol{\Omega}}$, system (5.1) has a unique positive equilibrium solution*

$$E_1^{**} = \left(C_0 C_t^*, \ \frac{k_s C_0 (1 - C_t^*)}{k_s + k_c}, \ \frac{k_c C_0 (1 - C_t^*)}{k_s + k_c} \right),$$

where C_t^* is the unique positive root in the interval

$$\left(0, \ \min\left(1, \frac{k_s}{k_g C_0}\right) \right)$$

to the equation

$$(k_s + k_c) k_n C_0^{n-1} C_t^n - k_c k_g C_0 C_t^2 + (k_g C_0 + k_s) k_c C_t - k_s k_c = 0.$$

Furthermore, E_1^{**} is globally asymptotically stable with respect to the set $\widehat{\boldsymbol{\Omega}}$.

Mathematical analysis of model II

Using rigorous numerical simulations (see in Section 5.2), we established that nucleation has insignificant effect on the overall microtubule dynamics. For this reason, we analyze model II for the special case when $n = 1$. Model II then becomes

$$\frac{dC_t}{dt} = k_c C_d - \frac{k_n C_t}{k_m + C_t} - k_g C_m C_t \tag{5.9a}$$

$$\frac{dC_d}{dt} = k_s C_m - k_c C_d \tag{5.9b}$$

$$\frac{dC_m}{dt} = \frac{k_n C_t}{k_m + C_t} + k_g C_m C_t - k_s C_m \tag{5.9c}$$

$$C_m(0) \geq 0; \quad C_t(0) \geq 0; \quad C_d(0) \geq 0.$$

The law of conservation of mass is satisfied in system (5.9); that is, the relation

$$\frac{d}{dt}[C_t(t) + C_d(t) + C_m(t)] = 0$$

holds, implying that the total concentration of all the variables in the system is a constant:

$$C_m(t) + C_t(t) + C_d(t) = C_0 > 0, \qquad \forall\, t \geq 0. \tag{5.10}$$

Obviously, the origin $(0,\ 0,\ 0)$ is the trivial equilibrium solution of (5.9). This equilibrium corresponds to the case when $C_0 = 0$; that is, the case when there is no tubulin in the experiment.

The Jacobian matrix of system (5.9), evaluated at the origin, is given by

$$\mathbf{J}_{(0,0,0)} = \begin{bmatrix} -\frac{k_n}{k_m} & k_c & 0 \\ 0 & -k_c & k_s \\ \frac{k_n}{k_m} & 0 & -k_s \end{bmatrix}$$

The characteristic equation of the Jacobian is

$$k_m\lambda^3 + \lambda^2(k_ck_m + k_sk_m + k_n) + \lambda(k_mk_ck_s + k_ck_n + k_sk_n) = 0,$$

whose roots are

$$\lambda_1 = 0,$$
$$\lambda_2 = \frac{-(k_ck_m + k_sk_m + k_n) + \sqrt{(k_ck_m + k_sk_m - k_n)^2 - 4k_ck_sk_m^2}}{2k_m},$$

and

$$\lambda_3 = \frac{-(k_ck_m + k_sk_m + k_n) - \sqrt{(k_ck_m + k_sk_m - k_n)^2 - 4k_ck_sk_m^2}}{2k_m}.$$

Since

$$\sqrt{(k_ck_m + k_sk_m - k_n)^2 - 4k_ck_sk_m^2} < \sqrt{(k_ck_m + k_sk_m - k_n)^2} = k_ck_m + k_sk_m - k_n,$$

it follows that

$$\lambda_2 < -\frac{k_n}{k_m} \quad \text{and} \quad \lambda_3 < -(k_c + k_s)$$

Thus, the Jacobian matrix has two negative eigenvalues, λ_2 and λ_3, and one zero eigenvalue, implying that $(0,\ 0,\ 0)$ is a non-hyperbolic equilibrium solution. The zero eigenvalue comes from the conservation of mass. By the stable and centre manifold theorems (Theorems 2.3.1 and 2.3.2, respectively), there exists a local two-dimensional stable manifold through the origin, and a one-dimensional local centre manifold tangent to the eigenspace associated to λ_1. We therefore conclude that the origin is locally asymptotically stable.

Let us now look for the non-trivial equilibrium solution(s) of (5.9); that is, the equilibrium solution(s) of (5.9) when $C_0 > 0$.

The set

$$\check{\boldsymbol{\Omega}} = \{(C_t, C_d, C_m) \in \mathbb{R}^3_+ : C_t \geq 0;\ C_d \geq 0;\ C_m \geq 0;\ C_t + C_d + C_m = C_0\}$$

is positively invariant under the flow of (5.9). It thus follows that system (5.9) is well posed with bounded solutions. Using (5.10), we can reduce system (5.9) to a two-dimensional system of differential equations by dropping the equation for C_m to obtain

$$\frac{dC_t}{dt} = k_c C_d - \frac{k_n C_t}{k_m + C_t} - (C_0 - C_t - C_d) k_g C_t \tag{5.11a}$$

$$\frac{dC_d}{dt} = (C_0 - C_t - C_d) k_s - k_c C_d \tag{5.11b}$$

Let us define the variables C_m, C_t, and C_d of system (5.9) in terms of proportions:

$$\tilde{C}_m = \frac{C_m}{C_0}, \quad \tilde{C}_t = \frac{C_t}{C_0}, \quad \tilde{C}_d = \frac{C_d}{C_0},$$

with

$$\tilde{C}_m + \tilde{C}_t + \tilde{C}_d = 1$$

Then, after dropping the tildes for notational simplicity, system (5.11) becomes

$$\frac{dC_t}{dt} = (k_g C_0 C_t + k_c)C_d - \frac{k_n C_t}{k_m + C_0 C_t} - (1 - C_t)k_g C_0 C_t \tag{5.12a}$$

$$\frac{dC_d}{dt} = (1 - C_t)k_s - (k_s + k_c)C_d \tag{5.12b}$$

The set

$$\widetilde{\boldsymbol{\Omega}} = \{(C_t, C_d) \in \mathbb{R}^2_+ : C_t \geq 0;\ C_d \geq 0;\ C_t + C_d \leq 1\}$$

is positively invariant under the flow of (5.12). Therefore, (5.12) is well posed, with bounded solutions.

Remark 5.1.7. From (5.10), the dynamics of C_m (in proportions) is deduced from

$$C_m(t) = 1 - C_t(t) - C_d(t).$$

The equivalence of system (5.9) and system (5.12) is thus established by noting that the solutions of (5.9) can be obtained from the solutions of (5.12) together with (5.10). That is, multiplying the solutions of (5.12) by C_0 and using (5.10), we have the solutions of (5.9).

We now consider the analysis of system (5.12).

Equilibrium of system (5.12)

Theorem 5.1.8. *If $C_0 > 0$, then on the set $\widetilde{\boldsymbol{\Omega}}$, system* (5.12) *has a unique positive equilibrium*

$$E_2^* = \left(C_t^*, \frac{(1 - C_t^*)k_s}{k_s + k_c}\right),$$

where C_t^* is the unique positive root in the interval $(0,1)$ to the cubic equation

$$k_c k_g C_0^2 C_t^3 - [k_s - (k_m - C_0)k_g]\, k_c C_0 C_t^2 + k_m k_s k_c$$

$$- [(k_s + k_c)k_n + (k_g C_0 + k_s)k_m k_c - k_s k_c C_0]\, C_t = 0.$$

Proof. Setting the left-hand sides of system (5.12) to zero, we obtain

$$0 = (k_g C_0 C_t + k_c)C_d - \frac{k_n C_t}{k_m + C_0 C_t} - (1 - C_t)k_g C_0 C_t \tag{5.13a}$$

$$0 = (1 - C_t)k_s - (k_s + k_c)C_d \tag{5.13b}$$

From (5.13b), we have that

$$C_d = \frac{(1 - C_t)k_s}{k_s + k_c}$$

Substituting this value in Eq. (5.13a) and simplifying the resulting equation, we obtain

$$k_c k_g C_0^2 C_t^3 - [k_s - (k_m - C_0)k_g]\, k_c C_0 C_t^2 + k_m k_s k_c$$

$$- [(k_s + k_c)k_n + (k_g C_0 + k_s)k_m k_c - k_s k_c C_0]\, C_t = 0 \tag{5.14}$$

The LHS of Eq. (5.14) can be written as a difference of two polynomials $\Phi_3(C_t) - \Phi_4(C_t)$, where

$$\Phi_3(C_t) = k_c k_g C_0^2 C_t^3 + k_m k_s k_c$$

and

$$\Phi_4(C_t) = [k_s - (k_m - C_0)k_g]\, k_c C_0 C_t^2$$

$$+ \{[(k_m - C_0)k_c + k_n]\, k_s + (k_m k_g C_0 + k_n)k_c\}\, C_t$$

Now, $\Phi_3(C_t)$ is, for all values of C_t, an increasing polynomial function with $\Phi_3(0) = k_m k_s k_c > 0$. On the other hand, the zeros of $\Phi_4(C_t)$ are 0 and $C_t^{\text{int}_2}$, where

$$\begin{aligned} C_t^{\text{int}_2} &= \frac{\left[(k_m - C_0)k_c + k_n\right] k_s + (k_m k_g C_0 + k_n)k_c}{\left[(k_m - C_0)k_g - k_s\right] k_c C_0} \\ &= \frac{(k_m k_g - k_s)k_c C_0 + (k_s + k_c)k_n + k_m k_s k_c}{(k_m k_g - k_s)k_c C_0 - k_g k_c C_0^2} \end{aligned}$$

We consider the following two cases:

Case I: $k_m > \frac{k_s}{k_g} + C_0$. In this case,

- The above expression for $C_t^{\text{int}_2}$ must be greater than one because the numerator is greater than the denominator.
- The critical value of Φ_4; namely

$$C_t^{\text{crit}_2} = \frac{\left[(k_m - C_0)k_c + k_n\right] k_s + (k_m k_g C_0 + k_n)k_c}{2k_c C_0 \left[(k_m - C_0)k_g - k_s\right]},$$

  is positive, and
- Φ_4 is concave downwards on $(-\infty, \infty)$, increasing on $\left(-\infty, C_t^{\text{crit}_2}\right)$ and decreasing on $\left(C_t^{\text{crit}_2}, \infty\right)$.

In Figure 5.3a, the functions $\Phi_3(C_t)$ and $\Phi_4(C_t)$ are sketched. Both functions are monotonically increasing in C_t for all $C_t \in \left(0, C_t^{\text{crit}_2}\right)$.

Since

$$0 = \Phi_4(0) < \Phi_3(0) = k_m k_s k_c$$

and

$$k_c k_g C_0^2 + k_m k_s k_c = \Phi_3(1) < \Phi_4(1) = k_c k_g C_0^2 + k_m k_s k_c + (k_s + k_c)k_n,$$

a unique intersection (at $C_t = C_t^* \in (0, 1)$) of the curves defined by the functions $\Phi_3(C_t)$ and $\Phi_4(C_t)$ exists.

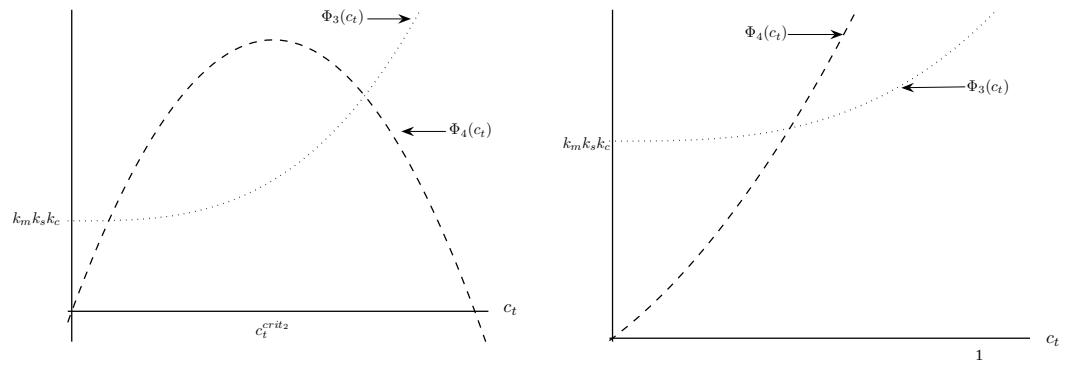

(a) The case when $k_m > \frac{k_s}{k_g} + C_0$ (b) The case when $k_m < \frac{k_s}{k_g} + C_0$

Figure 5.3: Illustration of the functions $\Phi_3(C_t)$ and $\Phi_4(C_t)$ of Eq. (5.14).

Case II: $k_m < \frac{k_s}{k_g} + C_0$. In this case,

- both $C_t^{\text{int}_2}$ and $C_t^{\text{crit}_2}$ are negative,
- Φ_4 is concave upwards at $C_t^{\text{crit}_2}$, decreasing on $\left(-\infty, C_t^{\text{crit}_2}\right)$ and increasing on $\left(C_t^{\text{crit}_2}, \infty\right)$, and
- Φ_4 is positive for all $C_t > 0$.

In Figure 5.3b, the functions $\Phi_3(C_t)$ and $\Phi_4(C_t)$ are sketched. Since

- both functions are monotonically increasing in C_t on $(0, 1)$,
- $0 = \Phi_4(0) < \Phi_3(0) = k_m k_s k_c$, and
- $k_c k_g C_0^2 + k_m k_s k_c = \Phi_3(1) < \Phi_4(1) = k_c k_g C_0^2 + k_m k_s k_c + (k_s + k_c) k_n$,

a unique intersection (at $C_t = C_t^* \in (0, 1)$) of the curves defined by the functions $\Phi_3(C_t)$ and $\Phi_4(C_t)$ exists.

Combining Case I and II, it follows that the functions Φ_3 and Φ_4 have a unique intersection point for $0 < C_t < 1$. The other intersection points are outside the interval $(0, 1)$ and are thus biologically irrelevant. Consequently, system (5.12) has a unique positive equilibrium

$$E_2^* = \left[C_t^*, \frac{(1 - C_t^*)k_s}{k_s + k_c}\right],$$

where C_t^* is the positive root to the cubic equation (5.14) satisfying $0 < C_t^* < 1$. This completes the proof of Theorem 5.1.8. □

Stability analysis of E_2^*

Theorem 5.1.9. *Providing that*

$$k_s + k_c > k_g C_0,$$

the equilibrium solution E_2^* of system (5.12) *is globally asymptotically stable with respect to the set $\widetilde{\boldsymbol{\Omega}}$.*

Proof. Computing the linearization matrix of system (5.12) around the equilibrium solution $E_2^* = \left[C_t^*, \frac{(1-C_t^*)k_s}{k_s+k_c}\right]$ we get

$$\mathbf{J}_{E_2^*} = \begin{bmatrix} -\frac{k_m k_n}{(k_m+C_0C_t^*)^2} + \frac{[(k_s+2k_c)C_t^*-k_c]k_gC_0}{k_s+k_c} & k_gC_0C_t^* + k_c \\ \\ -k_s & -(k_s+k_c) \end{bmatrix}$$

Now, the trace of $\mathbf{J}_{E_2^*}$ is given by

$$\mathrm{tr}(\mathbf{J}_{E_2^*}) = -\frac{k_m k_n}{(k_m + C_0C_t^*)^2} + \frac{[(k_s+2k_c)C_t^* - k_c]k_gC_0}{k_s+k_c} - (k_s+k_c)$$

$$= \frac{(k_m + C_0C_t^*)^2\left[(k_s+2k_c)k_gC_0C_t^* - k_ck_gC_0 - (k_s+k_c)^2\right] - k_mk_n(k_s+k_c)}{(k_m+C_0C_t^*)^2(k_s+k_c)}$$

$$= \frac{(k_m + C_0C_t^*)^2\big\{(k_s+k_c)\big[k_gC_0C_t^* - k_s - k_c\big] - k_ck_gC_0(1-C_t^*)\big\} - k_mk_n(k_s+k_c)}{(k_m+C_0C_t^*)^2(k_s+k_c)}$$

Imposing the condition

$$k_gC_0C_t^* < k_s + k_c,$$

the numerator of the above expression will be negative (recall that $C_t^* \in (0,1)$). Therefore,

$$C_t^* < \frac{k_s + k_c}{k_g C_0} \quad \Rightarrow \quad \text{tr}(\mathbf{J}_{E_2^*}) < 0 \, .$$

Taking $k_s + k_c > k_g C_0$, it follows that $\frac{k_s+k_c}{k_g C_0} > 1$ and, hence, the condition

$$C_t^* < \frac{k_s + k_c}{k_g C_0}$$

is satisfied (because $0 < C_t^* < 1$). Consequently, $\text{tr}(\mathbf{J}_{E_2^*}) < 0$ and, from Bendixson's criterion (Theorem 2.4.7), it follows that (5.12) has no nontrivial periodic solutions in $\mathbb{R}^2_+$ for all $C_t \in (0,1)$, provided that $k_s + k_c > k_g C_0$. Since E_2^* is unique, it follows by Poincaré-Bendixson theorem (Theorem 2.4.3) that all trajectories limit to the equilibrium E_2^*; that is, that E_2^* is globally asymptotically stable. This completes the proof of Theorem 5.1.9.□

Theorem 5.1.10. *If $C_0 > 0$, then on the set $\check{\boldsymbol{\Omega}}$, system* (5.9) *has a unique positive equilibrium solution*

$$E_2^{**} = \left(C_0 C_t^*, \ \frac{k_s C_0 (1 - C_t^*)}{k_s + k_c}, \ \frac{k_c C_0 (1 - C_t^*)}{k_s + k_c} \right),$$

where C_t^* is the unique positive root in the interval $(0,1)$ to the cubic equation

$$k_c k_g C_0^2 C_t^3 - \left[k_s - (k_m - C_0) k_g \right] k_c C_0 C_t^2 + k_m k_s k_c$$

$$- \left[(k_s + k_c) k_n + (k_g C_0 + k_s) k_m k_c - k_s k_c C_0 \right] C_t = 0.$$

Furthermore, providing that $k_s + k_c > k_g C_0$, E_2^{**} is globally asymptotically stable with respect to the set $\check{\boldsymbol{\Omega}}$.

Proof. This follows from remark 5.1.7. □

We mention here that on the basis of Theorem 5.1.9, we cannot provide a complete

analysis of the equilibria E_2^* and E_2^{**}. In other words, the theorem is silent on the stability of the equilibrium E_2^* in the case when $k_s + k_c < k_g C_0$ holds. In order to gain further insight on the asymptotic behaviour of the equilibrium solution E_2^{**}, we will conduct numerical simulations on the model for both the case when $k_s + k_c > k_g C_0$ and the case when $k_s + k_c < k_g C_0$.

Mathematical analysis of model III

We now analyze Model III for the special case $n = 1$; that is, we assume that the nucleation rate, k_n, linearly depends on the GTP-tubulin concentration. Then, system (4.13) becomes

$$\frac{dC_t}{dt} = k_c C_d - k_n C_t - k_g C_g C_t \tag{5.15a}$$
$$\frac{dC_d}{dt} = k_s C_s - k_c C_d \tag{5.15b}$$
$$\frac{dC_s}{dt} = k_{\text{cat}} C_g - (k_{\text{res}} + k_s) C_s \tag{5.15c}$$
$$\frac{dC_g}{dt} = k_n C_t + k_g C_g C_t + k_{\text{res}} C_s - k_{\text{cat}} C_g \tag{5.15d}$$

$$C_t(0) \geq 0, \quad C_d(0) \geq 0, \quad C_s(0) \geq 0, \quad C_g(0) \geq 0.$$

Summing the four equations in system (5.15), the conservation equation

$$\frac{d}{dt}\left[C_t(t) + C_d(t) + C_s(t) + C_g(t)\right] = 0$$

is obtained. This implies that the total concentration of all the variables in system (5.15) is a constant,

$$C_t(t) + C_d(t) + C_s(t) + C_g(t) = C_0 > 0, \qquad \forall\, t \geq 0.$$

The origin $(0,\ 0,\ 0,\ 0)$ is the trivial equilibrium solution of (5.15). This equilibrium corresponds to the case when the concentration of each variable in system (5.15) is equal to zero; that is, when $C_0 = 0$.

The Jacobian matrix of system (5.15), evaluated at the point (0, 0, 0, 0), is given by

$$\mathbf{J}_{(0,0,0,0)} = \mathbf{J_0} = \begin{bmatrix} -k_n & k_c & 0 & 0 \\ 0 & -k_c & k_s & 0 \\ 0 & 0 & -(k_{\text{res}} + k_s) & k_{\text{cat}} \\ k_n & 0 & k_{\text{res}} & -k_{\text{cat}} \end{bmatrix}$$

The matrix $\mathbf{J_0}$ is singular, implying that 0 is an eigenvalue of $\mathbf{J_0}$ associated with the left (row) eigenvector [1 1 1 1]. Furthermore, the digraph, $\mathcal{D}(\mathbf{J_0})$, associated with $\mathbf{J_0}$ is strongly connected, which implies that $\mathbf{J_0}$ is irreducible. Consequently, 0 is a simple eigenvalue of $\mathbf{J_0}$ [32]. This zero eigenvalue corresponds to the conservation of mass.
Using Gershgorin theorem[1], we know that all the eigenvalues of $\mathbf{J_0}$ have nonpositive real parts. In particular, defining

$$\hat{k} = \max\{k_n,\ k_c,\ k_{\text{res}} + k_s,\ k_{\text{cat}}\}, \tag{5.16}$$

all Gershgorin discs are contained in the disc centred at $-\hat{k}$ with radius $\hat{k}$.
We now need to show that [1 1 1 1] is (to a scalar) the only strictly positive[2] eigenvector of $\mathbf{J_0}$. We "shift" the matrix $\mathbf{J_0}$ by a multiple of the identity matrix $\mathbf{I}$ to make all of its elements nonnegative. Thus, we consider the matrix $\mathbf{J_0} + \hat{k}\mathbf{I}$, where $\hat{k}$ is given by (5.16). The new matrix $\mathbf{J_0} + \hat{k}\mathbf{I}$ inherits some spectral properties of an irreducible matrix. In particular, $\mathbf{J_0} + \hat{k}\mathbf{I}$ is irreducible, since the irreducibility of $\mathbf{J_0}$ is not affected by modifying

[1]

Theorem (Gershgorin)**.** [35] If $\mathbf{A} = (a_{ij})$ is an $n \times n$ matrix, then all the eigenvalues of $\mathbf{A}$ are located in the union of n discs $\cup_{j=1}^{n} D_j(\mathbf{A})$ where

$$D_j(\mathbf{A}) = \left\{ z \in \mathbb{C} : |z - a_{jj}| \leq \sum_{\substack{i=1 \\ i \neq j}}^{n} |a_{ij}| \right\}, \qquad j = 1, 2, \cdots, n.$$

Furthermore, if a union of k of these n disks forms a connected region that is disjoint from all the remaining $n - k$ discs, then there are precisely k eigenvalues of $\mathbf{A}$ in this region.

[2] A vector $\boldsymbol{x} = (x_1, \cdots, x_n)$ is said to be strictly (or strongly) positive, and we write $\boldsymbol{x} \gg 0$ if $x_i > 0$ for all $i = 1, \cdots, n$.

its diagonal entries.

By Perron-Frobenius theorem[3],

- the spectral radius of $\mathbf{J_0} + \hat{k}\mathbf{I}$ is a positive simple eigenvalue of $\mathbf{J_0} + \hat{k}\mathbf{I}$ strictly exceeding in modulus all other eigenvalues of $\mathbf{J_0} + \hat{k}\mathbf{I}$;
- there exists a positive eigenvector $\mathbf{v}$ corresponding to the eigenvalue $\rho(\mathbf{J_0} + \hat{k}\mathbf{I})$;
- any other nonnegative eigenvector of $\mathbf{J_0} + \hat{k}\mathbf{I}$ is a multiple of $\mathbf{v}$.

Using a left eigenvector, we have

$$\mathbf{v}^T(\mathbf{J_0} + \hat{k}\mathbf{I}) = \rho(\mathbf{J_0} + \hat{k}\mathbf{I})\mathbf{v}^T$$

for $\mathbf{v}^T \gg 0$ unique to a scalar multiple.

Since

$$[1\ 1\ 1\ 1](\mathbf{J_0} + \hat{k}\mathbf{I}) = [1\ 1\ 1\ 1]\mathbf{J_0} + \hat{k}[1\ 1\ 1\ 1] = \hat{k}[1\ 1\ 1\ 1],$$

it follows that $\rho(\mathbf{J_0} + \hat{k}\mathbf{I}) = \hat{k}$ and $\mathbf{v}^T = [1\ 1\ 1\ 1]$ is the eigenvector corresponding to the spectral radius $\hat{k}$ of $\mathbf{J_0} + \hat{k}\mathbf{I}$. We note that the spectra (the sets of all eigenvalues) $\sigma(\mathbf{J_0})$ and $\sigma(\mathbf{J_0} + \hat{k}\mathbf{I})$ of $\mathbf{J_0}$ and $\mathbf{J_0} + \hat{k}\mathbf{I}$, respectively, are translations of $\hat{k}$, which implies that $[1\ 1\ 1\ 1]$ is the only strictly positive (left) eigenvector of $\mathbf{J_0}$, and is associated to the eigenvalue 0.

Consequently, since $\sigma(\mathbf{J_0})$ and $\sigma(\mathbf{J_0} + \hat{k}\mathbf{I})$ are translations of $\hat{k}$, 0 is the dominant eigenvalue of $\mathbf{J_0}$ and is of multiplicity 1, and all other eigenvalues of $\mathbf{J_0}$ have negative real parts.

By the stable and centre manifold theorems (Theorems 2.3.1 and 2.3.2, respectively), we

[3]

Theorem (Perron-Frobenius)**.** [71] If $\mathbf{A} = (a_{ij})$ is an $n \times n$ nonnegative matrix, then $r = \rho(\mathbf{A})$ is an eigenvalue of $\mathbf{A}$ and there is a corresponding eigenvector $\mathbf{v} > 0$. If, in addition, $\mathbf{A}$ is irreducible, then $r > 0$ and $\mathbf{v} \gg 0$. Moreover, r has algebraic multiplicity one and if $\mathbf{u} > 0$ is an eigenvector of $\mathbf{A}$, then there exists $s > 0$ such that $\mathbf{u} = s\mathbf{v}$. If $\mathbf{B}$ is a matrix satisfying $\mathbf{B} > \mathbf{A}$, then $\rho(\mathbf{B}) > \rho(\mathbf{A})$. Finally, if $\mathbf{A} \gg 0$ then $|\lambda| < r$ for all other eigenvalues of $\mathbf{A}$.

deduce that there exists a local three-dimensional stable manifold through (0, 0, 0, 0) and a one-dimensional local centre manifold tangent to the eigenspace associated to the zero eigenvalue. It therefore follows that the origin is locally asymptotically stable.
We now turn to the search for the non-trivial equilibrium solution(s) of (5.15) − corresponding to the case $C_0 > 0$.The set

$$\overline{\boldsymbol{\Omega}} = \{(C_t, C_d, C_s, C_g) \in \mathbb{R}^4_+ : C_t \geq 0;\ C_d \geq 0;\ C_s \geq 0;\ C_g \geq 0;\ C_t + C_d + C_s + C_g = C_0\}$$

is positively invariant under the flow induced by system (5.15). It thus follows that system (5.15) is well posed with bounded solutions. Let us replace C_g in (5.15) with $C_0 - C_t - C_d - C_s$ to obtain a three-dimensional system

$$\begin{aligned}
\frac{dC_t}{dt} &= k_c C_d - k_n C_t - (C_0 - C_t - C_d - C_s)k_g C_t \\
\frac{dC_d}{dt} &= k_s C_s - k_c C_d \\
\frac{dC_s}{dt} &= k_{\text{cat}}(C_0 - C_t - C_d - C_s) - (k_{\text{res}} + k_s)C_s
\end{aligned}$$

That is

$$\frac{dC_t}{dt} = k_c C_d - k_n C_t - (C_0 - C_t)k_g C_t + (C_d + C_s)k_g C_t \tag{5.17a}$$

$$\frac{dC_d}{dt} = k_s C_s - k_c C_d \tag{5.17b}$$

$$\frac{dC_s}{dt} = (C_0 - C_t)k_{\text{cat}} - k_{\text{cat}} C_d - (k_{\text{cat}} + k_{\text{res}} + k_s)C_s \tag{5.17c}$$

It is convenient to describe system (5.17) in terms of relative proportions; that is,

$$\bar{C}_t = \frac{C_t}{C_0};\ \ \bar{C}_d = \frac{C_d}{C_0};\ \ \bar{C}_s = \frac{C_s}{C_0}.$$

With this transformation, system (5.17) becomes (after dropping the bars for notational simplicity)

$$\frac{dC_t}{dt} = k_c C_d - k_n C_t - (1 - C_t) k_g C_0 C_t + (C_s + C_d) k_g C_0 C_t \tag{5.18a}$$

$$\frac{dC_d}{dt} = k_s C_s - k_c C_d \tag{5.18b}$$

$$\frac{dC_s}{dt} = (1 - C_t - C_d) k_{\text{cat}} - (k_{\text{cat}} + k_{\text{res}} + k_s) C_s \tag{5.18c}$$

The set

$$\breve{\boldsymbol{\Omega}} = \{(C_t, C_d, C_s) \in \mathbb{R}^3_+ : C_t \geq 0;\ C_d \geq 0;\ C_s \geq 0;\ C_t + C_d + C_s \leq 1\}$$

is positively invariant with respect to system (5.18).

Equilibrium of system (5.18)

Theorem 5.1.11. *If $C_0 > 0$, then on the set $\breve{\boldsymbol{\Omega}}$, system* (5.18) *admits a unique positive equilibrium*

$$E_3^* = (C_t^*,\ C_d^*,\ C_s^*) = \left(C_t^*,\ \frac{k_s k_{\text{cat}}}{\kappa}(1 - C_t^*),\ \frac{k_c k_{\text{cat}}}{\kappa}(1 - C_t^*) \right),$$

where $\kappa = k_s k_{\text{cat}} + (k_{\text{cat}} + k_{\text{res}} + k_s) k_c$ and C_t^* is the unique positive root in the interval $(0, 1]$ to the equation

$$(k_{\text{res}} + k_s) k_g k_c C_0 C_t^2 - \left[\kappa k_n + (k_{\text{res}} + k_s) k_g k_c C_0 + k_s k_c k_{\text{cat}}\right] C_t + k_s k_c k_{\text{cat}} = 0.$$

Proof. The equilibrium solutions satisfy the following relations:

$$0 = k_c C_d - k_n C_t - (1 - C_t) k_g C_0 C_t + (C_s + C_d) k_g C_0 C_t \tag{5.19a}$$

$$0 = k_s C_s - k_c C_d \tag{5.19b}$$

$$0 = (1 - C_t) k_{\text{cat}} - k_{\text{cat}} C_d - (k_{\text{cat}} + k_{\text{res}} + k_s) C_s \tag{5.19c}$$

From Eq. (5.19b),

$$C_s = \frac{k_c}{k_s} C_d$$

Substituting this value in Eq. (5.19c) and solving for C_d gives

$$C_d = \frac{k_s k_{\text{cat}}}{\kappa}(1 - C_t) \tag{5.20}$$

where

$$\kappa = k_s k_{\text{cat}} + (k_{\text{cat}} + k_{\text{res}} + k_s)k_c \tag{5.21}$$

Hence

$$C_s = \frac{k_c k_{\text{cat}}}{\kappa}(1 - C_t) \tag{5.22}$$

Replacing the values of C_d and C_s in Eq. (5.19a) with (5.20) and (5.22), respectively, gives

$$-\kappa k_n C_t + E C_t^2 - (E + F)C_t + F = 0 \tag{5.23}$$

where

$$E = (k_{\text{res}} + k_s)k_g k_c C_0, \tag{5.24}$$

and

$$F = k_s k_c k_{\text{cat}}. \tag{5.25}$$

The positive roots, $C_t^* \in (0, 1]$, of Eq. (5.23) are the C_t components of the equilibrium solutions of (5.19).

The LHS of Eq. (5.23) can be written as a difference of two polynomials $P_8(C_t) - P_7(C_t)$, where

$$P_8(C_t) = E C_t^2 - (E + F)C_t + F$$

and

$$P_7(C_t) = \kappa k_n C_t$$

P_7 is linear and monotonically increasing in C_t for all $C_t \in (0, 1]$ and $P_7(0) = 0$, implying that $P_7(C_t) > 0$ for all $C_t \in (0, 1]$.

On the other hand, P_8 is quadratic in C_t, is concave upwards, and cuts the vertical axis at $F > 0$. Furthermore, $P_8(C_t)$

- cuts the C_t-axis at $C_t = 1$ and $C_t = \frac{F}{E} > 0$;
- is decreasing on the interval $\left(0, \frac{E+F}{2E}\right)$ and increasing on the interval $\left(\frac{E+F}{2E}, \infty\right)$, and
- is positive on the intervals $\left(0,\ \min(1, \frac{F}{E})\right)$ and $\left(\max(1, \frac{F}{E}),\ \infty\right)$.

We consider the following two cases.

Case I: $\min(1, \frac{F}{E}) = \frac{F}{E}$. In this case (see Figure 5.4a),

- $P_8(C_t) > 0, \ \forall\, C_t \in \left(0, \frac{F}{E}\right) \subset (0, 1)$,
- $P_7(C_t) > 0, \ \forall\, C_t \in (0, 1)$,
- $P_7(C_t)$ is monotonically increasing in C_t on $(0, 1)$, and
- $P_8(C_t)$ is monotonically decreasing in C_t on $\left(0, \frac{F}{E}\right)$.

Since

$$0 = P_7(0) < P_8(0) = F,$$

and

$$\kappa k_n = P_7(1) > P_8(1) = 0,$$

it follows that $P_7(C_t)$ and $P_8(C_t)$ have a unique intersection at $0 < C_t^* < \frac{F}{E}$ on $(0, 1)$. The other intersection point, if it exists, is biologically irrelevant since the state variables in system (5.18) are in proportions.

Case II: $\min(1, \frac{F}{E}) = 1$. In this case (see Figure 5.4b),

- $P_8(C_t) > 0, \ \forall\, C_t \in (0, 1)$,
- $P_7(C_t) > 0, \ \forall\, C_t \in (0, 1)$,

– $P_7(C_t)$ is monotonically increasing in C_t on $(0, 1)$, and

– $P_8(C_t)$ is monotonically decreasing in C_t on $(0, 1)$.

Since

$$0 = P_7(0) < P_8(0) = F,$$

and

$$\kappa k_n = P_7(1) > P_8(1) = 0,$$

it follows that $P_7(C_t)$ and $P_8(C_t)$ have a unique intersection at $0 < C_t^* < 1$. The other intersection point, if it exists, is biologically irrelevant.

Combining Case I and II, it follows that $P_7(C_t)$ and $P_8(C_t)$ have a unique intersection at

$$0 < C_t^* < \min\left(1, \frac{F}{E}\right).$$

To obtain the precise expression of C_t^*, we write Eq. (5.23) as

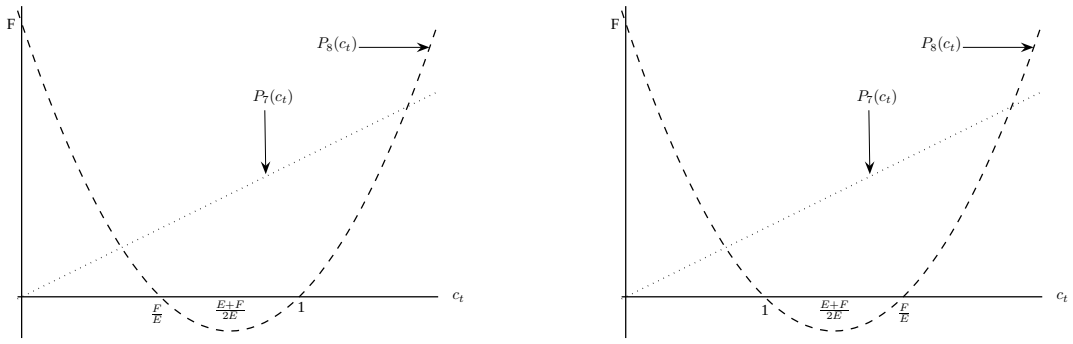

(a) The case when $\min(1, \frac{F}{E}) = \frac{F}{E}$ (b) The case when $\min(1, \frac{F}{E}) = 1$

Figure 5.4: Illustration of the functions $P_7(C_t)$ and $P_8(C_t)$ of Eq. (5.23).

$$EC_t^2 - (\kappa k_n + E + F)C_t + F = 0 \tag{5.26}$$

and solve (5.26) for C_t to obtain the roots C_t^* and C_t^u ($C_t^* < C_t^u$), where

$$C_t^* = \frac{\kappa k_n + E + F - \sqrt{(\kappa k_n + E + F)^2 - 4EF}}{2E};$$

that is,

$$\begin{aligned} C_t^* &= \frac{\kappa k_n + E + F - \sqrt{(\kappa k_n + E - F)^2 + 4\kappa k_n F}}{2E} \\ \Rightarrow C_t^* &< \frac{\kappa k_n + E + F - (\kappa k_n + E - F)}{2E} = \frac{F}{E} \qquad \text{(Recall that } \frac{F}{E} > 0\text{)} \end{aligned}$$

and

$$\begin{aligned} C_t^u &= \frac{\kappa k_n + E + F + \sqrt{(\kappa k_n + E - F)^2 + 4\kappa k_n F}}{2E} \\ \Rightarrow C_t^u &> \frac{\kappa k_n + E + F + (\kappa k_n + E - F)}{2E} = 1 + \frac{\kappa k_n}{E} > 1 \end{aligned}$$

Consequently, system (5.18) has a unique positive equilibrium

$$E_3^* = \left(C_t^*,\ \frac{k_s k_{\text{cat}}}{\kappa} (1 - C_t^*),\ \frac{k_c k_{\text{cat}}}{\kappa} (1 - C_t^*) \right),$$

where κ is given by (5.21) and

$$C_t^* = \frac{\kappa k_n + E + F - \sqrt{(\kappa k_n + E + F)^2 - 4EF}}{2E} \in \left(0, \min\left(\frac{F}{E},\ 1\right) \right)$$

This completes the proof of Theorem 5.1.11. □

Remark 5.1.12. With respect to system (5.15), the unique positive equilibrium is given by

$$E_3^{**} = \left(C_0 C_t^*,\ \frac{k_s k_{\text{cat}} C_0}{\kappa} (1 - C_t^*),\ \frac{k_c k_{\text{cat}} C_0}{\kappa} (1 - C_t^*),\ \frac{(k_{\text{res}} + k_s) k_c C_0}{\kappa} (1 - C_t^*) \right),$$

where C_t^* is the unique positive root in the interval $(0,1)$ to the equation (5.23). This is obtained by multiplying each component in the equilibrium solution of (5.18) by C_0 and using the fact that $C_g(t) = C_0 - C_s(t) - C_t(t) - C_d(t)$.

Stability analysis of E_3^*

Theorem 5.1.13. *The unique positive equilibrium E_3^* of system* (5.18) *is globally asymptotically stable in the domain*

$$\hat{\boldsymbol{\Omega}} = \Big\{(C_t, C_d, C_s) \in \mathbb{R}^3_+ : C_t \geq 0,\ \ C_d > \frac{3k_s k_{\text{cat}}}{\kappa}\left(1 - C_t^*\right),$$

$$C_s > \frac{k_{\text{cat}}}{k_{\text{cat}} + k_{\text{res}} + k_s} + \left[k_c - \frac{k_s k_{\text{cat}}}{2(k_{\text{cat}} + k_{\text{res}} + k_s)}\right]\frac{k_{\text{cat}}}{\kappa}\left(1 - C_t^*\right),\ \ C_t + C_d + C_s \leq 1\Big\}$$

Proof. Consider the Lyapunov function

$$V_1(C_t, C_d, C_s) = \frac{1}{2}\Big[A(C_d - C_d^*)^2 + B(C_s - C_s^*)^2 + C(C_t - C_t^*)^2\Big], \tag{5.27}$$

where the constants A, B and C are to be determined. Then,

- V_1 is continuously differentiable on $\hat{\boldsymbol{\Omega}}$,
- $V_1(C_t^*, C_d^*, C_s^*) = 0$, and
- $V_1(C_t, C_d, C_s) > 0, \quad \forall\ (C_t,\ C_d,\ C_s) \in \hat{\boldsymbol{\Omega}} \setminus \{(C_t^*, C_d^*, C_s^*)\}$

Time differentiating (5.27) along the solutions of (5.18) we get

$$\dot{V}_1 = A(C_d - C_d^*)\dot{C}_d + B(C_s - C_s^*)\dot{C}_s + C(C_t - C_t^*)\dot{C}_t$$

$$= A(C_d - C_d^*)(k_s C_s - k_c C_d) + B(C_s - C_s^*)\big[k_{\text{cat}}(1 - C_t - C_d - C_s) - (k_{\text{res}} + k_s)C_s\big]$$

$$+ C(C_t - C_t^*)\big[k_c C_d - k_n C_t - (1 - C_t)k_g C_0 C_t + (C_d + C_s)k_g C_0 C_t\big]$$

$$= -\Big\{ \big[(k_{\text{cat}} + k_{\text{res}} + k_s)B(C_s - C_s^*) + Ak_sC_d^* - Bk_{\text{cat}}\big]C_s + Bk_{\text{cat}}C_s^*$$

$$+ (Ak_c(C_d - C_d^*) - Bk_{\text{cat}}C_s^*)C_d + (Bk_{\text{cat}} - Ak_s)C_dC_s + (C_s - C_s^*)Bk_{\text{cat}}C_t$$

$$+ C(C_t - C_t^*)\left[k_nC_t + (1 - C_t)k_gC_0C_t - k_cC_d - (C_d + C_s)k_gC_0C_t\right]\Big\}$$

If we now take $A = 1$, $B = \frac{2k_s}{k_{\text{cat}}}$, and $C = 0$, then $\dot{V}_1$ will be negative if the following four inequalities hold simultaneously:

$$(k_{\text{cat}} + k_{\text{res}} + k_s)B(C_s - C_s^*) + Ak_sC_d^* - Bk_{\text{cat}} > 0 \quad \Leftrightarrow \quad C_s > C_s^* + \frac{\left(k_{\text{cat}} - \frac{Ak_sC_d^*}{B}\right)}{k_{\text{cat}} + k_{\text{res}} + k_s} \tag{5.28}$$

$$Ak_c(C_d - C_d^*) - Bk_{\text{cat}}C_s^* > 0 \quad \Leftrightarrow \quad C_d > C_d^* + \frac{Bk_{\text{cat}}}{Ak_c}C_s^* \,, \tag{5.29}$$

$$Bk_{\text{cat}} - Ak_s > 0 \quad \Leftrightarrow \quad B > \frac{Ak_s}{k_{\text{cat}}} \,, \tag{5.30}$$

$$C_s - C_s^* > 0 \quad \Leftrightarrow \quad C_s > C_s^* \,. \tag{5.31}$$

Replacing the values of C_d^* and C_s^* in inequalities (5.28 - 5.31), we obtain

$$C_s > \frac{k_{\text{cat}}}{k_{\text{cat}} + k_{\text{res}} + k_s} + \left[k_c - \frac{k_sk_{\text{cat}}}{2(k_{\text{cat}} + k_{\text{res}} + k_s)}\right]\frac{k_{\text{cat}}}{\kappa}(1 - C_t^*) \tag{5.32}$$

$$C_d > \frac{3k_sk_{\text{cat}}}{\kappa}(1 - C_t^*) \tag{5.33}$$

$$\frac{2k_s}{k_{\text{cat}}} > \frac{k_s}{k_{\text{cat}}} \tag{5.34}$$

$$C_s > \frac{k_ck_{\text{cat}}}{\kappa}(1 - C_t^*) \tag{5.35}$$

Now, inequality (5.32) can be rewritten as

$$C_s > \frac{k_c k_{\text{cat}}}{\kappa}\,(1 - C_t^*) + \frac{k_{\text{cat}}\big(1 - C_d^*/2\big)}{k_{\text{cat}} + k_{\text{res}} + k_s},$$

and, since $C_d^* < 1$, the region defined by inequality (5.35) is contained in the region defined by inequality (5.32). Consequently,

$$\dot{V}_1 < 0 \quad \forall\, (C_t,\ C_d,\ C_s) \in \hat{\boldsymbol{\Omega}} \setminus \{(C_t^*, C_d^*, C_s^*)\}.$$

By Lyapunov's stability theorem, it follows that the equilibrium solution, $E_3^* = [C_t^*,\ C_d^*,\ C_s^*]$, is globally asymptotically stable for system (5.18) on the domain $\hat{\boldsymbol{\Omega}}$. This completes the proof of Theorem 5.1.13. □

Remarks. Note that the global stability of the equilibrium solution E_3^* is proved in a very restricted region of the phase space, such that for any transients around C_s^*, for example, the function V_1 fails to be a Lyapunov function. From Remark 5.1.12, we state the following theorem.

Theorem 5.1.14. *If $C_0 > 0$, then on the set $\overline{\boldsymbol{\Omega}}$, system* (5.15) *admits a unique positive equilibrium*

$$E_3^{**} = \left(C_0 C_t^*,\ \frac{k_s k_{\text{cat}} C_0}{\kappa}\,(1 - C_t^*)\,,\ \frac{k_c k_{\text{cat}} C_0}{\kappa}\,(1 - C_t^*)\,,\ \frac{(k_{\text{res}} + k_s) k_c C_0}{\kappa}\,(1 - C_t^*)\right),$$

where $\kappa = k_s k_{\text{cat}} + (k_{\text{cat}} + k_{\text{res}} + k_s) k_c$ and C_t^* is the unique positive root in the interval $(0, 1]$ to the equation

$$(k_{\text{res}} + k_s) k_g k_c C_0 C_t^2 - \left[\kappa k_n + (k_{\text{res}} + k_s) k_g k_c C_0 + k_s k_c k_{\text{cat}}\right] C_t + k_s k_c k_{\text{cat}} = 0.$$

Furthermore, E_3^{**} is globally stable on the domain $\hat{\boldsymbol{\Omega}}$.

Mathematical analysis of model IV

We will analyze model IV for the special case when $n = 1$; that is, we consider the following system:

$$\frac{dC_t}{dt} = k_c C_d - \frac{k_n C_t}{k_m + C_t} - k_g C_g C_t \tag{5.36a}$$

$$\frac{dC_d}{dt} = k_s C_s - k_c C_d \tag{5.36b}$$

$$\frac{dC_s}{dt} = k_{\text{cat}} C_g - (k_s + k_{\text{res}})\, C_s \tag{5.36c}$$

$$\frac{dC_g}{dt} = \frac{k_n C_t}{k_m + C_t} + (k_g C_t - k_{\text{cat}}) C_g + k_{\text{res}} C_s \tag{5.36d}$$

$$C_t(0) \geq 0, \quad C_d(0) \geq 0, \quad C_s(0) \geq 0, \quad C_g(0) \geq 0.$$

We note that

$$\frac{d}{dt}\left(C_t(t) + C_d(t) + C_g(t) + C_s(t)\right) = 0;$$

that is, the total concentration in the system is a constant

$$C_t(t) + C_d(t) + C_g(t) + C_s(t) = C_0$$

This constraint guarantees the boundedness of solutions of (5.36).

The origin $(0,\ 0,\ 0,\ 0)$ is the trivial equilibrium solution of (5.36). The trivial equilibrium occurs when $C_0 = 0$; that is, when there is no tubulin in the experiment.

The Jacobian matrix of system (5.36), evaluated at the point $(0,\ 0,\ 0,\ 0)$, is given by

$$\mathbf{J}_{(0,0,0,0)} = \mathbf{J_0} = \begin{bmatrix} -\frac{k_n}{k_m} & k_c & 0 & 0 \\ 0 & -k_c & k_s & 0 \\ 0 & 0 & -(k_{\text{res}} + k_s) & k_{\text{cat}} \\ \frac{k_n}{k_m} & 0 & k_{\text{res}} & -k_{\text{cat}} \end{bmatrix}$$

The matrix $\mathbf{J_0}$ is singular, implying that 0 is an eigenvalue of $\mathbf{J_0}$ associated with the left (row) eigenvector [1 1 1 1]. Furthermore, the digraph, $\mathcal{D}(\mathbf{J_0})$, associated with $\mathbf{J_0}$ is strongly connected, which implies that $\mathbf{J_0}$ is irreducible. Consequently, 0 is a simple eigenvalue of $\mathbf{J_0}$ [32]. The existence of this zero eigenvalue is due to the conservation of mass.

Using Gershgorin theorem, we know that all the eigenvalues of $\mathbf{J_0}$ have nonpositive real parts. In particular, defining

$$\tilde{k} = \max\left\{\frac{k_n}{k_m},\ k_c,\ k_{\text{res}} + k_s,\ k_{\text{cat}}\right\}, \tag{5.37}$$

all Gershgorin discs are contained in the disc centred at $-\tilde{k}$ with radius $\tilde{k}$.

We now need to show that [1 1 1 1] is (to a scalar) the only strictly positive eigenvector of $\mathbf{J_0}$. We "shift" the matrix $\mathbf{J_0}$ by a multiple of the identity matrix $\mathbf{I}$ to make all of its elements nonnegative. Thus, we consider the matrix $\mathbf{J_0} + \tilde{k}\mathbf{I}$, where $\tilde{k}$ is given by (5.37). The new matrix $\mathbf{J_0} + \tilde{k}\mathbf{I}$ inherits some spectral properties of an irreducible matrix. In particular, $\mathbf{J_0} + \tilde{k}\mathbf{I}$ is irreducible, since the irreducibility of $\mathbf{J_0}$ is not affected by modifying its diagonal entries.

By Perron-Frobenius theorem,

- the spectral radius of $\mathbf{J_0} + \tilde{k}\mathbf{I}$ is a positive simple eigenvalue of $\mathbf{J_0} + \tilde{k}\mathbf{I}$ strictly exceeding in modulus all other eigenvalues of $\mathbf{J_0} + \tilde{k}\mathbf{I}$;
- there exists a positive eigenvector $\mathbf{v}$ corresponding to the eigenvalue $\rho(\mathbf{J_0} + \tilde{k}\mathbf{I})$;
- any other nonnegative eigenvector of $\mathbf{J_0} + \tilde{k}\mathbf{I}$ is a multiple of $\mathbf{v}$.

Using a left eigenvector, we have

$$\mathbf{v}^T(\mathbf{J_0} + \tilde{k}\mathbf{I}) = \rho(\mathbf{J_0} + \tilde{k}\mathbf{I})\mathbf{v}^T$$

for $\mathbf{v}^T \gg 0$ unique to a scalar multiple.

Since

$$[1\ 1\ 1\ 1](\mathbf{J_0} + \tilde{k}\mathbf{I}) = [1\ 1\ 1\ 1]\mathbf{J_0} + \tilde{k}[1\ 1\ 1\ 1] = \tilde{k}[1\ 1\ 1\ 1],$$

it follows that $\rho(\mathbf{J_0} + \tilde{k}\mathbf{I}) = \tilde{k}$ and $\mathbf{v}^T = [1\ 1\ 1\ 1]$ is the eigenvector corresponding to the spectral radius $\tilde{k}$ of $\mathbf{J_0} + \tilde{k}\mathbf{I}$. We note that the spectra (the sets of all eigenvalues) $\sigma(\mathbf{J_0})$ and $\sigma(\mathbf{J_0} + \tilde{k}\mathbf{I})$ of $\mathbf{J_0}$ and $\mathbf{J_0} + \tilde{k}\mathbf{I}$, respectively, are translations of $\tilde{k}$, which implies that [1 1 1 1] is the only strictly positive (left) eigenvector of $\mathbf{J_0}$, and is associated to the eigenvalue 0.

Consequently, since $\sigma(\mathbf{J_0})$ and $\sigma(\mathbf{J_0} + \tilde{k}\mathbf{I})$ are translations of $\tilde{k}$, 0 is the dominant eigenvalue of $\mathbf{J_0}$ and is of multiplicity 1, and all other eigenvalues of $\mathbf{J_0}$ have negative real parts. By the stable and centre manifold theorems (Theorems 2.3.1 and 2.3.2, respectively), we deduce that there exists a local three-dimensional stable manifold through $(0,\ 0,\ 0,\ 0)$ and a one-dimensional local centre manifold tangent to the eigenspace associated to the zero eigenvalue. Therefore, the origin is locally asymptotically stable.

Let us now consider the non-trivial equilibrium solution(s) of (5.36); that is, the equilibrium solution(s) of (5.36) when $C_0 > 0$.

The set

$$\boldsymbol{\Omega}_4 = \{(C_t, C_d, C_s, C_g) \in \mathbb{R}^4_+ : C_t \geq 0;\ C_d \geq 0;\ C_s \geq 0;\ C_g \geq 0;\ C_t + C_d + C_s + C_g = C_0\}$$

is positively invariant under the flow of (5.36). It thus follows that system (5.36) is well posed with bounded solutions. We can reduce system (5.36) to a three-dimensional system by introducing

$$C_g(t) = C_0 - C_t(t) - C_d(t) - C_s(t)$$

to obtain

$$\frac{dC_t}{dt} = k_c C_d - \frac{k_n C_t}{k_m + C_t} - (C_0 - C_t - C_d - C_s)k_g C_t \tag{5.38a}$$

$$\frac{dC_d}{dt} = k_s C_s - k_c C_d \tag{5.38b}$$

$$\frac{dC_s}{dt} = (C_0 - C_t - C_d - C_s)k_{\text{cat}} - (k_s + k_{\text{res}})C_s \tag{5.38c}$$

Next, define

$$\bar{C}_t = \frac{C_t}{C_0}, \quad \bar{C}_d = \frac{C_d}{C_0}, \quad \bar{C}_s = \frac{C_s}{C_0},$$

so that from Eqns. (5.38a-5.38c), we have

$$\begin{aligned}
\frac{d\bar{C}_t}{dt} &= k_c\bar{C}_d - \frac{k_n\bar{C}_t}{k_m + C_0\bar{C}_t} - (1 - \bar{C}_t - \bar{C}_d - \bar{C}_s)k_g C_0\bar{C}_t \\
\frac{d\bar{C}_d}{dt} &= k_s\bar{C}_s - k_c\bar{C}_d \\
\frac{d\bar{C}_s}{dt} &= (1 - \bar{C}_t - \bar{C}_d - \bar{C}_s)k_{\text{cat}} - (k_{\text{res}} + k_s)\bar{C}_s
\end{aligned}$$

Thus by dropping the bar for notational simplicity, we have

$$\frac{dC_t}{dt} = k_c C_d - \frac{k_n C_t}{k_m + C_0 C_t} - (1 - C_t - C_d - C_s)k_g C_0 C_t \tag{5.39a}$$

$$\frac{dC_d}{dt} = k_s C_s - k_c C_d \tag{5.39b}$$

$$\frac{dC_s}{dt} = (1 - C_t - C_d - C_s)k_{\text{cat}} - (k_{\text{res}} + k_s)C_s \tag{5.39c}$$

The set

$$\tilde{\boldsymbol{\Omega}}_4 = \{(C_t, C_d, C_s) \in \mathbb{R}^3_+ : C_t \geq 0;\ C_d \geq 0;\ C_s \geq 0;\ C_t + C_d + C_s \leq 1\}$$

is positively invariant with respect to system (5.39).

Equilibria of system (5.39)

Theorem 5.1.15. *If $C_0 > 0$, then on the set $\tilde{\boldsymbol{\Omega}}_4$, system* (5.39) *admits a unique positive equilibrium*

$$E_4^* = \left(C_t^*,\ \frac{k_s k_{\text{cat}}}{\kappa}(1 - C_t^*),\ \frac{k_c k_{\text{cat}}}{\kappa}(1 - C_t^*)\right),$$

where $\kappa = k_s k_{\text{cat}} + (k_{\text{cat}} + k_{\text{res}} + k_s)k_c$ *and* C_t^* *is the unique positive root in the interval* $(0, 1)$ *to the equation*

$$(k_{\text{res}} + k_s)k_g k_c C_0^2 C_t^3 - \left[k_s k_{\text{cat}} - (k_m - C_0)(k_{\text{res}} + k_s)k_g\right] k_c C_0 C_t^2$$

$$- \left[(k_m - C_0)k_s k_c k_{\text{cat}} + (k_{\text{res}} + k_s)k_g k_c C_0 k_m + \kappa k_n\right] C_t + k_s k_c k_{\text{cat}} k_m = 0$$

Proof. Setting the time derivatives of system (5.39) equal to zero, we have

$$0 = k_c C_d - \frac{k_n C_t}{k_m + C_0 C_t} - (1 - C_t - C_d - C_s)k_g C_0 C_t \tag{5.40a}$$

$$0 = k_s C_s - k_c C_d \tag{5.40b}$$

$$0 = (1 - C_t - C_d - C_s)k_{\text{cat}} - (k_{\text{res}} + k_s)C_s \tag{5.40c}$$

From Eq. (5.40b),

$$C_s = \frac{k_c}{k_s} C_d$$

Substituting this value in Eq. (5.40c) and solving for C_d gives

$$C_d = \frac{k_s k_{\text{cat}}}{\kappa}(1 - C_t) \tag{5.41}$$

where κ is given by (5.21).

Therefore,

$$C_s = \frac{k_c k_{\text{cat}}}{\kappa}(1 - C_t) \tag{5.42}$$

Replacing the values of C_d and C_s with (5.41) and (5.42), respectively, in Eq. (5.40a) gives

$$\frac{k_s k_c k_{\text{cat}}}{\kappa}(1 - C_t) - \frac{k_n C_t}{k_m + C_0 C_t} - \frac{(k_{\text{res}} + k_s)k_c}{\kappa}(1 - C_t)k_g C_0 C_t = 0$$

This gives a cubic polynomial in C_t:

$$EC_0C_t^3 - [FC_0 - (k_m - C_0)E]\,C_t^2 - [(k_m - C_0)F + Ek_m + \kappa k_n]\,C_t + Fk_m = 0, \quad (5.43)$$

where E and F are given by (5.24) and (5.25), respectively. The positive roots, C_t^*, of Eq. (5.43) are the C_t components of the equilibrium solutions of (5.40).
We write the left hand side of Eq. (5.43) as a difference of two polynomials $\Phi_1(C_t) - \Phi_2(C_t)$, where

$$\Phi_1(C_t) = EC_0C_t^3 + Fk_m$$

and

$$\Phi_2(C_t) = [FC_0 - (k_m - C_0)E]\,C_t^2 + [(k_m - C_0)F + Ek_m + \kappa k_n]\,C_t$$

The function $\Phi_1(C_t)$ is monotonically increasing in C_t on the interval $(0, 1)$. We consider the following cases.

Case I: $k_m > \frac{E+F}{E}C_0$. In this case

- $\Phi_2(C_t)$ cuts the C_t-axis at the points

$$C_t = 0 \qquad \text{and} \qquad C_t^{\text{int}_6} = \frac{(k_m - C_0)F + Ek_m + \kappa k_n}{(k_m - C_0)E - FC_0} > 0$$

- $\Phi_2(C_t)$ is concave downwards, increasing on $(0,\, C_t^{\text{crit}_6})$ and decreasing on $(C_t^{\text{crit}_6},\, \infty)$, where

$$C_t^{\text{crit}_6} = \frac{(k_m - C_0)F + Ek_m + \kappa k_n}{2\,[(k_m - C_0)E - FC_0]} > 0$$

– $\Phi_2(C_t)$ is positive for all $C_t \in \left(0, C_t^{\text{int}_6}\right)$.

In Figure 5.5a, the functions $\Phi_1(C_t)$ and $\Phi_2(C_t)$ are sketched. Since

$$0 = \Phi_2(0) < \Phi_1(0) = Fk_m$$

and

$$EC_0 + Fk_m = \Phi_1(1) < \Phi_2(1) = EC_0 + Fk_m + \kappa k_n,$$

a unique intersection (at $C_t = C_t^* \in (0,1)$) of the curves defined by the functions $\Phi_1(C_t)$ and $\Phi_2(C_t)$ exists.

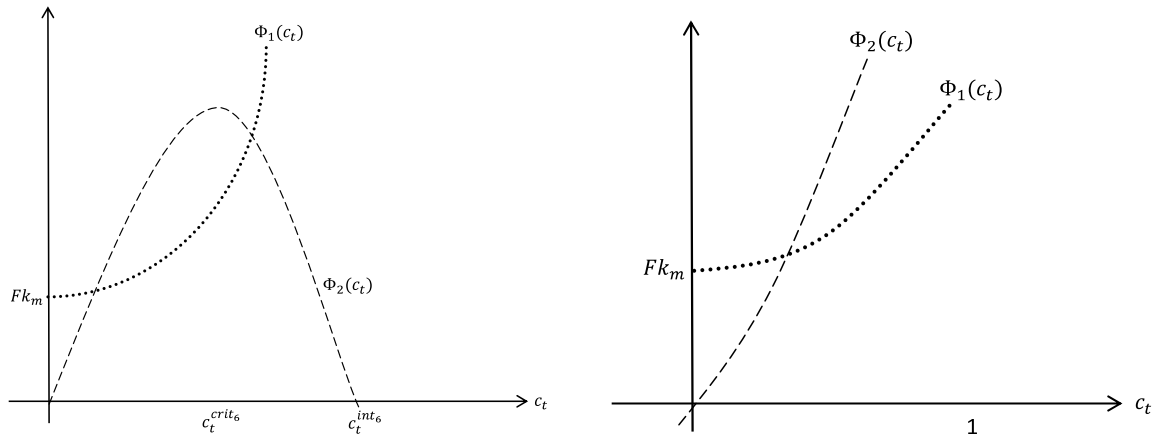

(a) The case when $k_m > \frac{E+F}{E}C_0$ (b) The case when $C_0 < k_m < \frac{E+F}{E}C_0$

Figure 5.5: Illustration of the functions $\Phi_1(C_t)$ and $\Phi_2(C_t)$ of Eq. (5.43).

Case II: $C_0 < k_m < \frac{E+F}{E}C_0$. In this case

- $\Phi_2(C_t)$ cuts the C_t-axis at the points

$$C_t = 0 \qquad \text{and} \qquad C_t^{\text{int}_6} = \frac{(k_m - C_0)F + Ek_m + \kappa k_n}{(k_m - C_0)E - FC_0} < 0$$

- $\Phi_2(C_t)$ is concave upwards, decreasing on $(-\infty,\, C_t^{\text{crit}_7})$ and increasing on $(C_t^{\text{crit}_7},\, 1)$, where

$$C_t^{\text{crit}_7} = \frac{(k_m - C_0)F + Ek_m + \kappa k_n}{2\left[(k_m - C_0)E - FC_0\right]} < 0$$

- $\Phi_2(C_t)$ is positive for all $C_t \in (0,1)$.

Both functions, $\Phi_1(C_t)$ and $\Phi_2(C_t)$, are monotonically increasing in C_t on the interval $(0,1)$. Since

$$0 = \Phi_2(0) < \Phi_1(0) = Fk_m$$

and

$$EC_0 + Fk_m = \Phi_1(1) < \Phi_2(1) = EC_0 + Fk_m + \kappa k_n,$$

a unique intersection (at $C_t = C_t^* \in (0,1)$) of the curves defined by the functions $\Phi_1(C_t)$ and $\Phi_2(C_t)$ exists.

Combining Case I and II, we conclude that $\Phi_1(C_t)$ and $\Phi_2(C_t)$ have a unique intersection point at $C_t = C_t^* \in (0,1)$. Consequently, system (5.39) has a unique equilibrium

$$E_4^* = \left(C_t^*,\ \frac{k_s k_{\text{cat}}}{\kappa}(1 - C_t^*),\ \frac{k_c k_{\text{cat}}}{\kappa}(1 - C_t^*) \right),$$

where C_t^* is the unique positive root to the cubic equation (5.43) on the interval $(0,1)$. This completes the proof of Theorem 5.1.15. □

Remark 5.1.16. With respect to system (5.36), the unique positive equilibrium is given by

$$E_4^{**} = \left(C_0 C_t^*,\ \frac{k_s k_{\text{cat}} C_0}{\kappa}\left(1 - C_t^*\right),\ \frac{k_c k_{\text{cat}} C_0}{\kappa}\left(1 - C_t^*\right),\ \frac{(k_{\text{res}} + k_s) k_c C_0}{\kappa}\left(1 - C_t^*\right) \right),$$

where $\kappa = k_s k_{\text{cat}} + (k_{\text{cat}} + k_{\text{res}} + k_s)k_c$ and C_t^* is the unique positive root in the interval $(0,1)$ to the equation

$$(k_{\text{res}} + k_s)k_g k_c C_0^2 C_t^3 - \left[k_s k_{\text{cat}} - (k_m - C_0)(k_{\text{res}} + k_s)k_g\right] k_c C_0 C_t^2$$

$$- \left[(k_m - C_0)k_s k_c k_{\text{cat}} + (k_{\text{res}} + k_s)k_g k_c C_0 k_m + \kappa k_n\right] C_t + k_s k_c k_{\text{cat}} k_m = 0.$$

E_4^{**} is obtained by multiplying each component in the equilibrium solution of (5.38) by C_0 and using the fact that $C_g(t) = C_0 - C_s(t) - C_t(t) - C_d(t)$.

Stability analysis of E_4^*

Theorem 5.1.17. *The unique positive equilibrium E_4^* of system* (5.39) *is globally asymptotically stable in the domain*

$$\overline{\boldsymbol{\Omega}}_4 = \Big\{(C_t, C_d, C_s) \in \mathbb{R}^3_+ : C_t \geq 0,\ \ C_d > \frac{3k_s k_{\text{cat}}}{\kappa}\left(1 - C_t^*\right),$$

$$C_s > \frac{k_{\text{cat}}}{k_{\text{cat}} + k_{\text{res}} + k_s} + \left[k_c - \frac{k_s k_{\text{cat}}}{2(k_{\text{cat}} + k_{\text{res}} + k_s)}\right]\frac{k_{\text{cat}}}{\kappa}\left(1 - C_t^*\right),\ \ C_t + C_d + C_s \leq 1\Big\}$$

Proof. Consider the Lyapunov function

$$V_2(C_t, C_d, C_s) = \frac{A_1}{2}(C_d - C_d^*)^2 + A_2(C_s - C_s^*)^2 + \frac{A_3}{2}(C_t - C_t^*)^2, \tag{5.44}$$

where the constants A_1, A_2 and A_3 are to be determined. Then,

- V_2 is continuously differentiable on $\overline{\boldsymbol{\Omega}}_4$,
- $V_2(C_t^*, C_d^*, C_s^*) = 0$, and
- $V_2(C_t, C_d, C_s) > 0, \quad \forall\ (C_t,\ C_d,\ C_s) \in \overline{\boldsymbol{\Omega}}_4 \setminus \{(C_t^*, C_d^*, C_s^*)\}$

Time differentiating (5.44) along the solutions of (5.39) we get

$$\dot{V}_2 = A_1(C_d - C_d^*)\dot{C}_d + 2A_2(C_s - C_s^*)\dot{C}_s + A_3(C_t - C_t^*)\dot{C}_t$$

$$= A_1(C_d - C_d^*)(k_s C_s - k_c C_d) + 2A_2(C_s - C_s^*)\big[k_{\text{cat}}(1 - C_t - C_d - C_s) - (k_{\text{res}} + k_s)C_s\big]$$

$$+ A_3(C_t - C_t^*)\left[k_c C_d - \frac{k_n C_t}{k_m + C_0 C_t} - (1 - C_t - C_d - C_s)k_g C_0 C_t\right]$$

$$= -\Big\{ \big[(k_{\text{cat}} + k_{\text{res}} + k_s)2A_2(C_s - C_s^*) + A_1 k_s C_d^* - 2A_2 k_{\text{cat}}\big] C_s + 2A_2 k_{\text{cat}} C_s^*$$

$$+ (A_1 k_c (C_d - C_d^*) - 2A_2 k_{\text{cat}} C_s^*) C_d + (2A_2 k_{\text{cat}} - A_1 k_s) C_d C_s + (C_s - C_s^*) 2A_2 k_{\text{cat}} C_t$$

$$+ A_3 (C_t - C_t^*) \big[\frac{k_n C_t}{k_m + C_0 C_t} + k_g C_0 C_t - k_c C_d - (C_t + C_d + C_s) k_g C_0 C_t \big] \Big\}$$

If we now take $A_1 = 1$, $A_2 = \frac{k_s}{k_{\text{cat}}}$, and $A_3 = 0$, then $\dot{V}_2$ will be negative if the following four inequalities hold simultaneously:

$$(k_{\text{cat}} + k_{\text{res}} + k_s)2A_2(C_s - C_s^*) + A_1 k_s C_d^* > 2A_2 k_{\text{cat}} \quad \Leftrightarrow \quad C_s > C_s^* + \frac{\left(k_{\text{cat}} - \frac{A_1 k_s C_d^*}{2A_2}\right)}{k_{\text{cat}} + k_{\text{res}} + k_s} \tag{5.45}$$

$$A_1 k_c (C_d - C_d^*) - 2A_2 k_{\text{cat}} C_s^* > 0 \quad \Leftrightarrow \quad C_d > C_d^* + \frac{2A_2 k_{\text{cat}}}{A_1 k_c} C_s^* \tag{5.46}$$

$$2A_2 k_{\text{cat}} - A_1 k_s > 0 \quad \Leftrightarrow \quad A_2 > \frac{A_1 k_s}{2k_{\text{cat}}} \tag{5.47}$$

$$C_s - C_s^* > 0 \quad \Leftrightarrow \quad C_s > C_s^* \tag{5.48}$$

Replacing the values of C_d^* and C_s^* in inequalities (5.45 - 5.48), we obtain

$$C_s > \frac{k_{\text{cat}}}{k_{\text{cat}} + k_{\text{res}} + k_s} + \left[k_c - \frac{k_s k_{\text{cat}}}{2(k_{\text{cat}} + k_{\text{res}} + k_s)} \right] \frac{k_{\text{cat}}}{\kappa} (1 - C_t^*) \tag{5.49}$$

$$C_d > \frac{3k_s k_{\text{cat}}}{\kappa} (1 - C_t^*) \tag{5.50}$$

$$\frac{k_s}{k_{\text{cat}}} > \frac{k_s}{2k_{\text{cat}}} \tag{5.51}$$

$$C_s > \frac{k_c k_{\text{cat}}}{\kappa} (1 - C_t^*) \tag{5.52}$$

Now, inequality (5.49) can be rewritten as

$$C_s > \frac{k_c k_{\text{cat}}}{\kappa}\,(1 - C_t^*) + \frac{k_{\text{cat}}\big(1 - C_d^*/2\big)}{k_{\text{cat}} + k_{\text{res}} + k_s},$$

and, since $C_d^* < 1$, the region defined by inequality (5.52) is contained in the region defined by inequality (5.49). Consequently,

$$\dot{V}_2 < 0 \quad \forall\, (C_t,\ C_d,\ C_s) \in \overline{\boldsymbol{\Omega}}_4 \setminus \{(C_t^*, C_d^*, C_s^*)\}.$$

By Lyapunov's stability theorem, it follows that the equilibrium solution, $E_4^* = (C_t^*,\ C_d^*,\ C_s^*)$, is globally asymptotically stable for system (5.39) on $\overline{\boldsymbol{\Omega}}_4$. This completes the proof of Theorem 5.1.17. □

Remarks. Note that the global stability of the equilibrium solution E_4^* is confined to a very specific region of the phase space. For instance, for any transients around C_s^*, the function V_2 fails to be a Lyapunov function. From Remark 5.1.16, we state the following theorem.

Theorem 5.1.18. *If $C_0 > 0$, then on the set $\boldsymbol{\Omega}_4$, system* (5.36) *admits a unique positive equilibrium*

$$E_4^{**} = \left(C_0 C_t^*,\ \frac{k_s k_{\text{cat}} C_0}{\kappa}\,(1 - C_t^*)\,,\ \frac{k_c k_{\text{cat}} C_0}{\kappa}\,(1 - C_t^*)\,,\ \frac{(k_{\text{res}} + k_s) k_c C_0}{\kappa}\,(1 - C_t^*)\right),$$

where $\kappa = k_s k_{\text{cat}} + (k_{\text{cat}} + k_{\text{res}} + k_s) k_c$ and C_t^* is the unique positive root in the interval $(0, 1)$ to the equation

$$(k_{\text{res}} + k_s) k_g k_c C_0^2 C_t^3 - \left[k_s k_{\text{cat}} - (k_m - C_0)(k_{\text{res}} + k_s) k_g\right] k_c C_0 C_t^2$$

$$- \left[(k_m - C_0) k_s k_c k_{\text{cat}} + (k_{\text{res}} + k_s) k_g k_c C_0 k_m + \kappa k_n\right] C_t + k_s k_c k_{\text{cat}} k_m = 0$$

Furthermore, E_4^{**} is globally stable on the domain $\overline{\boldsymbol{\Omega}}_4$.

5.2 Numerical simulations

In this section, we present numerical simulations of the models. All simulations and subsequent analysis were conducted in MATLAB [55].

Symbol	Description	Value	Unit	Source
All models				
k_n	Rate constant for nucleation	5.127×10^{-6}	s^{-1}	[69]
k_g	Rate constant for elongation	9.3	$\mu m \text{min}^{-1}$	[8]
k_s	Rate constant for shrinking	12.8	$\mu m \text{min}^{-1}$	[8]
k_c	Rate constant for recycling	10	min^{-1}	U
II & IV only				
k_{m}	Maximal rate of nucleation	6		U
III & IV only				
k_{cat}	Catastrophe frequency	0.96	min^{-1}	[8]
k_{res}	Rescue frequency	1.86	min^{-1}	[8]
V only				
a_{cat}	Velocity of the catastrophe rate	0.5	min^{-1}	U
a_{res}	Velocity of the rescue rate	10	min^{-1}	U
b_{cat}	Maximal magnitude of the catastrophe rate	2	min^{-1}	U
b_{res}	Minimal magnitude of the rescue rate	2	min^{-1}	U

Table 5.1: Parameter values used in the numerical simulation of the models. The symbol U indicates that the parameter was arbitrarily chosen.

Numerical simulation of model I

Table 5.1 gives the parameters of model (5.1), their description, and the numerical values that are used for the simulations, while Figure 5.6 shows the time evolution of the variables

$C_t(t)$, $C_d(t)$, and $C_m(t)$ (in proportion) of system (5.1), for various initial conditions. In Figure 5.6, notice that only about 34% of the solution polymerizes to form microtubules.

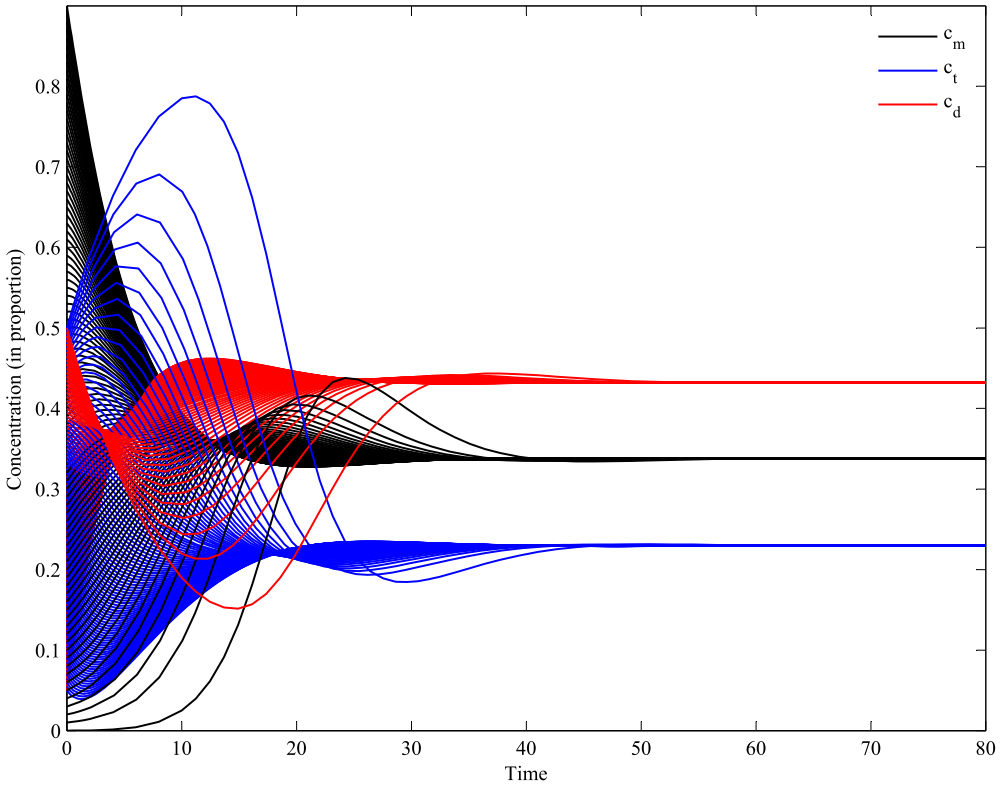

Figure 5.6: Solution curves for model I in proportions. Parameter values are as given in Table 5.1.

Numerical simulation of model II

Using the parameter values in Table 5.1, we carried out numerical simulation of model (5.9). Figures 5.7 and 5.8 show the solution curves of model (5.9) for various initial conditions, the former in the case when $k_s + k_c < k_g C_0$ holds, and the latter in the case when $k_s + k_c > k_g C_0$ holds. Although the case $k_s + k_c < k_g C_0$ has not been proved mathematically, it appears that E_2^{**} is globally stable in both cases.

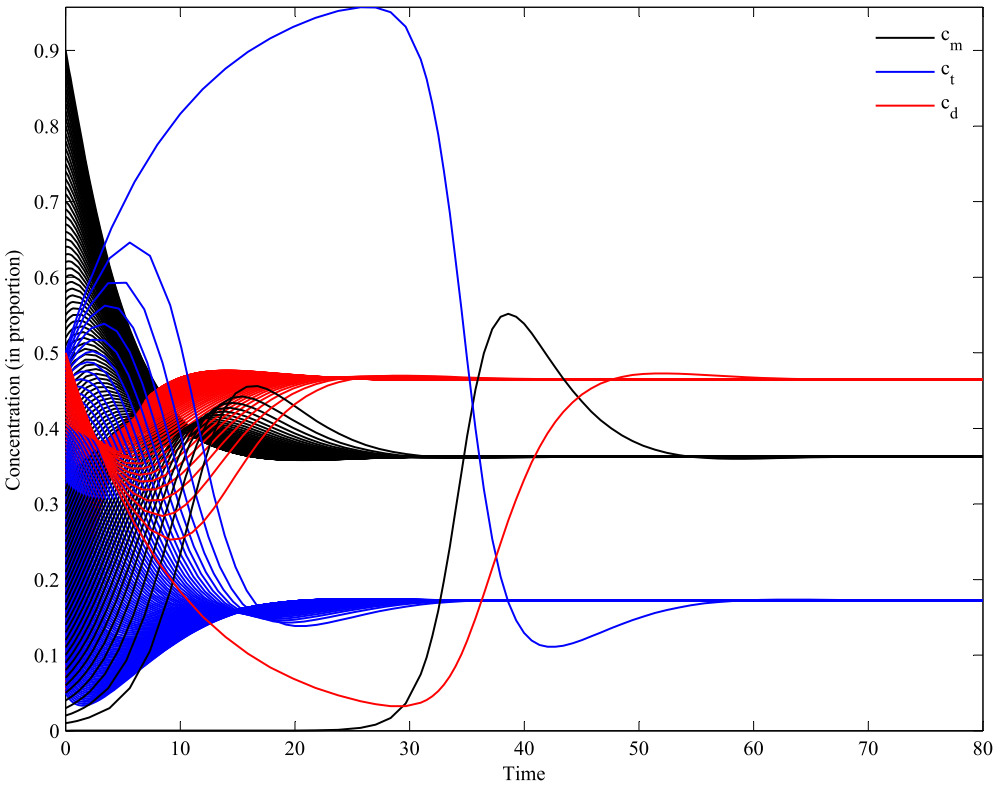

Figure 5.7: Solution curves for model II in proportions when the condition of Theorem 5.1.9 does not hold; that is, when $k_s + k_c < k_g C_0$.

Numerical simulation of model III

We carried out numerical simulation of model (5.15). Table 5.1 gives the parameters of the model, their description, and the numerical values that are used for the simulations. Figure 5.9 shows the time evolution of the variables $C_t(t)$, $C_d(t)$ and $C_m = C_s(t) + C_g(t)$ of system (5.15) for various initial conditions. In contrast to Models I and II, Figure 5.9 now suggests that ultimately, 66% of the solution polymerizes into microtubules.

Numerical simulation of model IV

The solution curves of the variables $C_t(t)$, $C_d(t)$ and $C_m = C_s(t) + C_g(t)$ of system (5.36) are shown in Figure 5.10. The parameters used in this simulation are given in Table 5.1. Again notice that in Figure 5.10, the percentage of microtubules formed is about 66%.

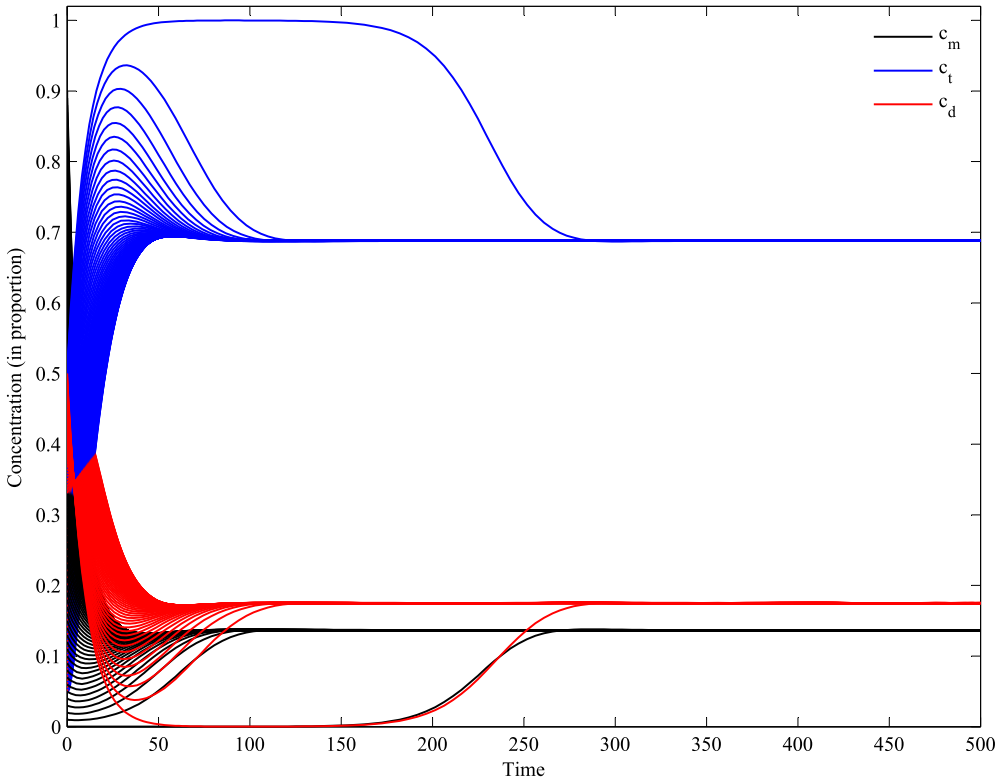

Figure 5.8: Solution curves for model II in proportions when the condition of Theorem 5.1.9 is satisfied; that is, when $k_s + k_c > k_g C_0$.

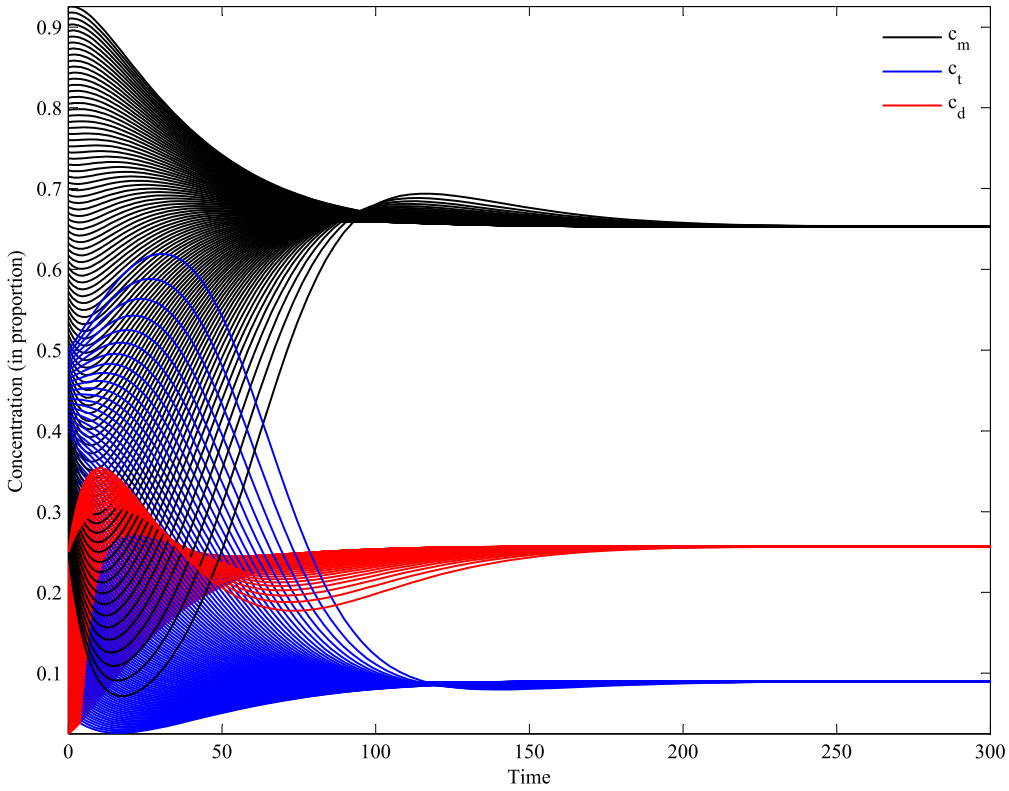

Figure 5.9: Solution curves for model III in proportions. Parameter values are as given in Table 5.1.

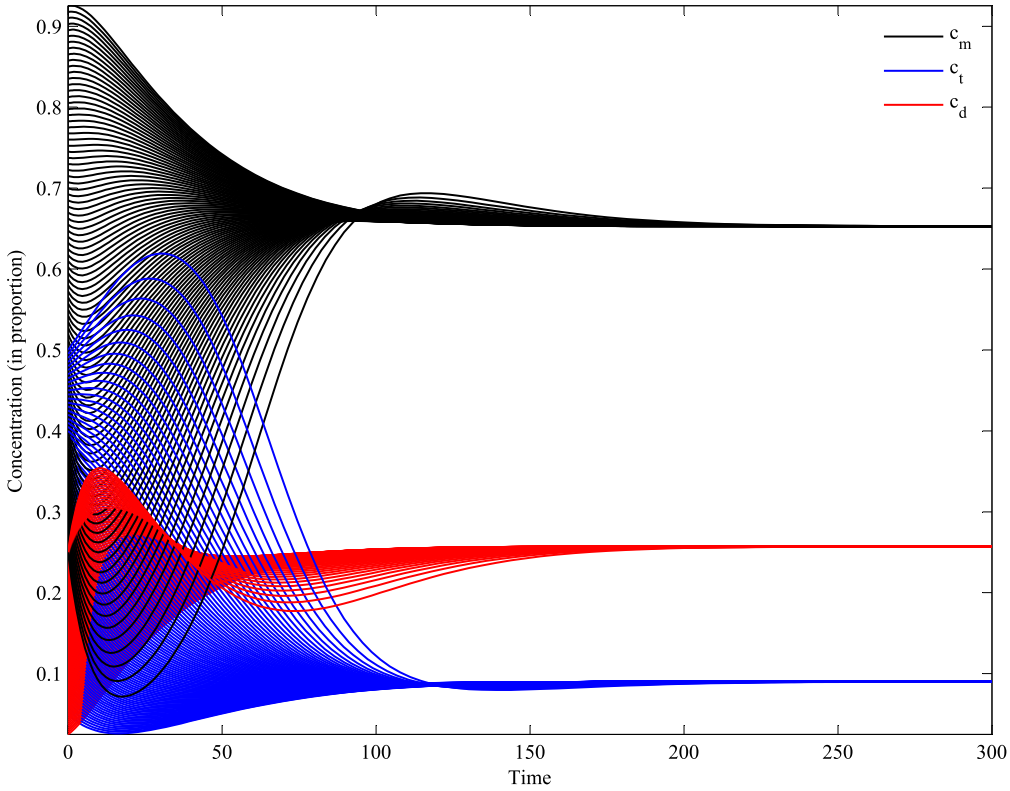

Figure 5.10: Solution curves for model IV in proportions. Parameter values are as given in Table 5.1.

Numerical simulation of model V

Figure 5.11 shows the time evolution of the variables $C_t(t)$, $C_d(t)$ and $C_m = C_s(t) + C_g(t)$ of system (4.15). Table 5.1 gives the parameters for this simulation. From Figure 5.11, we notice that ultimately, close to 60% of the solution polymerizes into microtubules.

Comparing Figures 5.6 and 5.7 on one hand, and Figures 5.9, 5.10 and 5.11 on the other, it seems that the introduction of dynamic instability in the system induces an increase in the level of polymerization of microtubules.

5.3 Sensitivity analysis

To assess the effect of the parameters on the variables, we conducted sensitivity analysis. This involved solving (and normalizing) the system of first partial derivatives of the variables with respect to the parameter estimates as described in Section 2.6.2. Thus in

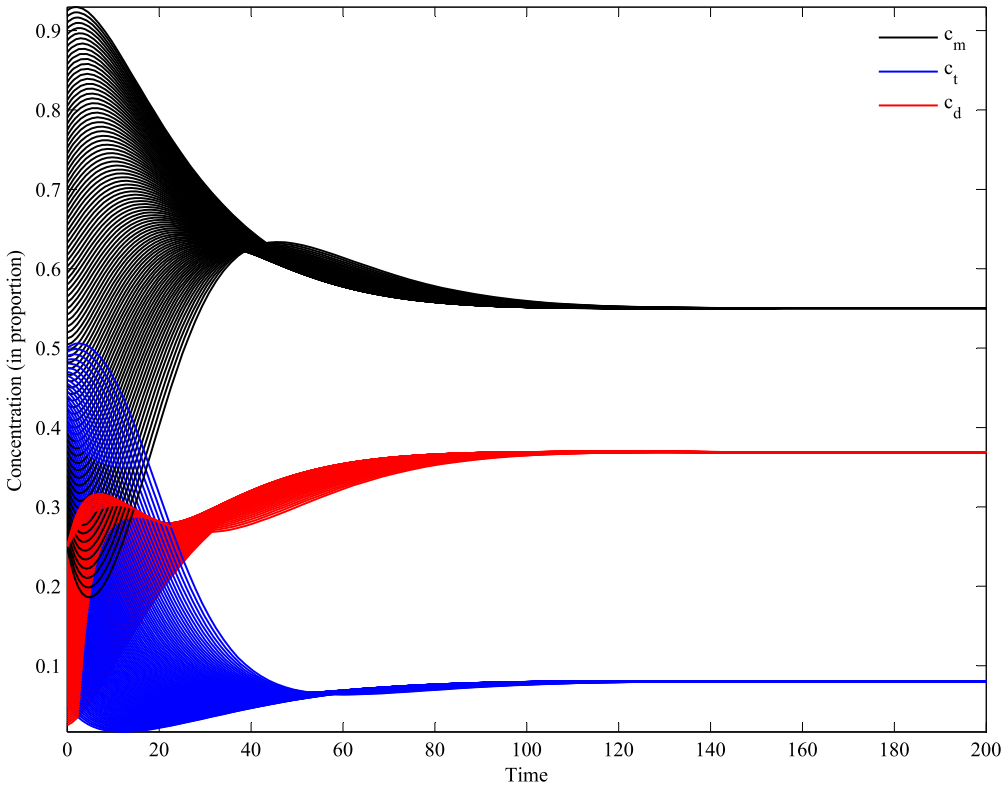

Figure 5.11: Solution curves for model V in proportions. Parameter values are as given in Table 5.1.

Model I, for example, we solved the following system of ordinary differential equations:

$$\dot{C}_t = k_c C_d - k_n C_t^n - k_g C_m C_t,$$

$$\dot{C}_d = k_s C_m - k_c C_d,$$

$$\dot{C}_m = k_n C_t^n + k_g C_m C_t - k_s C_m,$$

$$\frac{d}{dt}\left(\frac{\partial \boldsymbol{C}}{\partial \boldsymbol{p}}\right) = \frac{\partial \boldsymbol{f}}{\partial \boldsymbol{C}}\frac{\partial \boldsymbol{C}}{\partial \boldsymbol{p}} + \frac{\partial \boldsymbol{f}}{\partial \boldsymbol{p}},$$

$$\boldsymbol{C}(0) = [C_{t0}\ C_{d0}\ C_{m0}]^T, \quad \frac{\partial \boldsymbol{C}}{\partial \boldsymbol{p}}(\mathbf{0}) = \frac{\partial}{\partial \boldsymbol{p}}\big(\boldsymbol{C}(\mathbf{0})\big) = \mathbf{0},$$

where

$$\boldsymbol{C} = [C_t\ C_d\ C_m]^T, \quad \boldsymbol{f} = [f_1\ f_2\ f_3]^T = [\dot{C}_t\ \dot{C}_d\ \dot{C}_m]^T,$$

$$\frac{\partial \boldsymbol{C}}{\partial \boldsymbol{p}} = \begin{bmatrix} \frac{\partial C_t}{\partial k_n} & \frac{\partial C_t}{\partial k_g} & \frac{\partial C_t}{\partial k_s} & \frac{\partial C_t}{\partial k_c} \\ \frac{\partial C_d}{\partial k_n} & \frac{\partial C_d}{\partial k_g} & \frac{\partial C_d}{\partial k_s} & \frac{\partial C_d}{\partial k_c} \\ \frac{\partial C_m}{\partial k_n} & \frac{\partial C_m}{\partial k_g} & \frac{\partial C_m}{\partial k_s} & \frac{\partial C_m}{\partial k_c} \end{bmatrix}, \quad \frac{\partial \boldsymbol{f}}{\partial \boldsymbol{C}} = \begin{bmatrix} \frac{\partial f_1}{\partial C_t} & \frac{\partial f_1}{\partial C_d} & \frac{\partial f_1}{\partial C_m} \\ \frac{\partial f_2}{\partial C_t} & \frac{\partial f_2}{\partial C_d} & \frac{\partial f_2}{\partial C_m} \\ \frac{\partial f_3}{\partial C_t} & \frac{\partial f_3}{\partial C_d} & \frac{\partial f_3}{\partial C_m} \end{bmatrix}, \quad \frac{\partial \boldsymbol{f}}{\partial \boldsymbol{p}} = \begin{bmatrix} \frac{\partial f_1}{\partial k_n} & \frac{\partial f_1}{\partial k_g} & \frac{\partial f_1}{\partial k_s} & \frac{\partial f_1}{\partial k_c} \\ \frac{\partial f_2}{\partial k_n} & \frac{\partial f_2}{\partial k_g} & \frac{\partial f_2}{\partial k_s} & \frac{\partial f_2}{\partial k_c} \\ \frac{\partial f_3}{\partial k_n} & \frac{\partial f_3}{\partial k_g} & \frac{\partial f_3}{\partial k_s} & \frac{\partial f_3}{\partial k_c} \end{bmatrix}$$

5.3.1 Transient versus long-term sensitivity analysis results

Figure 5.12 shows the solution curves of the normalized sensitivity coefficients of the variables in model I (i.e., C_t, C_d and C_m) to the parameters (k_n, k_g, k_s and k_c). The figure captures two aspects of the sensitivity: the transient and the long-term sensitivity. In the long-run, the sensitivity coefficients lie within the $[-1, 1]$ interval. This was the general trend across the models.

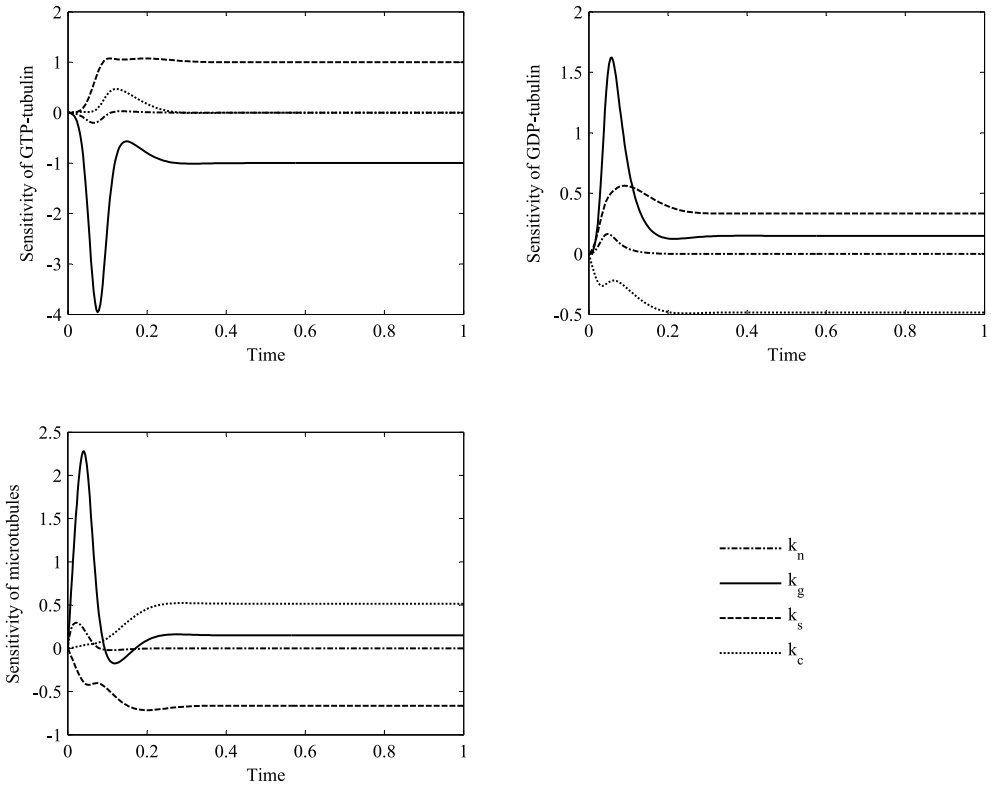

Figure 5.12: The curves of normalized sensitivity coefficients of the variables C_t, C_d and C_m in model I with respect to the parameters.

5.3.2 Qualitative sensitivity analysis results

As we would, of course, expect, in Figure 5.12, and in all the other models, the normalized sensitivity coefficient of the microtubules with respect to the elongation parameter, $\frac{\partial \ln C_t}{\partial \ln k_g}$, is positive, meaning that an increase in the parameter k_g induces an increase in the

microtubule. The shrinking parameter, k_s, has an opposite effect on the microtubule in all the models - increasing the value of k_s causes a decrease in the microtubule concentration. The qualitative sensitivity analysis results are summarized in Table 5.2. The table shows the signs of the normalized sensitivity coefficients for all the models. A $+$ means that an increase in the parameter will induce an increase in the variable's population, while a $-$ means that an increase in the parameter will induce a decrease in the variable's population. In Table 5.2, we notice that in the absence of dynamic instability (models I and II), shrinkage has a mixed effect on the GDP-tubulin. The recycling parameter (k_c) has a positive effect on GTP-tubulin in models I, III and IV, a positive effect on microtubules in all the models, a mixed effect on the GTP-tubulin in model II, and a negative effect on GTP-tubulin in model V. Nucleation has a negative effect on GTP-tubulin in models I, II and IV, has a mixed effect on GTP-tubulin in models III and V, and has a positive effect on GDP-tubulin in all the models. It (nucleation) has a positive effect on microtubules in model I, II and V, and a mixed effect on microtubules in models III and IV. It seems that in model V, the magnitude of the positive effect of nucleation on GDP-tubulin cancels the negative effect of nucleation on GTP-tubulin, resulting in a positive effect on microtubules. In general, it appears that the presence of dynamic instability inhibits the positive effect of nucleation on microtubules. The maximal rate of nucleation (k_m) has no effect on all the variables in models II and IV.

The contour plots resulting from the sensitivity analysis provided an insight into the effect of simultaneously varying pairs of parameters on the GTP-tubulin, GDP-tubulin and microtubule concentrations. When the contour curves are linear or nearly so, then this implies that the interaction effect of the two parameters on the variable's population is insignificant. If, on the other hand, the contour curves have considerable curvature, then this implies that the interaction term is large and important. A sample of the contour plots is shown in Figures 5.13 and 5.14. The magnitudes of the sensitivity coefficients in the sensitivity analysis are shown in Table 5.3. When the parameters k_g, k_s and k_c pairwise interacted, models III and IV showed low sensitivity to the nucleation

	I	II	III	IV	V
t_{kn}	−	−	±	−	±
t_{kg}	−	−	−	−	−
t_{ks}	+	+	+	+	+
t_{kc}	+	±	+	+	−
t_{km}	$n.a.$	0	$n.a.$	0	$n.a.$
t_{kcat}	$n.a.$	$n.a.$	+	+	$n.a.$
t_{kres}	$n.a.$	$n.a.$	−	−	$n.a.$
t_{acat}	$n.a.$	$n.a.$	$n.a.$	$n.a.$	−
t_{ares}	$n.a.$	$n.a.$	$n.a.$	$n.a.$	−
t_{bcat}	$n.a.$	$n.a.$	$n.a.$	$n.a.$	+
t_{bres}	$n.a.$	$n.a.$	$n.a.$	$n.a.$	−
d_{kn}	+	+	+	+	+
d_{kg}	+	+	+	+	+
d_{ks}	±	±	+	+	+
d_{kc}	−	−	−	−	−
d_{km}	$n.a.$	0	$n.a.$	0	$n.a.$
d_{kcat}	$n.a.$	$n.a.$	+	+	$n.a.$
d_{kres}	$n.a.$	$n.a.$	−	−	$n.a.$
d_{acat}	$n.a.$	$n.a.$	$n.a.$	$n.a.$	−
d_{ares}	$n.a.$	$n.a.$	$n.a.$	$n.a.$	−
d_{bcat}	$n.a.$	$n.a.$	$n.a.$	$n.a.$	+
d_{bres}	$n.a.$	$n.a.$	$n.a.$	$n.a.$	−
m_{kn}	+	+	±	±	+
m_{kg}	+	+	+	+	+
m_{ks}	−	−	−	−	−
m_{kc}	+	+	+	+	+
m_{km}	$n.a.$	0	$n.a.$	0	$n.a.$
m_{kcat}	$n.a.$	$n.a.$	+	+	$n.a.$
m_{kres}	$n.a.$	$n.a.$	−	−	$n.a.$
m_{acat}	$n.a.$	$n.a.$	$n.a.$	$n.a.$	−
m_{ares}	$n.a.$	$n.a.$	$n.a.$	$n.a.$	−
m_{bcat}	$n.a.$	$n.a.$	$n.a.$	$n.a.$	+
m_{bres}	$n.a.$	$n.a.$	$n.a.$	$n.a.$	−

Table 5.2: Sensitivity analysis: influences of reaction rates on the dynamics of GTP-tubulin (t), GDP-tubulin (d), and polymers (m). t_{kg}, for example, denotes $\frac{\partial \ln C_t}{\partial \ln k_g}$. The symbol + (resp. −) denotes positive (resp. negative) value of normalized sensitivity coefficient, while ± denotes positive and negative values of normalized sensitivity coefficients. *n.a.* stands for 'not applicable'.

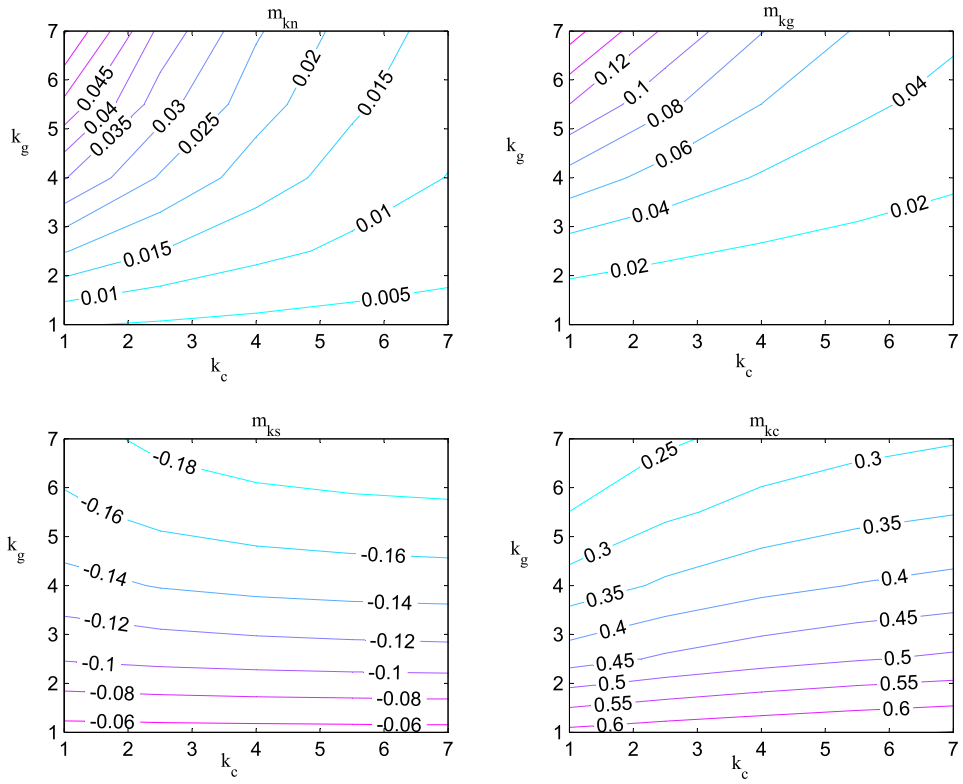

Figure 5.13: A contour plot for the variability of sensitivity coefficients of microtubule concentration derived from the sensitivity analysis of k_g and k_c in model I.

parameter, k_n, while models I and II showed high sensitivity to k_n (Table 5.3). This seemed to suggest that dynamic instability inhibits nucleation in microtubule dynamics.

5.3.3 Quantitative sensitivity analysis results

The quantitative sensitivity analysis results were summarized using box plots. A *box plot* (sometimes referred to as a *box-and-whisker plot*) is a graphical device that simultaneously displays several important features of a given data set. At a glance, a box plot reveals the centre, dispersion and skewness of a data set. It displays the following features:

- the 25th percentile (Q1),
- the 75th percentile (Q3),
- the median,

	$k_g - k_n$			$k_n - k_s$			$k_c - k_n$			$k_g - k_s$			$k_c - k_g$			$k_c - k_s$		
	II	IV	V	II	IV	V	II	IV	V	II	IV	V	II	IV	V	II	IV	V
t_{kn}	−	−	−	−	−	−	−	−	−	· − ·	−	·−	·−	−	−	−	−	±
t_{kg}	·−	−	−	−	−	−	−	−	−	· − ·	−	·−	−	−	−	−	−	−
t_{ks}	+	+	+	+	+	+	+	+	+	+	+	+	+	+	+	+	+	+
t_{kc}	+	+	−	+	+	−	+	+	−	+	+	−	−	+	−	±	+	−
d_{kn}	+	+	+	+	+	+	+	+	+	·+	+	· + ·	·+	+	+	+	+	+
d_{kg}	+	+	+	+	+	+	+	+	+	·+	+	·+	+	+	+	+	+	+
d_{ks}	±	+	+	+	+	+	+	+	+	±	+	+	±	+	+	·+	+	+
d_{kc}	−	−	· − ·	−	·−	· − ·	−	·−	−	−	−	· − ·	−	·−	−	·−	·−	·−
m_{kn}	+	+	+	+	+	+	+	±	+	+	+	· + ·	+	+	+	+	+	+
m_{kg}	+	+	+	+	+	+	+	+	+	·+	+	+	+	+	+	+	+	+
m_{ks}	−	−	−	−	−	−	−	−	−	−	−	−	−	−	·−	·−	−	−
m_{kc}	+	+	· + ·	+	+	· + ·	+	·+	·+	+	+	· + ·	+	·+	· + ·	·+	·+	·+

	$k_g - k_n$			$k_n - k_s$			$k_c - k_n$			$k_g - k_s$			$k_c - k_g$			$k_c - k_s$		
	I	III	V	I	III	V	I	III	V	I	III	V	I	III	V	I	III	V
t_{kn}	−	−	−	−	−	−	−	−	−	· − ·	−	·−	· − ·	−	−	· − ·	+	±
t_{kg}	−	−	−	−	−	−	−	−	−	·−	−	·−	−	−	−	−	−	−
t_{ks}	+	+	+	+	+	+	+	+	+	+	+	+	+	+	+	+	+	+
t_{kc}	+	+	−	+	+	−	+	+	−	+	+	−	+	+	−	+	−	−
d_{kn}	+	+	+	+	+	+	+	+	+	· + ·	+	· + ·	· + ·	+	+	· + ·	+	+
d_{kg}	+	+	+	+	+	+	+	+	+	+	+	·+	+	+	+	+	+	+
d_{ks}	+	+	+	+	+	+	+	+	+	+	+	+	+	+	+	·+	+	+
d_{kc}	−	·−	· − ·	−	·−	· − ·	−	·−	−	−	·−	· − ·	−	−	−	·−	·−	·−
m_{kn}	+	+	+	+	+	+	+	−	+	· + ·	+	· + ·	· + ·	+	+	· + ·	−	+
m_{kg}	+	+	+	+	+	+	+	+	+	+	+	+	+	+	+	+	+	+
m_{ks}	−	−	−	−	−	−	−	−	−	−	−	−	−	−	·−	·−	−	−
m_{kc}	+	·+	· + ·	+	·+	· + ·	+	·+	·+	+	·+	· + ·	+	·+	· + ·	·+	·+	·+

Table 5.3: Sensitivity analysis: influences of reaction rates on the dynamics of GTP-tubulin (t), GDP-tubulin (d), and polymers (m). The symbol $\cdot + \cdot$ (resp. $\cdot - \cdot$) denotes a positive (resp. negative) value, x, of normalized sensitivity coefficient such that $|x| > 1.2$, $\cdot+$ (resp. $\cdot-$) denotes a positive (resp. negative) value, x, of normalized sensitivity coefficient such that $|x| \in [0.4, 1.2]$, $+$ (resp. $-$) denotes a positive (resp. negative) value, x, of normalized sensitivity coefficient such that $|x| < 0.4$, while $\pm$ denotes positive and negative values of normalized sensitivity coefficients.

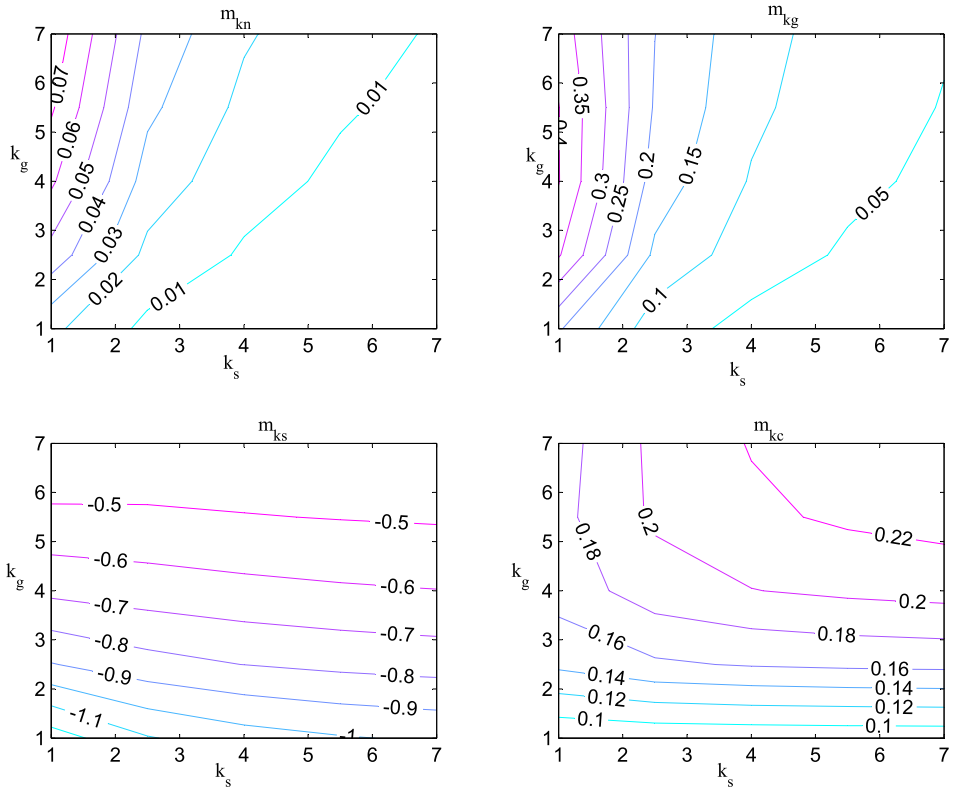

Figure 5.14: A contour plot for the variability of sensitivity coefficients of microtubule concentration derived from the sensitivity analysis of k_g and k_s in model I.

- the minimum and maximum values,
- outliers, if any.

The Q1 and Q3 are at the lower and upper ends, respectively, of the box. The distance between Q1 and Q3 is the interquartile range (IQR). A line (whisker) extends from Q1 to the smallest value that is inside a distance of $1.5 \times IQR$. Similarly, a whisker extends from Q3 to the largest value that is inside a distance of $1.5 \times IQR$. The median is the line inside of the box. The data is skewed if the median is not centred in the box. An outlier is any data point that is more than $1.5 \times IQR$ from either end of the box.

The box plots in Figure 5.15c, for example, show the sensitivity of the GTP-tubulin in model III as a function of the parameters.

From the sensitivity analysis, we noted that nucleation rate (k_n) and the maximal rate of nucleation (k_m) had negligible effect in the models.

Table 5.4 gives the parameter with the highest model sensitivity among all the parameters

in each population for each model. In the absence of dynamic instability, the elongation and shrinkage parameters account for the highest model sensitivity, while in the presence of dynamic instability, the catastrophe parameter is inducing the highest sensitivity in the variables. An interesting observation is the dispersion of the data. For models without dynamic instability, the standard deviations are, in general, higher than in the presence of dynamic instability. Intuitively, we would expect the data from dynamic instability models to display more dispersion, given the stochastic nature of catastrophe and rescue frequencies. Dynamic instability could thus be viewed as a smoothing process in the long run.

	I	II	III	IV	V
C_t	k_g -0.0251 (0.0009)	k_g -0.0319 (0.0155)	k_{cat} 0.0172 (0.0036)	k_{cat} 0.0190 (0.0041)	b_{cat} 0.0109 (0.0022)
C_d	k_s -0.0214 (0.0025)	k_c -0.0184 (0.0012)	k_{cat} 0.0578 (0.0103)	k_{cat} 0.0566 (0.0095)	b_{cat} 0.0337 (0.0041)
C_m	k_s -0.0237 (0.0057)	k_s -0.0283 (0.0034)	k_{cat} -0.0720 (0.0127)	k_{cat} -0.0755 (0.0135)	b_{cat} -0.0446 (0.0062)

Table 5.4: The parameter with the highest model sensitivity. The data shown in each cell is mean and standard deviation (in parentheses) of the normalized sensitivity coefficient of the variable with respect to the given parameter.

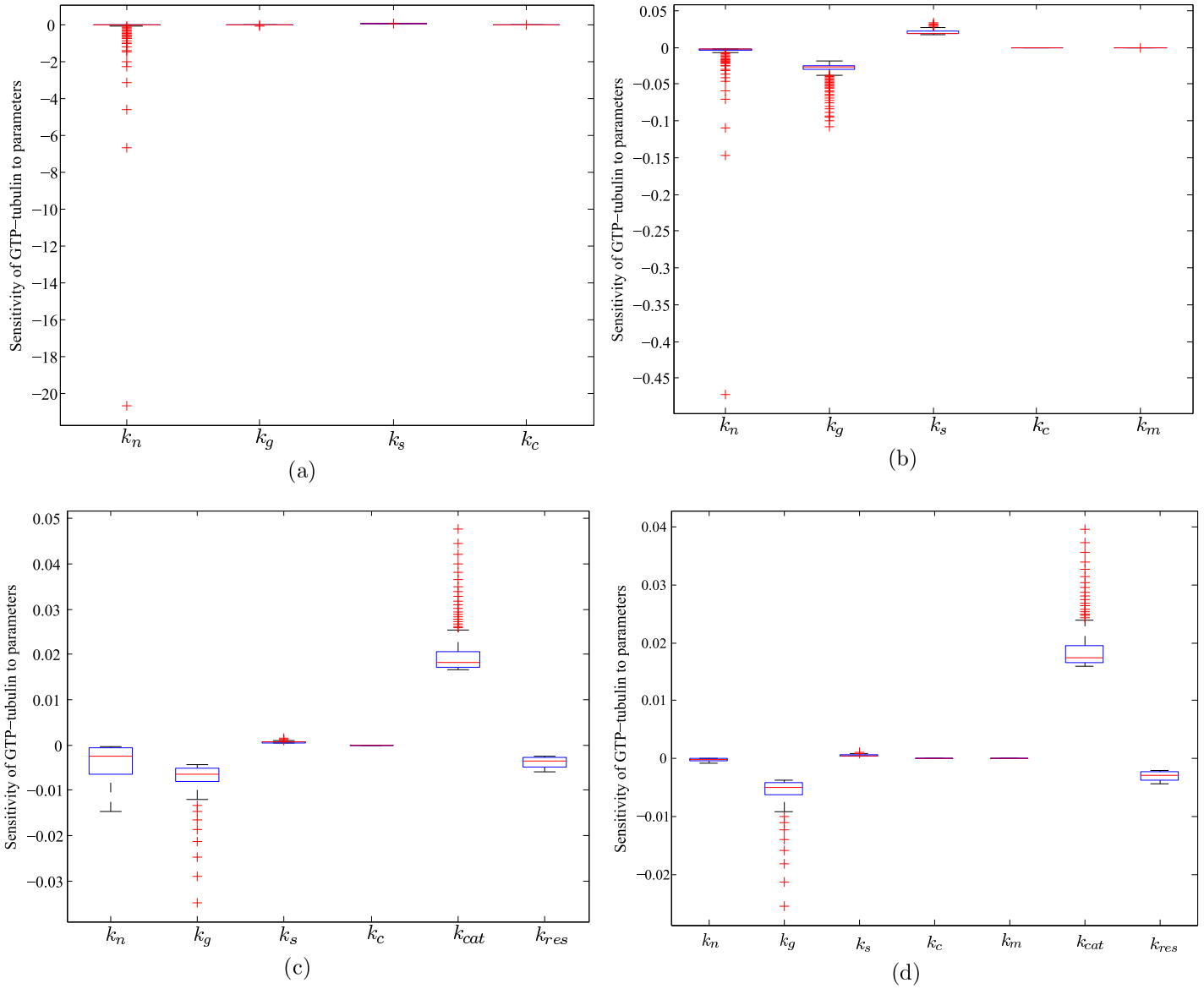

Figure 5.15: Box plots showing the sensitivity of GTP-tubulin to the parameters in (a) model I (b) model II (c) model III and (d) model IV.

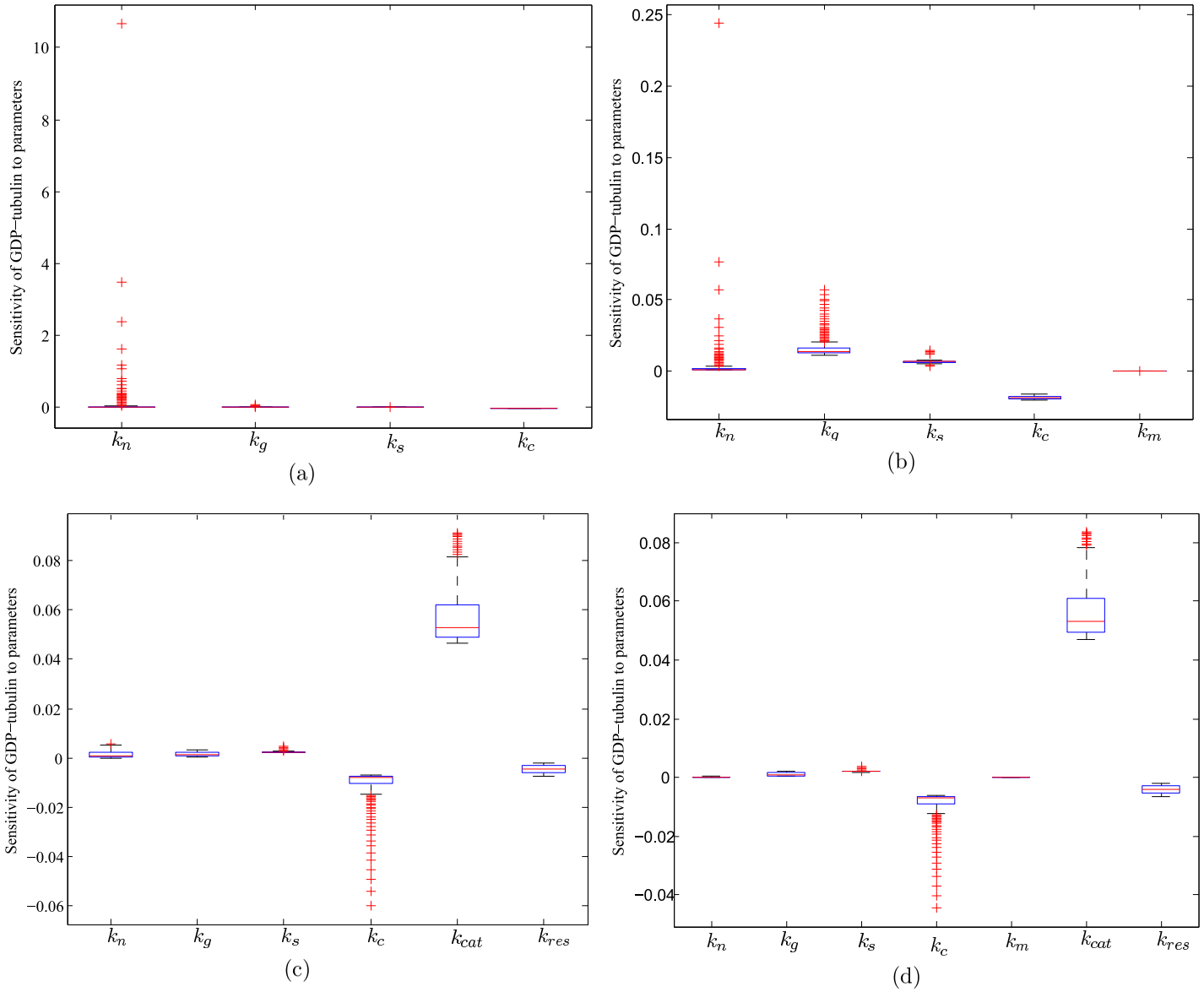

Figure 5.16: Box plots showing the sensitivity of GDP-tubulin to the parameters in (a) model I (b) model II (c) model III and (d) model IV.

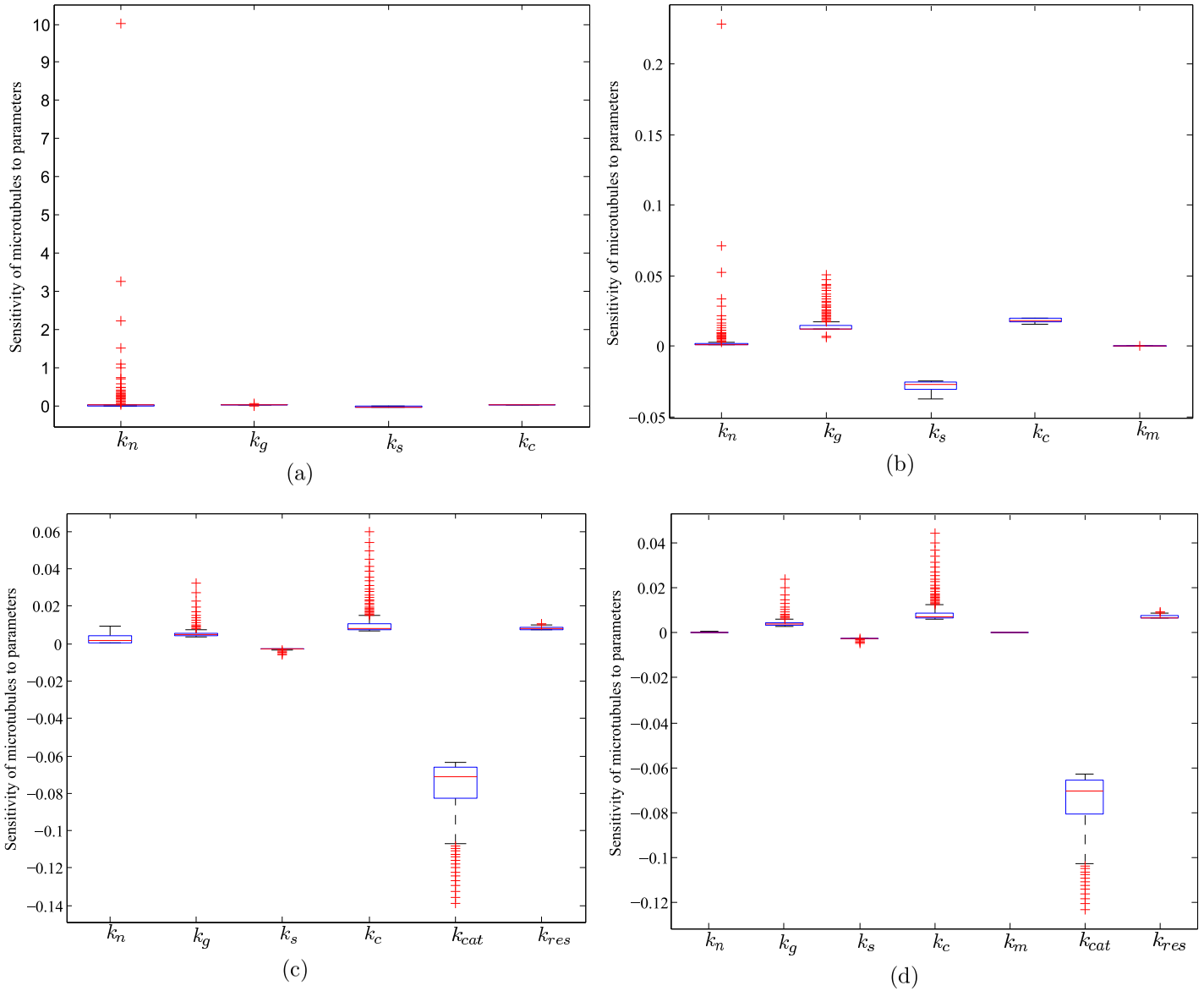

Figure 5.17: Box plots showing the sensitivity of microtubules to the parameters in (a) model I (b) model II (c) model III and (d) model IV.

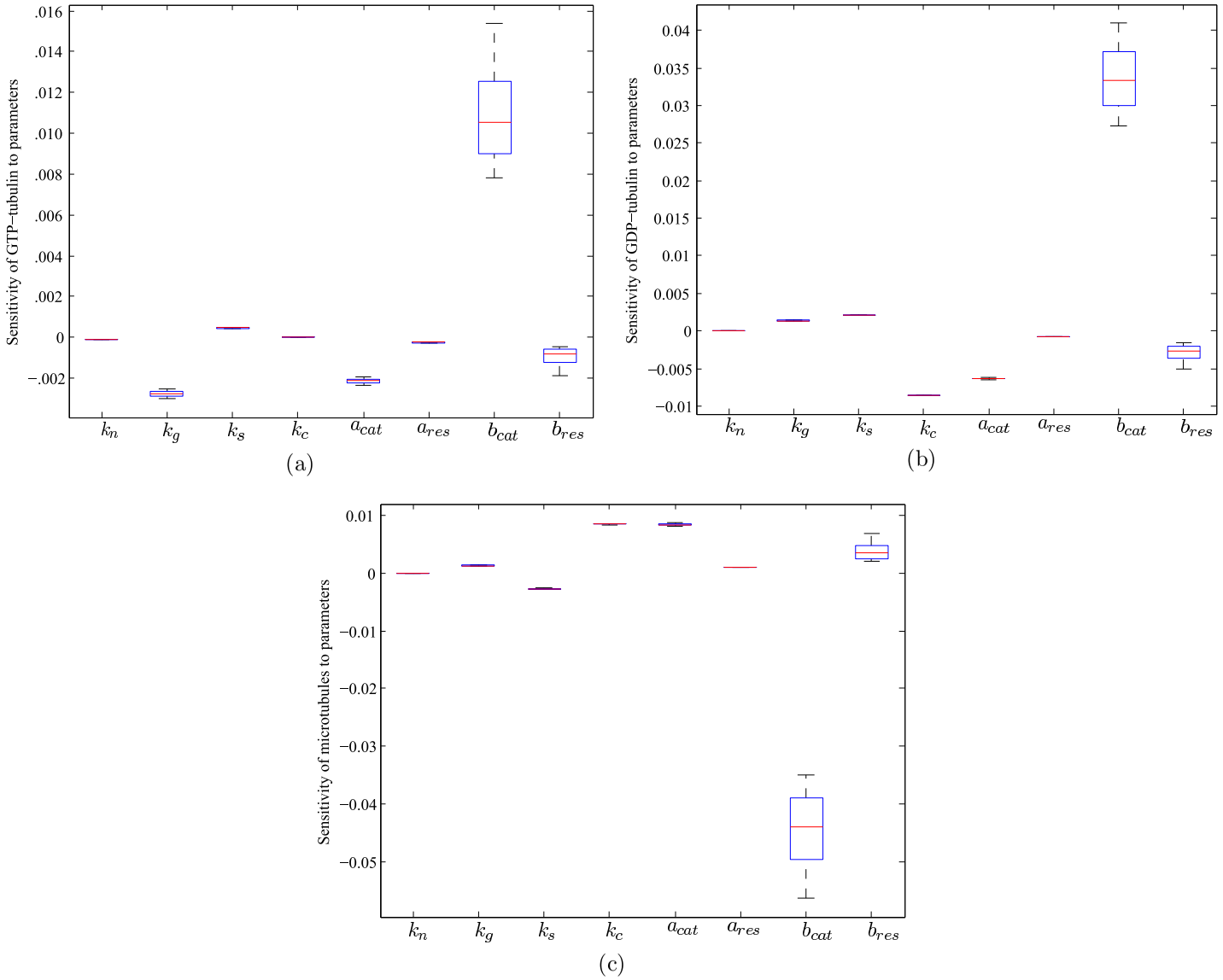

Figure 5.18: Box plots showing the sensitivity of variables in model V to the parameters.

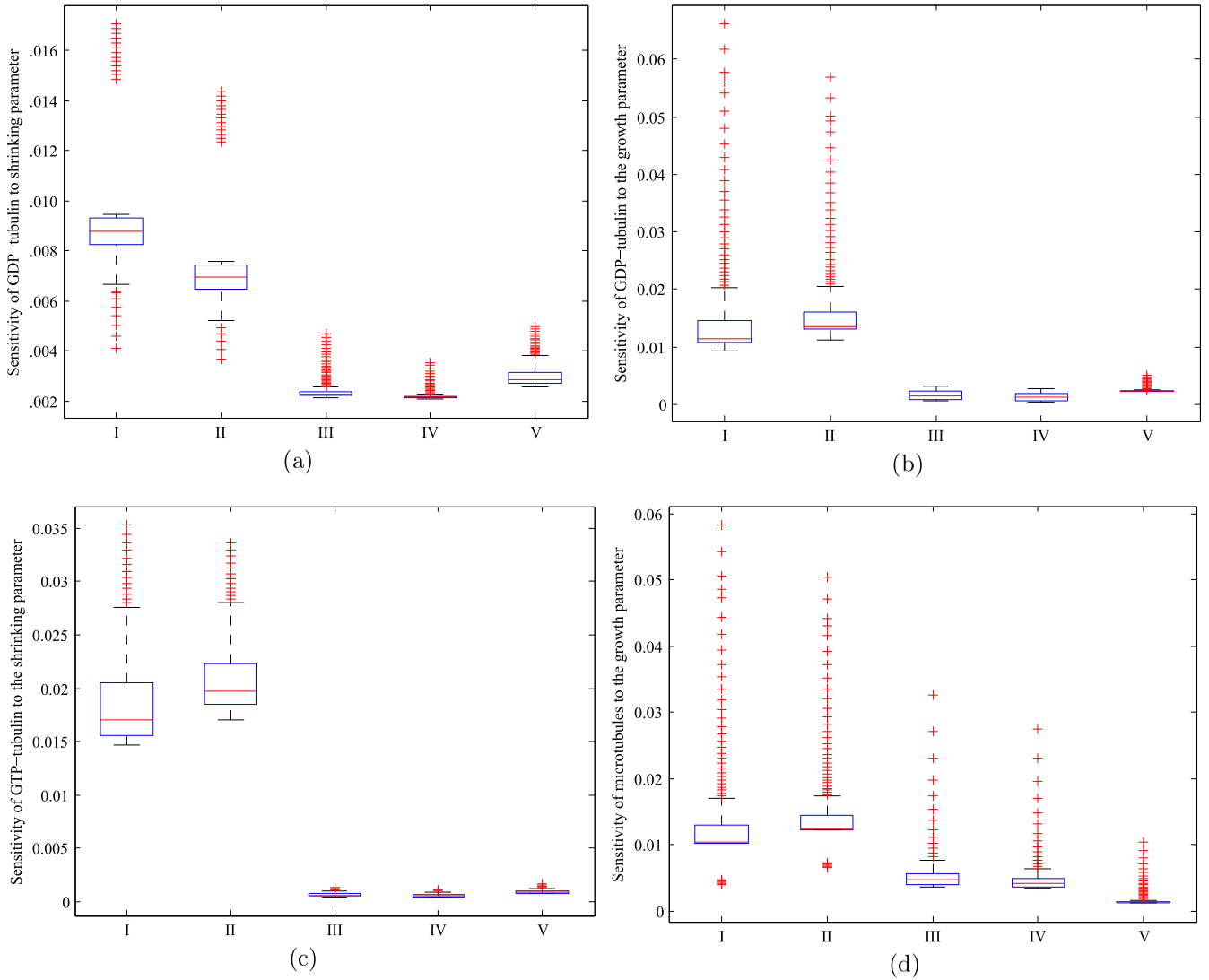

Figure 5.19: Box plot showing sensitivity of variables to the growth and shrinkage parameters. In (a) and (b), we have the sensitivity of GDP-tubulin to k_s and k_g, respectively. In (c) we have the sensitivity of GTP-tubulin as a function of k_s, while in (d), we have the sensitivity of microtubules as a function of k_g

When GTP-tubulin concentration-dependence on the dynamic instability parameters k_{cat} and k_{res} is assumed in model V, we observed some high sensitivity to the recycling (k_c) and elongation (k_g) parameters (Table 5.3 and Figure 5.18).

From Table 5.3, we notice that in model V, any pair of parameters involving the recycling parameter induces relatively high interaction effects on the sensitivity coefficients. This implies that recycling of GDP-tubulin has a greater effect in microtubule dynamics when rescue and catastrophe frequencies depend on GTP-tubulin concentration. This inference is further reinforced by the box plots obtained in Model V (Figure 5.18). By comparing models I and III in Table 5.3, we notice a substantial number of relatively higher sensitivities in model I. A similar observation is made if we compare models II and IV, with model II recording some high sensitivities on a number of coefficients. A related observation is made in Figure 5.19, where the sensitivity of the variables in model I and II is relatively higher compared to that in models III, IV and V. This seems to suggest that dynamic instability inhibits sensitivity of the variables to the parameters.

5.4 Discussion

From the analysis of the models, two key points are identified. Firstly, our results suggest that dynamic instability is an essential and indispensable property of microtubules. From the solution curves of the models, we notice that the level of polymerization of microtubules is higher in the presence than in the absence of dynamic instability (compare Figures 5.6, 5.7, 5.9, 5.10 and 5.11). That is, the proportion of solution that polymerizes to form microtubules is higher when dynamic instability is present. This seems to underscore the importance of dynamic instability in the maintenance of abundant supply of microtubules in the cells.

Secondly, our results support the long held view [24] and experimental observations [27, 82] that dynamic instability depends on the GTP-tubulin concentration. It is believed that the energy source that powers dynamic instability is the hydrolysis of GTP-tubulin.

In model V, where the rescue and catastrophe parameters are assumed to depend on the GTP-tubulin concentration, we notice that the sensitivity coefficient of recycling parameter, k_c is relatively high compared to the other models (Table 5.3). A high value of k_c, on the other hand, means an increase in microtubules (see Table 5.2).

In general, the box plots revealed a rather counterintuitive observation; in the absence of dynamic instability, the data showed more dispersion than in the presence of dynamic instability. Dynamic instability is an out-of-equilibrium phenomenon. As such, we would expect the data from models with dynamic instability to display more dispersion than those without it. It appears that in the long-run, dynamic instability is a smoothing process for the microtubule dynamics.

Chapter 6

Conclusions and suggestions for future work

The overall objective of this thesis was to contribute to our understanding of the role of dynamic instability in the assembly-disassembly dynamics of microtubules *in vitro*. We have constructed and analyzed a set of mathematical models of the dynamics of microtubule assembly and disassembly, considering several biologically plausible mechanisms. Numerical simulations have confirmed our analytic results. In line with the long-held view, numerical simulations have shown that nucleation has an insignificant effect on the overall microtubule dynamics. In the models where dynamic instability is present, we noted that the proportion of solution that polymerizes to form microtubules is higher than in models where dynamic instability is absent. This suggests that dynamic instability induces the formation of microtubules from the tubulin subunits. Thus dynamic instability provides the mechanism for the supply of microtubules in the areas where they are needed. Numerical simulations have also supported the notion that dynamic instability depends on GTP-tubulin concentration.

This work has generated some interesting problems for consideration in the future. Firstly we have assumed that the microtubules nucleate at random. While this may be true *in vitro*, it is a known fact from electron microscopic studies that microtubules form

at specific regions *in vivo* [72]. We thus need to incorporate the spatial component in the models. By compartmentalizing the cell, for example, we can study the dynamics of the concentrations of GDP-tubulin, GTP-tubulin and microtubules across the cell.

Secondly, we have taken that the newly formed seeds during the nucleation phase are growing microtubules. It would be interesting to consider the seeds as also existing in two states; growing and shrinking state.

Lastly, experiments [27] show that the two ends of the microtubule grow at different rates. Besides, the minus ends are embedded within the microtubule-organizing centre (MTOC) where initiation of new microtubules occurs, while the plus ends grow into the cytoplasm [2, 81]. This feature could thus be incorporated by introducing distinct rates for the minus and plus end.

Bibliography

[1] Alber, M. S., Kiskowski, M. A., Glazier, J. A. & Jiang, Y. (2003). On cellular automaton approaches to modeling biological cells. In J. Rosenthal & D. S. Gilliam (Eds.), *Mathematical Systems Theory in Biology, Communication, and Finance IMA* **134**, Springer-Verlag, New York, pp.1-39.

[2] Alberts, B., Bray, D., Lewis, J. Raff, M., Roberts, K. & Watson, J. D. (1994). Molecular Biology of the Cell, 3rd ed., Garland, New York.

[3] Antal, T., Krapivsky, P. L. & Redner, S. (2007a). Dynamics of microtubule instabilities. *J. Stat. Mech.* L05004.

[4] Antal, T., Krapivsky, P. L., Redner, S., Mailman, M. & Chakraborty, B. (2007b). Dynamics of an idealized model of microtubule growth and catastrophe. *Phys. Rev. E* **76**: 041907.

[5] Baas, P. W. & Black, M. M. (1990). Individual microtubules in the axon consists of domains that differ in both composition and stability. *J. Cell Biol.* **111**: 495-509.

[6] Bassetti, B., Lagomarsino, M. C. & Jona, P. (2000). A model for the self-organization of microtubules driven by molecular motors. *Eur. Phys. J. B* **15**: 483-492.

[7] Beer, R. D. (2000). Dynamical approaches to cognitive science. *Trends in Cognitive Sciences* **4**: 91-99.

[8] Belmont, L. D., Hyman, A. A., Sawin, K. E. & Mitchison, T. J. (1990). Real-time visualisation of cell cycle-dependent changes in microtubule dynamics in cytoplasmic extracts. *Cell* **62**: 579-589

[9] Bicout, D. J. & Rubin, R. J. (1999). Classification of microtubule histories. *Phys. Rev. E* **59**: 913-920.

[10] Birkhoff, G. & Rota, G. C. (1962). Ordinary differential equations. Ginn & Co., Boston.

[11] Bolterauer, H., Limbach, H.-J. & Tuszyński, J. A. (1999a). Models of assembly and disassembly of individual microtubules: stochastic and averaged equations. *J. Biol. Phys.* **25**: 1-22.

[12] Bolterauer, H., Limbach, H.-J. & Tuszyński, J. A. (1999b). Microtubules: strange polymers inside the cell. *Bioelectrochem. Bioenerg.* **48**: 285-295.

[13] Bouchard, A. M., Warrender, C. E. & Osbourn, G. C. (2006). Harnessing microtubule dynamic instability for nanostructure assembly. *Phys. Rev. E* **74**: 041902.

[14] Burbank, K. S. & Mitchison, T. J. (2006). Microtubule dynamic instability. *Curr. Biol.* **16**: R516-R517.

[15] Casati, R., Costato, M. & Milani, M. (1996). Cellular automata simulation of the effects induced by an external electromagnetic field on microtubule formation dynamics. *Bioelectrochem. Bioenerg.* **41**: 63-69.

[16] Caudron, N., Valiron, O., Usson, Y., Valiron, P. & Job, D. (2000). A reassessment of the factors affecting microtubule assembly and disassembly in vitro. *J. Mol. Biol.* **297**: 211-220.

[17] Coley, A. A. (2003). Dynamical systems and cosmology. Kluwer Academic, Dordrech.

[18] Desai, A. & Mitchison, T.J. (1997). Microtubule polymerization dynamics. *Annu. Rev. Cell Dev. Biol.* **13**: 83-117.

[19] Dogterom, M. & Leibler, S. (1993). Physical aspects of the growth and regulation of microtubule structures. *Phys. Rev. Lett.* **70**: 1347-1350.

[20] Dogterom, M., Maggs, A. C. & Leibler, S. (1995). Diffusion and formation of microtubule asters: physical processes versus biochemical regulation. *Proc. Natl. Acad. Sci. USA* **92**: 6683-6688.

[21] Downing, K. H. & Nogales, E. (1998). Tubulin and microtubule structure. *Curr. Opin. Cell. Biol.* **10**: 16-22.

[22] Dustin, P. (1978). Microtubules. Springer-Verlag, New York.

[23] Edelstein-Keshet, L. (1988). Mathematical models in biology. McGraw-Hill, New York.

[24] Erickson, H. P. & O'Brien, E. T. (1992). Microtubule dynamic instability and GTP hydrolysis. *Ann. Rev. Biophys. Biomol. Struct.* **21**: 145-166

[25] Ermentrout, G. B. & Edelstein-Keshet, L. (1993). Cellular automata approaches to biological modeling. *J. Theor. Biol.* **160**: 97-133.

[26] Flyvbjerg, H., Holy, T. E. & Leibler, S. (1994). Stochastic dynamics of microtubules: a model for caps and catastrophes. *Phys. Rev. Lett.* **73**: 2372-2375.

[27] Fygenson, D. K., Braun, E. & Libchaber, A. (1994). Phase diagram of microtubules. *Phys. Rev. E* **50**: 1579-1588.

[28] Grego, S., Cantillana, V. & Salmon, E. D. (2001). Microtubule treadmilling in vitro investigated by fluorescence speckle and confocal microscopy. *Biophys. J.* **81**: 66-78.

[29] Gronwall, T. H. (1919). Note on the derivatives with respect to a parameter of the solutions of a system of differential equations. *Ann. Math.* **20**: 292-296.

[30] Hahn, W. (1967). Stability of motion. Springer-Verlag, Berlin.

[31] Hale, J. K. (1969). Ordinary differential equations. Wiley, New York.

[32] Hearon, J. Z. (1963). Theorems on linear systems. *Ann. N.Y. Acad. Sci.* **108**: 36-68.

[33] Hirsch, M. W. & Smale, S. (1974). Differential equations, dynamical systems, and linear algebra. Academic Press, New York.

[34] Horio, T. & Hotani, H. (1986). Visualization of the dynamic instability of individual microtubules by darkfield microscopy. *Nature* **321**: 605-607.

[35] Horn, R. A. & Johnson, C. R. (1985). Matrix analysis. Cambridge University Press, Cambridge, London.

[36] Howard, J. & Hymann, A. A. (2003). Dynamics and mechanics of the microtubule plus end. *Nature* **422**: 753-758.

[37] Jánosi, I. M., Chrétien, D. & Flyvbjerg, H. (1998). Modeling elastic properties of microtubule tips and walls. *Eur. Biophys. J.* **27**: 501-513.

[38] Jánosi, I. M., Chrétien, D. & Flyvbjerg, H. (2002). Structural microtubule cap: stability, catastrophe, rescue, and third state. *Biophys. J.* **83**: 1317-1330.

[39] Janulevicius, A., Van Pelt, J. & Van Ooyen, A. (2006). Compartment volume influences microtubule dynamic instability: a model study. *Biophys. J.* **90**: 788-798.

[40] Jeffries, C. (1974). Qualitative stability and digraphs in model ecosystems. *Ecology* **55**: 1415-1419.

[41] Job, D., Valiron, O. & Oakley, B. (2003). Microtubule nucleation. *Curr. Opin. Cell Biol.* **15**: 111-117.

[42] Johnson, K. A. & Borisy, G. G. (1977). Kinetic analysis of microtubule self-assembly in vitro. *J. Mol. Biol.* **117**: 1-31.

[43] Jordan, M. A., Hadfield, J. A., Lawrence, N. J. & McGown, A. T. (1998). Tubulin as a target for anticancer drugs: agents which interact with the mitotic spindle. *Med. Res. Rev.* **18**: 259-296.

[44] Jordan, M. A. & Wilson, L. (2004). Microtubules as a target for anticancer drugs. *Nat. Rev. Cancer* **4**: 253-265.

[45] Katrukha, K. A. & Guriya, G. T. (2006). Dynamic instabilities in the microtubule cytoskeleton: a state diagram. *Biophysics* **51**: 781-788.

[46] Khalil, H. K. (2002). Nonlinear systems, 3rd ed., Prentice Hall, New Jersey.

[47] Kirchner, K. & Mandelkow, E. M. (1985). Tubulin domains responsible for assembly of dimers and protofilaments. *EMBO J.* **4**: 2397-2402.

[48] Kirschner, M. & Mitchison, T. J. (1986). Beyond self-assembly: from microtubules to morphogenesis. *Cell* **45**: 329-342.

[49] Kunwar, A., Schadschneider, A. & Chowdhury, D. (2006). From aggressive driving to molecular motor traffic. *J. Phys. A: Math. Gen.* **39**: 14263-14287.

[50] Lakshmikantham, V., Leela, S. & Martynyuk, A. A. (1989). Stability analysis of nonlinear systems. Mercel Dekker, Inc. New York.

[51] Lodish, H., Berk, A., Matsudaira, P., Kaiser, C., Krieger, M., Scott, M., Zipursky, J. & Darnell, S. (2003). Molecular Cell Biology. W.H. Freeman & Company, New York.

[52] Mandelkow, E. M. & Mandelkow, E. (1992). Microtubule oscillations. *Cell. Motil. Cytoskeleton* **22**: 235-244.

[53] Margolis, R. L. & Wilson, L. (1998). Microtubule treadmilling: what goes around comes around. *Bioessays* **20**: 830-836.

[54] Marx, A. & Mandelkow, E. (1994). A model of microtubule oscillations. *Eur. Biophys. J.* **22**: 405-421.

[55] The MathWorks Inc. (2006). MATLAB: The language of technical computing, version 7.2.0.232 (R2006a). The MathWorks Inc., Natick, Massachusetts.

[56] May, R. M. (1973). Qualitative stability in model systems. *Ecology* **54**: 638-641.

[57] Michel, A. N., Hou, L. & Liu, D. (2007). Stability of dynamical systems: continuous, discontinuous and discrete systems. Birkhäuser, Boston.

[58] Mitchison, T. J. & Kirschner, M. (1984). Dynamic instability of microtubule growth. *Nature* **312**: 237-242.

[59] Molodtsov, M. I., Ermakova, E. A., Shnol, E. E., Grishchuk, E. L., McIntosh, J. R. & Ataullakhanov, F. I. (2005a). A molecular-mechanical model of the microtubule. *Biophys. J.* **88**: 3167-3179.

[60] Molodtsov, M. I., Grishchuk, E. L., Efremov, A. K., McIntosh, J. R. & Ataullakhanov, F. I. (2005b). Force production by depolymerizing microtubules: a theoretical study. *Proc. Natl. Acad. Sci. USA* **102**: 4353-4358.

[61] Nogales, E. (1999). A structural view of microtubule dynamics. *Cell. Mol. Life Sci.* **56**: 133-142.

[62] Nogales, E., Wolf, S. G. & Downing, K. H. (1998). Structure of the $\alpha\beta$-tubulin dimer by electron crystallography. *Nature* **391**: 199-203.

[63] Olmsted, J. B. & Borisy, G. G. (1973). Microtubule. *Annu. Rev. Biochem.* **42**: 507-540.

[64] Pérez-Delgado, C. A. & Cheung, D. (2007). Local unitary quantum cellular automata. *Phys. Rev. A* **76**: 032320.

[65] Perko, L. (1991). Differential equations and dynamical systems: Texts in Applied Mathematics 7. Springer-Verlag, New York.

[66] Quirk, J. & Ruppert, R. (1965). Qualitative economics and the stability of equilibrium. *Review of Economic Studies* **32**: 311-326.

[67] Rabitz, H., Kramer, M. & Dacol, D. (1983). Sensitivity analysis in chemical kinetics. *Annu. Rev. Phys. Chem.* **34**: 419-461.

[68] Sept, D. (1999). Model for spatial microtubule oscillations. *Phys. Rev. E* **60**: 838-841.

[69] Sept, D., Limbach, H. J., Bolterauer, H. & Tuszyński, J. A. (1999). A chemical kinetics model for microtubule oscillations. *J. Theor. Biol.* **197**: 77-88.

[70] Šiljak, D. D. (1978). Large scale dynamical systems: stability and structure. North-Holland, Amsterdam.

[71] Smith, H. L. (1995). Monotone dynamical systems: an introduction to the theory of competitive and cooperative systems. *Math. Surveys Monogr.* **41** *Amer. Math. Soc.*, Providence, Rhode Island.

[72] Snyder, J. A. & McIntosh, J. R. (1976). Biochemistry and physiology of microtubules. *Annu. Rev. Biochem.* **45**: 699-720.

[73] Stephens, R. E. & Edds, K. T. (1976). Microtubules: structure, chemistry and function. *Physiol. Rev.* **56**: 709-777.

[74] Troisi, A., Wong, V. & Ratner, M. A. (2005). An agent-based approach for modeling molecular self-organization. *Proc. Natl. Acad. Sci. USA* **102**: 255-260.

[75] Turányi, T. (1990). Sensitivity analysis of complex kinetic systems: tools and applications. *J. Math. Chem.* **5**: 203-248.

[76] Tuszyński, J. A., Luchko, T., Portet, S. & Dixon, J. M. (2005). Anisotropic elastic properties of microtubules. *Eur. Phys. J. E - Soft Matter* **17**: 29-35.

[77] Valiron, O., Caudron, N. & Job, D. (2001). Microtubule dynamics. *Cell. Mol. Life Sci.* **58**: 2069-2084.

[78] VanBuren, V., Odde, D. J. & Cassimeris, L. (2002). Estimates of lateral and longitudinal bond energies within the microtubule lattice. *Proc. Natl. Acad. Sci. USA* **99**: 6035-6040.

[79] VanBuren, V., Cassimeris, L. & Odde, D. J. (2005). Mechanochemical model of microtubule structure and self-assembly kinetics. *Biophys. J.* **89**: 2911-2926.

[80] Voter, W. A. & Erickson, H. P. (1984). The kinetics of microtubule assembly. Evidence for a two-stage nucleation mechanism. *J. Biol. Chem.* **25**: 10430-10438.

[81] Wade, R. H. & Hyman, A. A. (1997). Microtubule structure and dynamics. *Curr. Opin. Cell Biol.* **9**: 12-17.

[82] Walker, R. A., O'Brien, T. O., Pryer, N. K., Soboeiro, M. F., Voter, W. A., Erickson, H. P. & Salmon, E. D. (1988). Dynamic instability of individual microtubules analyzed by video light microscopy: rate constants and transition frequencies. *J. Cell Biol.* **107**: 1437-1448.

[83] Wang, C. Y., Ru, C. Q. & Mioduchowski, A. (2006). Vibration of microtubules as orthotropic elastic shells. *Physica E* **35**: 48-56.

[84] Wegner, A. (1976). Head to tail polymerization of actin. *J. Mol. Biol.* **108**: 139-150.